BIPHASIC EFFECTS OF NITRIC OXIDE ON SKELETAL MUSCLE MYOTUBE ATROPHY

By

QUINLYN ANN SOLTOW

A DISSERTATION PRESENTED TO THE GRADUATE SCHOOL
OF THE UNIVERSITY OF FLORIDA IN PARTIAL FULFILLMENT
OF THE REQUIREMENTS FOR THE DEGREE OF
DOCTOR OF PHILOSOPHY

UNIVERSITY OF FLORIDA

2008

To my family, who always believes in me, even when I do not

ACKNOWLEDGMENTS

First, I thank Dr. Criswell for all of his guidance, kindness, and support during my growth as a graduate student in his lab. I also thank the rest of my committee members, Drs. Scott Powers, Stephen Dodd, and Glenn Walter, for their numerous suggestions and intellectual discussions. The dedication and passion demonstrated in their work has had great influence on my professional career.

Second, I would like to acknowledge all of the current and past members of the Molecular Physiology lab, Jeff Sellman, Jodi Long, Jenna Betters, and Vitor Lira, for teaching me everything that I know about biological assays and cell culture; as well as Jason Drenning and Liz Zeanah for their compassion and friendship both in and out of the lab. I would especially like to thank Vitor for his words of encouragement and advice during our final semester together. The memories of our struggles and laughs will never be forgotten.

Finally, I commend all of my family and close friends for putting up with me throughout this entire process. I could not have had the confidence and perseverance to obtain this degree had it not been for their endless love and support.

TABLE OF CONTENTS

LIST OF FIGURES

LIST OF ABBREVIATIONS

Bcl-3	B-cell lymphoma-3
cGMP	cyclic guanosine monophosphate
DGC	dystrophin-glycoprotein complex
eNOS	endothelial nitric oxide synthase
FOXO	forkhead box O
GSK-3β	glycogen synthase kinase-3beta
IκB-α	I kappa B-alpha
iNOS	inducible nitric oxide synthase
L-NAME	N^G-nitro-L-arginine methyl ester
MAFbx	muscle atrophy F-box
MuRF1	muscle RING finger-1
NF-κB	nuclear factor-kappa B
nNOS	neuronal nitric oxide synthase
NO	nitric oxide
NOS	nitric oxide synthase
PI3K	phosphoinositide-3-kinase

Abstract of Dissertation Presented to the Graduate School
of the University of Florida in Partial Fulfillment of the
Requirements for the Degree of Doctor of Philosophy

BIPHASIC EFFECTS OF NITRIC OXIDE ON SKELETAL MUSCLE MYOTUBE ATROPHY

By

Quinlyn Ann Soltow

December 2008

Chair: David S. Criswell
Major: Health and Human Performance

Skeletal muscle disuse atrophy occurs during prolonged periods of reduced muscle activity often seen with bed rest, limb immobilization, and space flight. Muscle injury or lack of mechanical activity causes disruptive nitric oxide synthase (NOS) activity, which is sufficient to induce forkhead box O-3a, muscle RING finger-1, and muscle atrophy F-box, and nuclear factor-kappa B (NF-kappaB) through classical and alternative pathways, respectively. Paradoxically, increased nitric oxide production is caused by muscle loading and is essential for muscle growth. This is the first study to develop two completely intrinsic models of skeletal muscle atrophy *in vitro*: 1) withdrawal from moderate cyclic stretch, and 2) high magnitude cyclic strain. First, moderate cyclic mechanical stretch can be used as a model of activity in cultured skeletal muscle myotubes, and increased myotube size through NOS-dependent Akt signaling. Cessation of moderate stretch caused protein degradation, altered neuronal NOS localization, and a reduction in myotube size via downregulation of Akt, which may contribute to NF-kappaB signaling through an alternative pathway. Secondly, high magnitude cyclic strain induced the classical pathway of NF-kappaB signaling and upregulated inducible NOS. These data demonstrated *in vitro* models of atrophy independent of external factors and provide evidence to better understand the signaling pathways involved during skeletal muscle loss.

CHAPTER 1
INTRODUCTION

Background

Skeletal muscle atrophy is a clinically significant problem as it arises from a variety of factors, such as prolonged bed rest, limb immobilization, space flight, denervation, cancer, sepsis, and ageing. In addition to compromised mobility and balance, loss of muscle mass contributes to the metabolic syndrome and increased risk for heart disease. Mechanical injury or lack of mechanical activity during disuse causes high NOS activity (140, 149, 169), which is sufficient to induce FOXO3a, MuRF1, MAFbx, and skeletal muscle atrophy (11, 169). Paradoxically, increased NO production, albeit a lower level than shown in atrophy models, is caused by muscle loading (passive stretch, electrical stimulation, reloading) and is essential for muscle growth (145, 162, 178). Low concentrations of NO can inhibit GSK-3β activity via a cGMP/Akt-dependent mechanism (48) and, therefore, may coordinate FOXO and NF-κB regulation of atrophy signaling pathways (Figure 1-1).

Determining if NO can prevent and/or contribute to skeletal muscle atrophy by regulating FOXO and NF-κB is important and may lead to potential therapeutic strategies to alleviate skeletal muscle disuse atrophy. Therefore, we hypothesize that NOS is a vital signal transducer in skeletal muscle, in that mechanical load imposed upon the muscle membrane maintains moderate NO concentrations to preserve skeletal muscle mass. However, cessation of activity causes nNOS to dissociate from the sarcolemma and produce unregulated amounts of NO contributing to proteolysis and skeletal muscle atrophy. Likewise, excessive strain to the muscle leads to upregulation of iNOS and activation of atrophy signaling pathways.

Specific Aims and Hypotheses

Specific aim 1: To develop an *in vitro* model of skeletal muscle disuse atrophy. Cyclic stretch provides strain to the sarcolemma and through mechanotransduction, increases muscle integrity (213), metabolism (86, 155), NO production (178, 212), and protein synthesis (81). We tested if removal of the stretch stimulus reverses these processes to induce protein degradation and atrophy.

Hypothesis 1: Cessation of repetitive bouts of cyclic stretch to myotubes causes protein degradation and a reduction in myotube size and protein content.

Specific aim 2: To test if cessation of repetitive daily activity of skeletal muscle myotubes causes elevation of NO production (>20%) and activation of skeletal muscle disuse atrophy. We have shown that moderate magnitudes of cyclic stretch stimulate an approximately 10-20% increase in NO production. Low concentrations of NO inhibit GSK-3β activity, which is hypothesized to be the primary kinase responsible for activation of the NF-κB complexes ($p50_2$/Bcl-3) implicated in disuse atrophy (83, 84). Conversely, higher amounts of NO induce GSK-3β, Bcl-3 and FOXO3a (169) activity responsible for atrophy.

Hypothesis 2A: Moderate magnitudes of cyclic stretch in C_2C_{12} myotubes maintain nNOS localization, low levels of NO, and oppose skeletal muscle atrophy by inhibition of GSK-3β, FOXO3a, and NF-κB.

Hypothesis 2B: Cessation of stretch in C_2C_{12} myotubes causes dissociation of nNOS from the sarcolemma, elevated NO production and initiation of skeletal muscle disuse atrophy signaling.

Hypothesis 2C: NOS inhibition with L-NAME in C_2C_{12} or genetic knockout of nNOS in primary myotubes prevents the upregulation of atrophy signaling pathways following cessation of cyclic stretch.

Specific aim 3: To ascertain if excessive load applied to skeletal muscle myotubes causes production of high amounts of NO via iNOS and activation of proteolysis. Skeletal muscle injury leads to inflammation and upregulation of iNOS (140, 147), which is associated with the classical pathway of NF-κB (IκB-α/p50/p65) (102) to induce protein degradation (11).

Hypothesis 3A: High tensile strain of C_2C_{12} myotubes induce iNOS, elevated NO production and proteolysis via the classical pathway of NF-κB signaling.

Hypothesis 3B: NOS inhibition with L-NAME in C_2C_{12} or genetic knockout of iNOS in primary myotubes protects myotubes from degradation following high magnitudes of stretch through inhibition of NF-κB.

Clinical Significance

Skeletal muscle tissue constitutes about 40% of human body mass to maintain basic functions such as locomotion, respiration, and metabolism. Skeletal muscle has the innate ability to adapt to stessors. Resistance exercise and sufficient nutrient uptake leads to skeletal muscle hypertrophy characterized by an increase in fiber cross-sectional area, force production, and protein content. On the other hand, skeletal muscle atrophy can ensue following periods of inactivity, lack of nutrition, or disease. Atrophy is described as a loss in fiber size, protein content, and strength. Skeletal muscle atrophy is a product of and can contribute to numerous disease states. A loss of skeletal muscle leads to fatigability, a loss in mobility and insulin resistance; all of which are risk factors for type II diabetes and cardiovascular disease.

Much work has been done in the field of skeletal muscle atrophy. Various models, including limb immobilization, limb unloading, denervation, and endotoxin administration, have been used to research the causes of muscle atrophy. These models are all performed *in vivo*, and can provide little insight on the intrinsic factors leading to muscle degradation in the absence of humoral and neural influence. Therefore, an *in vitro* model of skeletal muscle atrophy, applying both disuse and inflammation-associated types, is necessary to study the signaling pathways leading to loss of muscle mass. Elucidating these signals may lead to therapeutic strategies, such as pharmaceutical interventions or rehabilitation techniques, to attenuate or eliminate skeletal muscle atrophy as a cause or side effect of disease.

Strengths and Limitations

With this project, we developed a novel approach to the study of skeletal muscle disuse atrophy. Although informative research can be done using *in vivo* models of atrophy (hindlimb suspension, immobilization, denervation), there is a need for an *in vitro* model that mimics the same signaling pathways revealed during the *in vivo* studies independent of potential extraneous effects of neural and humoral factors. The few *in vitro* models of atrophy that have been investigated include starvation, glucocorticoid treatment, and cytokine administration (interleukins and tumor necrosis factor-alpha (TNF-α)) (15, 126, 168). Although these strategies induce atrophy of myotubes, they do so by acting through the TNF receptor and the classical pathway of NF-κB signaling (IκB-α/p50/p65). New research suggests this pathway does not account for inactivity-related atrophy (83, 84); therefore, an *in vitro* model has yet to be designed which activates the alternative pathway of NF-κB signaling (p50/Bcl-3). Therefore, this is the first *in vitro* model of disuse atrophy to act via the same mechanisms seen *in vivo*.

By using cessation of stretch to induce disuse signaling and high strain to cause inflammation associated-atrophy, we are employing a completely intrinsic model which is independent of any external physiological influence. One limitation inherent to *in vitro* models, such as this, is the need to confirm observations *in vivo*. Nevertheless, this study establishes intrinsic cellular mechanisms and will lead to *in vivo* studies to confirm the physiological significance of NO in skeletal muscle disuse atrophy.

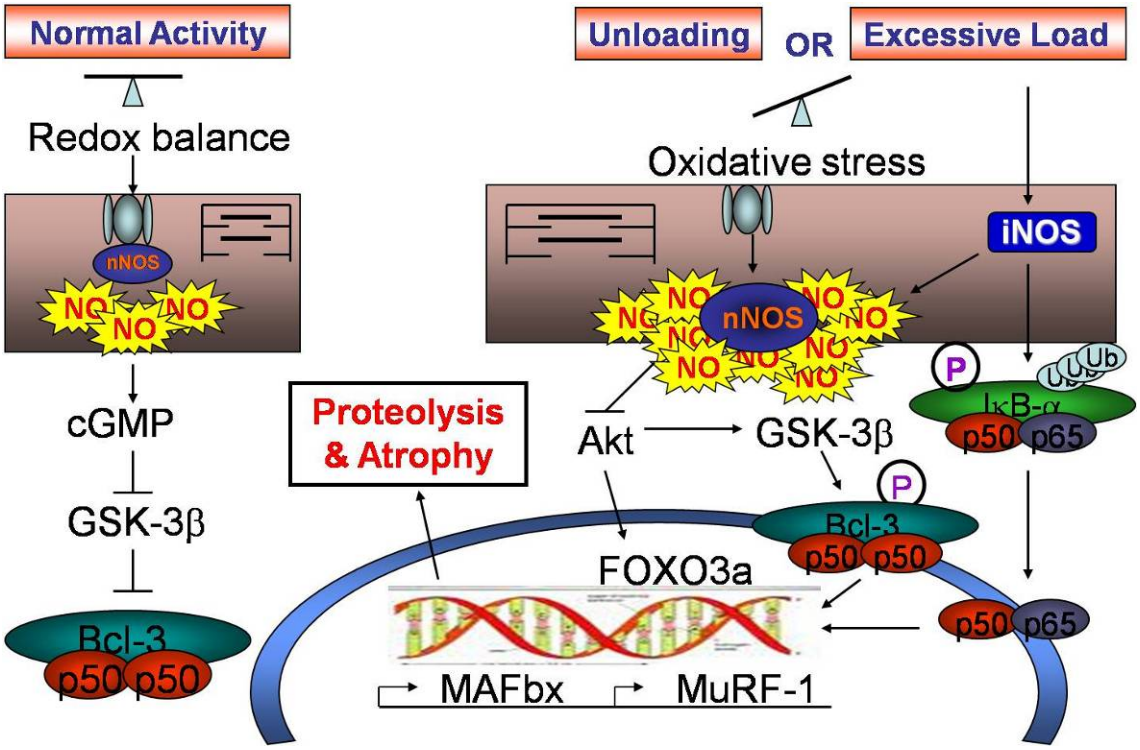

Figure 1-1. Proposed model of nitric oxide-dependent control of skeletal muscle size with alterations in loading stimuli.

CHAPTER 2
LITERATURE REVIEW

Skeletal muscle atrophy is a clinically significant problem as it arises from a variety of factors, such as prolonged bed rest, limb immobilization, space flight, denervation, cancer, sepsis, and ageing. Loss of muscle mass has been shown to contribute to inactivity, obesity, insulin resistance, hypertension, and hyperlipidemia (altogether termed metabolic syndrome). Minimization of muscle atrophy and its side effects will prevent the progression to more serious pathological disorders such as cardiovascular disease and cancer, and improve overall quality of life.

Overview of Disuse Skeletal Muscle Atrophy

Although skeletal muscle atrophy occurs with numerous pathologies such as cancer, sepsis, and diabetes (73, 87), muscle atrophy can also occur in the absence of disease during prolonged periods of reduced muscle activity (20). It is well established that prolonged best rest, limb immobilization, mechanical ventilation, or space flight can produce muscle atrophy in humans. However, investigation of mechanisms responsible for disuse atrophy in humans is difficult. Therefore, animal models have been utilized to mimic the various conditions that produce human disuse atrophy. For example, to imitate prolonged bed rest and space flight in humans, animal models of hindlimb suspension are used to unload the hindlimb locomotor muscles. Also, animal models of limb immobilization are commonly used to research disuse atrophy.

According to research employing both the aforementioned models, disuse muscle atrophy occurs due to both a decrease in muscle protein synthesis and an increase in the rate of proteolysis (21, 176). After the onset of muscle unloading, the rate of protein synthesis declines rapidly and reaches a new steady-state level at ~48 hours (176). The drop in protein synthesis is followed by a large and rapid increase in protein degradation peaking at approximately 14 days

(Figure 2-1). Fiber type disparities also affect the extent of muscle atrophy. Solei (predominantly type I fibers) show the greatest degree of atrophy during unloading and immobilized conditions (20). Collectively, the reduced activity of skeletal muscle negatively impacts muscle mass through alterations of the rates of protein synthesis and degradation that ultimately lead to muscle atrophy.

Although a decrease in protein synthesis initiates the drop in muscle mass, the predominant cause of atrophy is the dramatic increase in protein degradation. Therefore, strategies to attenuate proteolysis will be the most beneficial to counteracting muscle atrophy. Several proteolytic systems contribute to the degradation of muscle proteins. They include lysosomal proteases, calcium-activated proteases, and the proteasome system. Lysosomal proteases are activated in skeletal muscle undergoing disuse atrophy; however, the contribution of these proteases appears limited (58, 74, 139). It appears the bulk of muscle proteolysis involves both calpain and the proteasome system (139), and to some lesser extent, caspase-3 (50). The proteasome system can degrade monomeric contractile proteins, however, it is unable to degrade intact actomyosin complexes (65). Therefore, myofilaments must be released from the sarcomere before degradation by the proteasome system can occur. Evidence indicates that both calpain and caspase-3 are capable of producing actomyosin disassociation which is believed to be the rate-limiting step in protein degradation.

The proteasome system consists of the 20S core proteasome and the 26S proteasome complex (20S core + 19S regulatory complex) (43). The 26S proteasome recognizes ubiquitin-labeled proteins, unfolds, and degrades these proteins via an ATP-dependent mechanism. The binding of ubiquitin to protein substrates requires the ubiquitin-activating enzyme (E1), ubiquitin-conjugating enzyme (E2), and ubiquitin-ligase enzymes (E3). Specific E3 ligases

termed MAFbx and MuRF1 have been discovered in skeletal muscle and are essential in almost all models of skeletal muscle atrophy (19, 67).

Redox Balance

A potential mechanism that would trigger increased protein degradation and atrophy in skeletal muscle is oxidative stress, where antioxidant protein and scavenger protection are overwhelmed by oxidant production. Oxidation can alter the structure and function of proteins, lipids, and nucleic acids, leading to cellular injury and even cell death.

Kondo and colleagues provided the first evidence that oxidants contributed to disuse muscle atrophy. This work revealed that immobilization of skeletal muscles was associated with oxidative injury in the muscle, and the oxidant injury can contribute to muscle atrophy (101). Oxidative stress also increases in hindlimb muscle (soleus) with hindlimb unloading. Hindlimb unloading is linked to an imbalance in the antioxidant system and increased hydroperoxides. Unloading-induced disruption of the antioxidant enzyme and scavenger profile could also predispose skeletal muscle to inflammation and muscle damage upon reloading (108).

The exact mechanisms of how oxidative stress induces proteolysis are still unknown, but many possibilities exist. First, oxidative stress decreases membrane calcium-ATPase activity thereby retarding calcium removal from the cell and contributing to cellular calcium accumulation (160). Increased intracellular calcium levels would activate calpain and caspase resulting in augmented proteolysis. Second, oxidative stress upregulates the expression of MAFbx and MuRF1 and augments the 26S proteasome which would lead to accelerated proteolysis and muscle atrophy (19, 112). At present is uncertain which oxidant-producing pathways are responsible for the oxidative injury within inactive skeletal muscles, and oxidative stress in skeletal muscle may be due to the interaction of different oxidant production pathways.

Increased oxidant production during unloading may be due to a lack of neural stimulation or to reduced mechanical perturbation on the sarcolemma. Reduced nerve input can disrupt calcium release, reuptake and signaling within the sarcoplasm and stimulate calcium-activated proteolytic pathways. A decrement in contractile activity and metabolic demand may also disturb oxidative phosphorylation in the mitochondria unbalancing the redox state. Finally, and the focus of this proposal, is the lack of mechanical perturbation of the sarcolemma. Reduced mechanical strain on the muscle membrane may impair signaling from force transducers in the extracellular matrix to the cytoskeleton. The prolonged reduction in tension on the muscle fiber can cause dissociation of these mechanotransduction proteins and activate atrophic signaling pathways. Nitric oxide synthase is one such protein that can become dissociated from a complex of molecules localized at the membrane of muscle and produce oxidant stress during periods of unloading (169). The nitric oxide synthase pathway has been implicated in disuse atrophy and will be discussed in more detail.

Mechanotransduction

The dystrophin-glycoprotein complex (DGC) provides a transmembrane association between the extracelluar matrix and various intracellular proteins and protein complexes, comparable to other transmembrane complexes (Figure 2-2), such as the integrins (55). Disruption of the DGC, such as occurs in Duchene's muscular dystrophy or the mdx mouse, results in repetitive skeletal muscle injury/regeneration and muscle atrophy. Focal adhesion-associated proteins, including vinculin, talin, paxillin, and focal adhesion kinase (FAK), are associated with the DGC. Talin and vinculin are functionally similar to dystrophin because they serve as links between the actin cytoskeleton and a transmembrane receptor for extracellular matrix molecules (11, 102), and they are involved in the transmission of force between the actin cytoskeleton and the cell membrane. Integrin, the transmembrane binding partner for talin and

vinculin, is expressed at higher levels in mdx muscles (73), and recent investigations have shown that the transgenic overexpression of α7-integrin in mdx muscles could greatly reduce dystrophinopathy. However, the integrin complex is also rich in signaling molecules, so the possibility remains that repair of a signaling defect may contribute to the ameliorative effect of α7-integrin transgene expression and prevent muscle wasting.

One possible mechanism leading to muscle atrophy is through interruption of the DGC's interaction with the extracellular matrix and loss of cellular signaling through this complex (142). The DGC comprises of two dystroglycan protein subunits, α and β. β-dystroglycan is a transmembrane protein that binds to dystrophin in the cytoplasm and interacts with Grb2, an adapter protein linking signaling molecules containing phosphotyrosine residues and proline-rich domains (205), and FAK, another protein involved in transmembrane signaling (208). Both Grb2 and FAK function as mediators of survival signaling in numerous cell types, often working through PI3K and one of its downstream effectors, a serine/threonine kinase known as Akt (164). Cell adhesion to the extracellular matrix activates lipid-associated PI3K (26), which in turn induces translocation of Akt from the cytoplasmic pool to the cell membrane, where it is activated by phosphorylation (41). Akt activation has a protective effect, blocking induction of apoptosis in differentiated muscle cells in response to disruption of dystroglycan-laminin interactions (107). Downstream elements of the PI3K/Akt signaling pathway that may mediate cell survival include GSK-3β, members of the GLUT family of glucose transporters, transcription factors in the Forkhead family (FOXO), and members of the IκB family.

Overview of Akt Pathway Contribution to Atrophy

Akt affects transcription and translation of through modulation of a number of factors including mTOR, p70s6k, and NF-κB (Figure 2-3). Inhibition of PI3K reduces Akt and GSK-3β

phosphorylation and decreases myotube survival. Disruption of the dystroglycan-laminin interaction by a blocking antibody for α-dystroglycan significantly reduced Akt and GSK-3β phosphorylation suggesting these signals are modulated by DGC interactions with the extracellular matrix. A retroviral infection with a cDNA construct expressing a constitutively active form of Akt in combination with the blocking antibody restores GSK phosphorylation and promotes cell survival (107).

Various models of atrophy all lead to upregulation of the muscle specific E3 ligases, MAFbx and MuRF1 (19, 154) but can be antagonized by simultaneous treatment with IGF-1 (149) acting through the PI3K/Akt pathway (154, 166). This suggests a novel role for Akt inhibition of atrophy signaling. The mechanism by which Akt inhibits MAFbx and MuRF1 upregulation involves the FOXO family of transcription factors (110, 154, 166). FOXO transcription factors are excluded from the nucleus when phosphorylated by Akt and translocate upon dephosphorylation. The translocation of FOXO is required for upregulation of MuRF1 and MAFbx and is sufficient to induce atrophy (159). Another important substrate of Akt to note is glycogen synthase kinase 3 beta (GSK-3β), which is a negative regulator of protein synthesis. GSK-3β's activity is inhibited by phosphorylation by Akt. A role for GSK-3β in NF-κB signaling pathways of disuse atrophy will be discussed in later sections.

Disruption of DGC during Unloading

Evidence suggests that the DGC works as a regulator of muscle atrophy and serves as a scaffold for anti-atrophic signal transduction (169). The forced expression of dystrophin in skeletal muscle of cachexic mice is sufficient to attenuate muscle wasting (2). However, in tail-suspension-induced atrophy the expression patterns of the components of the DGC, dystrophin, β-dystrophin, α-sarcoglycan, dystrobrevin, laminin-α2, α1-syntrophin, and caveolin-3 are

normally expressed at the sarcolemma. Importantly, nNOS dissociates and translocates to the cytoplasm of the muscle during disuse (2). Normally, nNOS is present under the sarcolemma and accumulated at the NMJ (33) and at the myotendinous junction (32) (Figure 2-4). It is associated with the complex of DAPS and DAGs and with dystrophin through the intermediary of syntrophins, via a PDZ domain (194) (Figure 2-2). Neuronal NOS is a peripheral member of the DGC and may play a role in transducing mechanical signals into chemical ones. Sarcolemmal associated nNOS is reported to be a necessary signaling molecule for satellite cell activation, glucose uptake, muscle contraction, and vasodilation (7, 52, 68, 97). However, upon dissociation from the DGC, nNOS generates an overabundance of nitric oxide leading to skeletal muscle atrophy (2).

Disruption of α-sarcoglycan or dystroglycans dissociates the DGC, including nNOS, and can mimic models of muscular dystrophy. However, during disuse atrophy both of these molecules remain bound to the sarcolemma while nNOS dissociates from the DGC. This suggests that localization of nNOS may be the key component of the DGC that impacts muscle maintenance and atrophy.

Nitric Oxide Contribution to Atrophy

Nitric oxide (NO) is a gaseous free radical promoting many biological effects. Due to its high chemical reactivity, NO can be a powerful signaling molecule and antioxidant or can be harmful through the nitrosylation of many proteins. NO is generated exclusively by three NO synthase isoforms. Two of them are constitutively expressed in cells and have been identified as neuronal NOS (nNOS) and endothelial NOS (eNOS). The expression of the third form, inducible NOS (iNOS), is induced by various cytokines. All three isoforms catalyze the formation of NO from arginine, oxygen, and NADPH. Cofactors also required for NOS activity include, tetrahydrobiopterin (BH_4), FAD and FMN, in addition to a heme prosthetic group. To acquire the

active state, nNOS and eNOS also require calmodulin (CaM) and Ca^{2+} ions, indicating that NO synthesis is triggered by an elevation of free $[Ca^{2+}]_i$. Conversely, iNOS is insensitive to Ca^{2+} ions due to its high affinity for the CaM binding site at basal Ca^{2+} levels.

A number of structural differences characterize the three NOS isoforms. At the N-terminal region, nNOS contains a PDZ domain through which it interacts with α1-syntrophin in the membrane cytoskeleton-dystrophin complex of skeletal muscle or with postsynaptic density proteins in synaptic membranes and neuromuscular junctions. This segment is absent in eNOS and iNOS. The localization of each NOS isoform in skeletal muscle varies as shown in Figure 2-4. The myotendinous and neuromuscular junctions (32), like the costameres, are rich in nNOS, especially in type II fibers (69). Endothelial NOS is expressed in the cytoplasm of all fibers, but more abundantly in types I and IIa (76), where it is mainly localized in mitochondria (98). Inducible NOS is present at very low levels in healthy skeletal muscle of rodents (177) but is enhanced in response to endotoxin (177). The presence of iNOS is either cytosolic or concentrated at the neuromuscular junction (206).

The two constitutive isoforms, nNOS and eNOS, produce pico-nanomolar amounts of NO; whereas, iNOS tends to release NO at nano-micromolar concentrations (161). The quantity of NO produced in skeletal muscle may be a testament to the favorable versus unfavorable effects of NO signaling. The lower concentrations of NO produced may have more beneficial effects including satellite cell activation (7), enhanced myotube fusion (118), and muscle fiber hypertrophy (162, 163); whereas, "higher" amounts of NO, such as those produced by iNOS, are implicated in pathophysiology of inflammatory conditions and degenerative diseases. As mentioned previously, greater concentrations of endogenous NO can result in the formation of

several reactive nitrogen species causing cellular injury due to increased lipid peroxidation and nitrosylation of proteins.

Evidence indicates that NOS activity is increased in immobilized muscle, resulting in altered production of NO (100). Suzuki and colleagues demonstrate that nNOS is dislocated from the sarcolemma during hindlimb unloading leading to an increase in the production of NO (169). Neuronal NOS null mice suffered much milder atrophy, decreased nuclear accumulation of FOXO3a, and prevented upregulation of MAFbx and MuRF1 (169). This data indicates that dislocation of nNOS from the DGC increases nNOS production of higher than healthy muscle and mediates muscle atrophy via regulation of FOXO transcription factors.

Conversely, nNOS expression and activity has also been shown to increase with mechanical activity (178), training (10), and electrical stimulation (145). NOS is also necessary for muscle hypertrophy (162). Tidball and colleagues show that after 10 days of unloading nNOS protein and mRNA expression drop only to return to control levels after 7 days of reloading (178). NO release was not measured in the unloaded or reloaded muscles. However, after passive stretch and electrical stimulation of soleus muscles and C_2C_{12}s, NO release increases 20% above control levels (178). More recently,Wozniak and cohorts demonstrated that a 10% mechanical stretch applied to primary cultured myotubes transiently increased fluorescence of the NO probe, DAF-2DA; whereas in myotubes from mdx mice, which contain little nNOS at the sarcolemma, exhibited much less NO release after stretch (201). These results suggest that mechanical loading is a positive regulator of NOS expression and activity in myotubes and fully differentiated muscle, and this response in essential for muscle growth.

If elevated NOS activity is essential for both skeletal muscle hypertrophy and atrophy, what is the mechanism of its effects? The answer to this question is likely related to intracellular

NOS localization, NO concentration and its effect on redox balance, and NO targets in skeletal muscle. Agarwal and colleagues have demonstrated using cyclic stretch in chondrocytes that moderate amounts of strain increases NO production by about 20%, which is the same induction that Tidball measured in muscle cells with response to loading stimuli. The moderate cyclic stretch (8-10%) did not induce NF-κB translocation; however, more intensive strain (15-18%) greatly induced NO production (100% above control levels) and induced NF-κB nuclear translocation. Interestingly, a cytokine challenge induced translocation of NF-κB, but after initiating moderate cyclic strain (6%), NF-κB became progressively more cytosolic. This suggests that low levels of NO produced during activity contribute to maintenance of redox balance, inhibiting NF-κB activity, and suppressing atrophy signaling pathways. Whereas, high levels of NO induce oxidative stress, activate NF-κB, and contribute to turning on atrophy signals.

Secondly, the targets of NO in skeletal muscle vary based on its concentration. The main protein targets *in vivo* include Ca^{2+}-ATPase, the ryanodine receptor-calcium release channel and guanylate cyclase. The ryanodine receptor and Ca^{2+}-ATPase are susceptible to S-nitrosylation which increases open channel probability (203) and decreases calcium uptake (191), respectively, at relatively high concentrations of NO (167). This may disrupt calcium homeostasis in muscle and activate the calcium-dependent proteases discussed earlier. On the other hand, at lower concentrations, NO activates guanylate cyclase and produces cGMP (8), which has proven to be an essential signaling pathway in skeletal muscle to increase glucose transport (209) and control myoblast fusion (138).

The explanation of nitric oxide's effects on cellular signaling may be two-fold. First, we hypothesize that activity-induced nitric oxide production (moderate levels) contributes to the

maintenance of redox balance and primes the cell for optimal signaling and potential for hypertrophy and adaptation. Second, reduced activity causes nNOS dissociation from the DGC leading to high NO production, a shift in redox toward oxidative stress, and activation of proteolysis and atrophy signaling (Figure 2-5).

Nuclear Factor of κB Pathway of Atrophy

NF-κB is a long known signaling molecule of muscle atrophy, and there are five identified NF-κB transcription factors (p65, Rel B, c-Rel, p52, and p50) that mediate a variety of processes. All family members are expressed in skeletal muscle. Activation of NF-κB is achieved by nuclear transport of heterodimers of NF-κB family members and often occurs by ubiquitination and degradation of the inhibitory protein IκB, which otherwise binds NF-κB heterodimers and retains their cytosolic residence (9). NF-κB members p50 and p52 can form homodimers (75) and undergo nuclear translocation following partial processing of their cytoplasmic precursor molecules, p105 and p100, respectively. Generally, p50 and p52, which lack transactivation domains, function as transcriptional repressors. However, upon binding with B cell lymphoma 3 (Bcl-3), an IκB family member, these complexes can activate transcription through the Bcl-3 transactivation domain (22, 57, 133) when Bcl-3 becomes phosphorylated (25, 129). Thus, Bcl-3 is an unusual member of the IκB family because it can function as a transcriptional coactivator.

Activation of NF-κB is required for muscle degradation due to TNF-α treatment; however, the classical pathway that is activated due to TNF-α appears to be different than the NF-κB pathway that is activated during unloading atrophy (Figure 2-6). The classical pathway involves the nuclear transport of p65/p50 heterodimers by degradation of IκB-α triggered by its phosphorylation by IκB kinase β (IKKβ). NO production by iNOS has been shown to induce this classic pathway (5, 12). However, with unloading, Hunter colleagues demonstrated that nuclear

levels of the prototypical NF-κB family member p65 were not elevated, but p50 and Bcl-3 were markedly increased (84). Although both the classical and alternative pathways to muscle loss converge at the ubiquitin-proteasome (109, 170), the NF-κB pathway activated in inactivity is clearly distinct from that found in cachexia and injury.

Hindlimb suspension of NF-κB1$^{(-/-)}$ (p105/p50) and Bcl-3$^{(-/-)}$ mice further marked the necessity of p50 and Bcl-3 for skeletal muscle disuse atrophy. These genetic knockouts abrogated all NF-κB transcriptional activity and soleus fiber atrophy following 10 days of unloading (83). Judge and colleagues have also shown that incorporation of the IκB super repressor into mice skeletal muscle reversed muscle atrophy, NF-κB activity, and significantly reduced FOXO3a and MAFbx expression after 7 days of unloading (91). Further, mice with muscle-specific expression of a constitutively active form of IKKβ and given the proteasome inhibitor MG-132 blocked the increased proteolysis suggesting that NF-κB activation alone can activate proteasome-dependent proteolysis (31). Taken together, these results demonstrate the requirement of NF-κB signaling, specifically through p50 and Bcl-3, in disuse muscle atrophy.

A potential link between NO signaling and NF-κB lies within the nuclear p50/Bcl-3 complex required for disuse atrophy signaling. Bcl-3 is necessary for p50 dimer transcriptional activity since it contains the transactivation domain. However, phosphorylation of Bcl-3 is required prior to its activation. One likely kinase implicated in Bcl-3 phosphorylation and activation is GSK-3β. Our lab has demonstrated that low levels of NO can inhibit GSK-3β dephosphorylation and translocation to the nucleus via PI3K/Akt signaling (Drenning et al. unpublished). Inhibition of GSK-3β translocation would thereby prevent activation of the p50/Bcl-3 complex and subsequent transcription of atrophy genes. The NF-κB pathway is highly

implicated in the progression of disuse skeletal muscle atrophy, and strategies to attenuate its activity could provide potential therapeutic benefits.

Summary

Disuse skeletal muscle atrophy is mainly due to an increase in proteolysis. Lack of mechanical strain on the sarcolemma with inactivity may cause nNOS dissociation from the DGC and reduce PI3K/Akt activity thereby inducing FOXO3a and GSK-3β nuclear translocation and upregulation of the E3 ligases (MAFbx and MuRF1) and NF-κB (p50/Bcl-3), respectively. Movement of nNOS from the membrane to the cytosol initiates altered NOS activity potentially leading to oxidative stress and further activation of proteolytic pathways. Normal nNOS localization and mechanical activity can produce beneficial effects in muscle, attenuate GSK-3β through a cGMP dependent mechanism, and suppress NF-κB activation. Both NOS and NF-κB play a role in redox balance, have been deemed necessary for disuse skeletal muscle atrophy and found sufficient to induce FOXO3a and E3 ligase expression. Therefore, determining if nitric oxide can prevent and/or contribute to skeletal muscle atrophy by regulating NF-κB signaling is important and may lead to potential therapeutic strategies to alleviate skeletal muscle disuse atrophy.

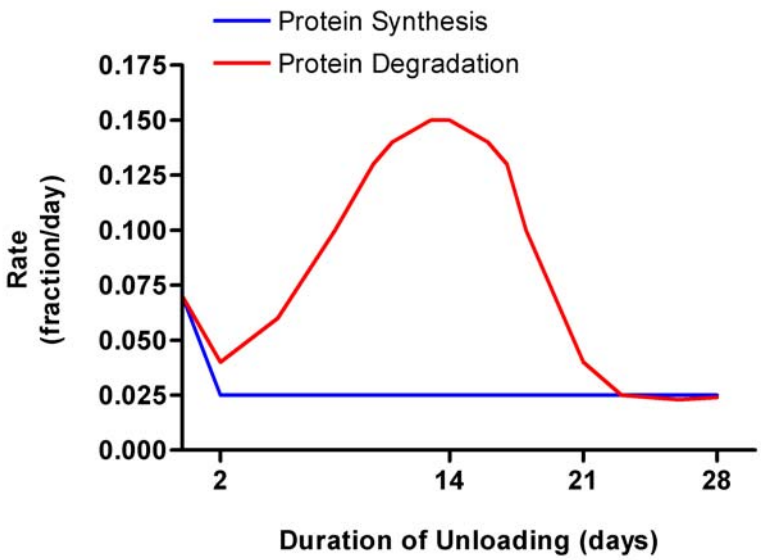

Figure 2-1. Contributions to skeletal muscle protein loss during unloading.

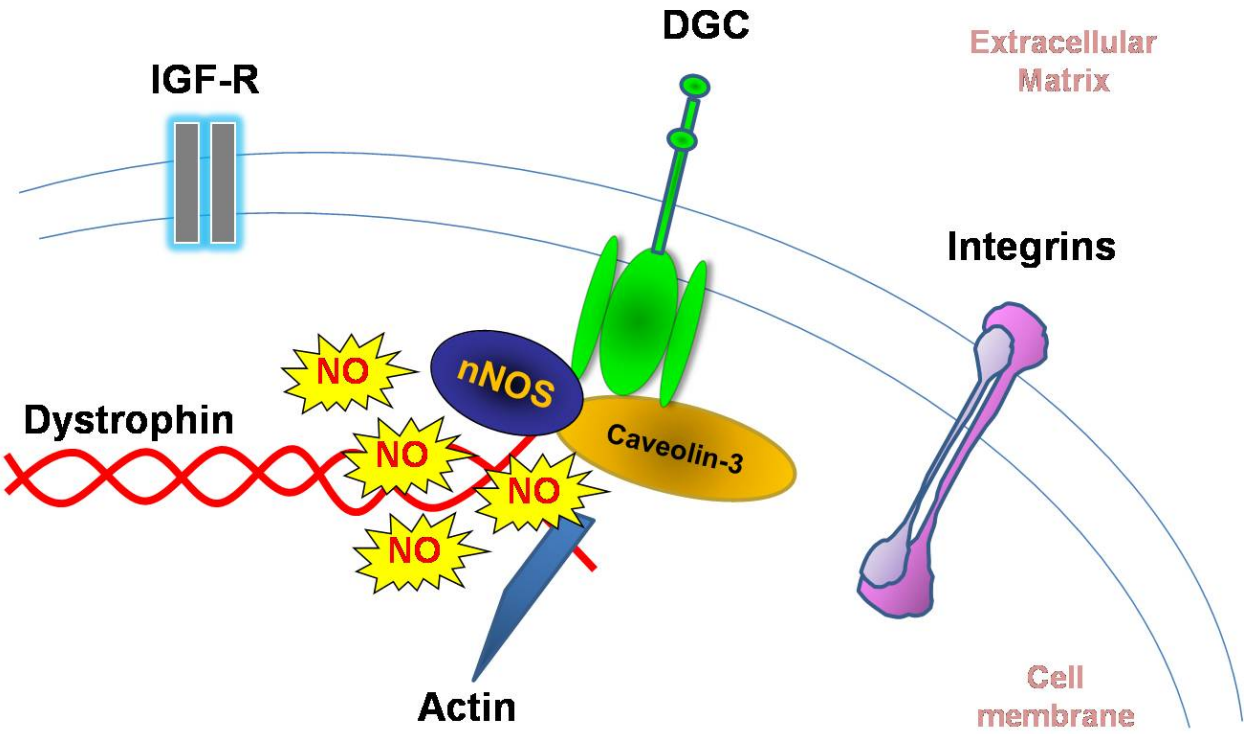

Figure 2-2. Model of the dystrophin-glycoprotein complex as a transsarcolemmal linker between the subsarcolemmal cytoskeleton and the extracellular matrix.

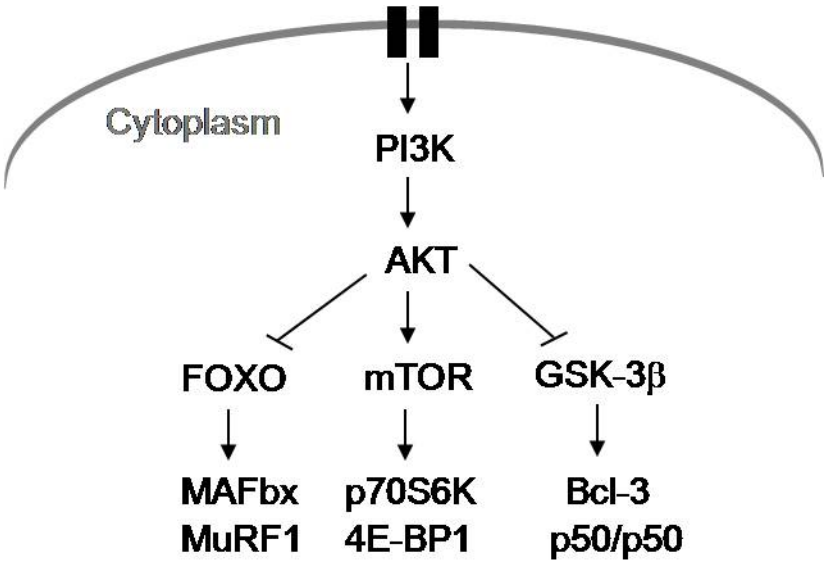

Figure 2-3. Overview of PI3K/Akt signaling network. Note the link between membrane receptors and Akt control of atrophic pathways.

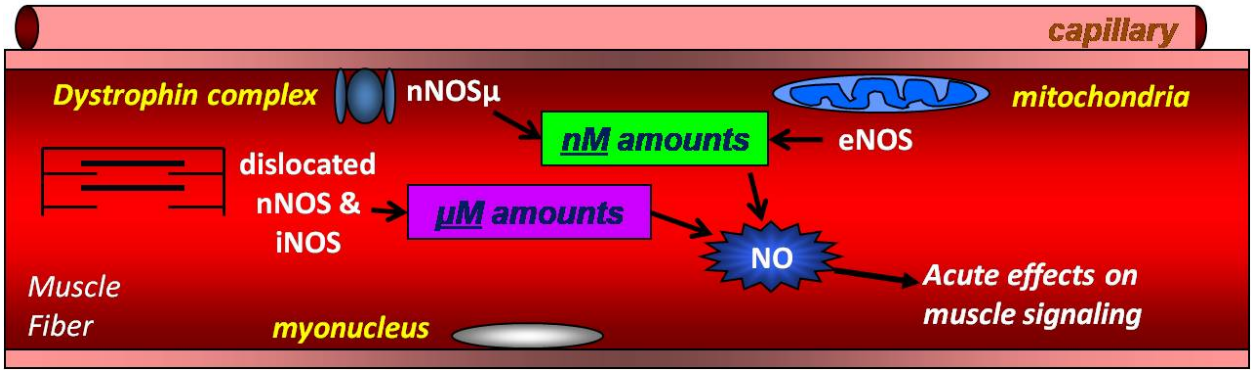

Figure 2-4. Subcellular compartmentalisation of NOS isoforms in skeletal muscle. nNOS is present below the plasma membrane and is particularly accumulated at the muscular and myotendinous junctions. eNOS is present in the cytoplasm of muscle, principally in the mitochondria. Lastly, iNOS is present in the muscle cytoplasm.

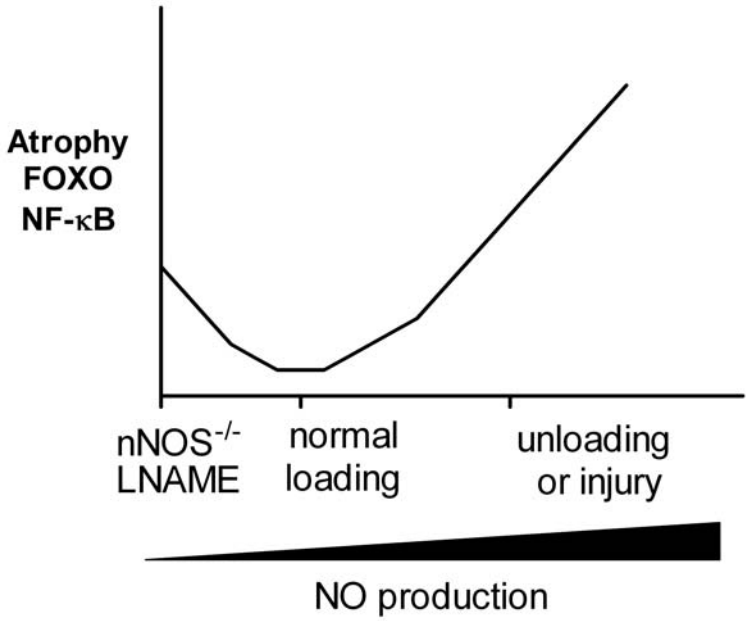

Figure 2-5. Degree of skeletal muscle atrophy as a function of NO production during various conditions.

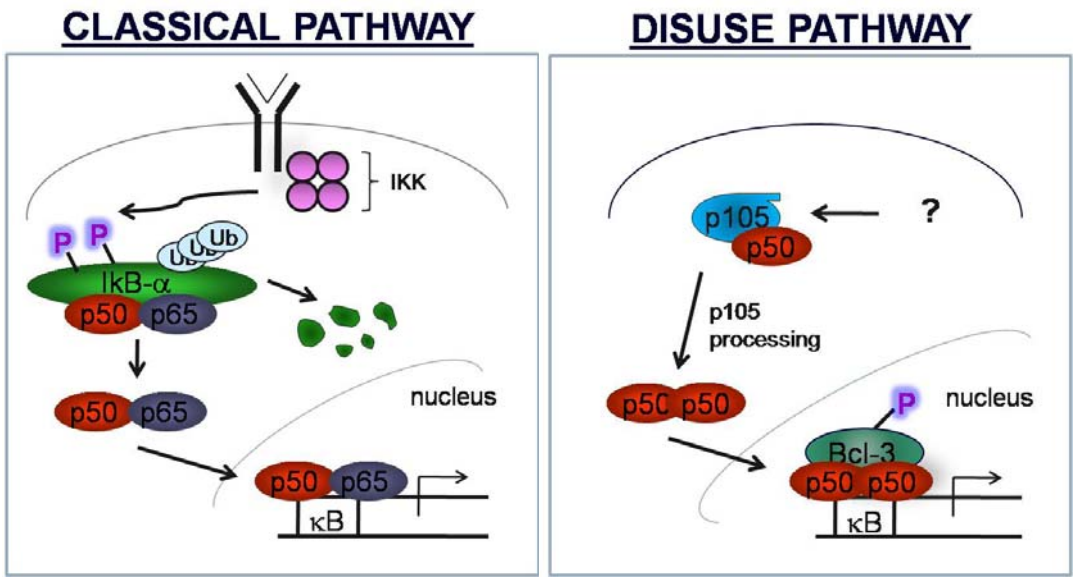

Figure 2-6. Pathways of NF-κB signaling in cachexia/cytokine-induced muscle atrophy (classical pathway) versus disuse muscle atrophy.

CHAPTER 3
MATERIALS AND METHODS

Experimental Designs

Five experiments were performed in order to develop an *in vitro* model of disuse muscle atrophy and to determine the role of nitric oxide in two different types of skeletal muscle atrophy. The first three experiments tested if cessation of repetitive cyclic mechanical strain can be used to mimic disuse muscle atrophy as seen *in vivo*. The final two experiments assessed if high mechanical strain is sufficient to induce the classical pathway of atrophy as seen in cachexia and inflammatory models.

Because many complex pathways have been implicated in skeletal muscle atrophy (e.g., Akt, NF-κB, calpain, caspase), we chose to study some of the main players implicated in several *in vivo* studies to determine their importance during our *in vitro* model of myotube atrophy. Our study incorporated two separate methods of *in vitro* culture. The first is an immortal mouse cell line of skeletal muscle cells called C_2C_{12}s. These cells were originally obtained by Yaffe and Saxel through selective serial passage of myoblasts cultured from the thigh muscle of C3H mice 70 h after a crush injury (204). These cells are capable of differentiation and are a widely used model to study differentiated skeletal muscle cells. Our second model, termed primary culture, involves isolating satellite cells from mouse skeletal muscle and inducing myoblast lineage under appropriate medium and growth factor conditions. Primary cultured cells play a role as a bridge between cell lines and cells *in vivo*, and this technique allowed us to utilize transgenic mouse strains to elucidate the signals that are dependent upon NOS gene expression during atrophy of myotubes.

Experimental 1 Design – Aims 1 and 2 (Figure 3-1). Experiment one was used to test Specific aims 1 and 2. C_2C_{12} myotubes were subjected to a 12% cyclic stretch (1h/d; 1 Hz) for

two days (2dSTR) or five days (5dSTR). One group underwent two days of activity (stretch) followed by three days of inactivity (2dSTR3dCES) to induce myotube atrophy. A non-stimulated control group was used at each time point to control for myotube maturation (2dCON and 5dCON). To test hypothesis one, images were taken of each group at the end of the experimental period and analyzed for myotube length, diameter, and area. Whole cell lysate was collected and used to assess total protein content and protein degradation. To examine hypotheses 2A and 2B, culture medium was collected at 48 h intervals to test for NO production by means of the nitrate/nitrite fluorometric kit (Cayman Chemical). Three samples from each group were fixed and immunostained against nNOS to confirm its localization within the cell. To test hypothesis 2C, L-NAME (5 mM) was administered in parallel to all groups to assess NO regulation of myotube atrophy.

Experimental 2 Design – Aim 2 (Figure 3-2). C_2C_{12} myotubes were subjected to a 12% cyclic stretch (1 h/d; 1 Hz) for two days and then remained inactive for 1, 12, 24, or 48 h before harvesting for protein or luciferase activity. We chose to use a 12% magnitude stretch based on results that that a moderate degree of cyclic stretch stimulates an approximately 10-20% increase in NO production (5, 178). We confirmed these NO levels by measurement of the NO probe, 4-amino-5-methylamino-2',7'-difluorofluorescein (DAF-FM) diacetate, at 6, 12, 18% stretch (Figure 3-3). The aforementioned time points were chosen to test for a time course of upregulation of atrophy signaling pathways. According to our preliminary data, one hour of NO treatment was effective in altering the phosphorylation states of Akt, GSK-3β, FOXO3a, and nuclear translocation of Bcl-3; thus two bouts of a one hour stretch were chosen to test for changes in these proteins. L-NAME (5 mM) was administered 30 m prior to the first bout of

stretch and maintained in the medium throughout the experimental period to test for NO-dependent activation of all measures.

In experiment 2a, we examined the upregulation of atrophy signaling molecules during the cessation of stretch by assessing whole cell lysate as well as nuclear and cytosolic fractions by western blot to probe for the phosphorylation status of Akt, GSK-3β, FOXO3a and Bcl-3 and nuclear and/or cytosolic localization of the NF-κB members, p50, p65, Bcl-3, and IκB-α. In experiment 2b, we monitored NF-κB-dependent transcriptional activity in myotubes by transfection with a NF-κB-luciferase reporter plasmid.

Experimental 3 Design – Aim 2 – Hypothesis 2C (Figure 3-4). Primary cultured satellite cells from wild-type (WT) or $nNOS^{(-/-)}$ mice were harvested and plated to 100 mm culture dishes. However, our technique was unsuccessful in maintaining these satellite cells in culture. Therefore, we were unable to collect data for hypothesis 2C in Specifc aim two which was to subject primary cultured myotubes to 12% cyclic stretch (1 h/d; 1 Hz) for 2 d with cessation of stretch for 1, 12, 24, or 48 h before harvesting for protein as described in experiment two.

Experiment 4 – Aim 3 (Figure 3-5). C_2C_{12} myotubes were subjected to a high magnitude stretch (18%; 0.1 Hz) for 1, 2, 3 h. One group then remained inactive for 2 h following the stretch protocol (2hCES). High magnitude stretch (18-26%) has been shown to upregulate iNOS mRNA and induce NF-κB translocation in other cell types (5). According to our preliminary data, 18% stretch is sufficient to induce a 30% increase in NO production (Figure 3-3). Although 30% increase in NO is sufficient to induce iNOS mRNA and NF-κB translocation, higher amounts of NO have shown to produce the greatest effect (5) but also may cause detrimental and undesirable effects to the cell. Thus we chose to implement an 18% cyclic strain to skeletal muscle myotubes as a model for injury and to induce the classical pathway of NF-κB signaling.

The aforementioned time points were chosen to test for a time course of upregulation of iNOS mRNA and NF-κB translocation previously shown in other cell types by Agarwal and colleagues (5).

In experiment 4a, we examined the translocation or degradation of NF-κB family members associated inflammation and injury in the classical pathway of atrophy by isolating nuclear and cytosolic fractions and analyzing with western blots to probe for the nuclear localization of the NF-κB members, p50, p65, Bcl-3, and cytosolic content of p65 and IκB-α. MAFbx was used as an indirect measure ubiquitin-proteasome activity and protein degradation. In experiment 4b, we monitored NF-κB-dependent transcriptional activity in myotubes by transfection with a NF-κB-luciferase reporter plasmid. In experiment 4c, we isolated mRNA and performed real-time RT-PCR for iNOS expression.

Experimental 5 Design – Aim 3 – Hypothesis 3B (Figure 3-6). Primary cultured myotubes from wild-type (WT) or iNOS$^{(-/-)}$ mice were subjected to a high magnitude stretch (as determined from experiment 4) for 1, 2, and 3 h. One group then remained inactive for 2 h following the stretch protocol (2hCES). Measures for experiments 5a were identical to those in 4a.

General Methods

Myogenic Culture

Myoblasts derived from C_2C_{12} cells (ATCC, Manassas, VA) were cultured on 100 mm dishes in Dulbecoo's Modified Eagle's Medium (DMEM) (Mediatech, Herndon, VA) supplemented with 10% fetal bovine serum (FBS), 1% penicillin/streptomycin, and 0.1% funzigone at 37˚C in the presence of 5% CO2 until 50-60% confluence was reached as visualized by light microscopy. The cultures were then be trypsinized and replated at equal density to 6-

well Flexcell plates for mechanical stimulation as described below. Once the Flexcell plate cultures reach 60-80% confluency, myotube differentiation was initiated by switching to DMEM supplemented with 2% horse serum, 1% penicillin/streptomycin, and 0.1% fungizone.

Primary Culture

Muscles from both hindlimbs from 3 mice ($nNOS^{(-/-)}$, $iNOS^{(-/-)}$ or their respective wild-types) were pooled and satellite cells were isolated according to Pavlath *et al*. (136). Myogenic cells were purified by preplating and seeded in 100 mm dishes cultured in Ham's F-10 with 20% FBS, 5 ng/mL basic FGF, 1% penicillin/streptomycin, and 0.1% fungizone. Once cells reached 80% confluence, they were trypsinized and replated to Flexcell plates under the same conditions as described above.

Mechanical Stimulation Using Cyclic Strain

Myoblasts were plated on type I collagen-coated flexible-bottom plates (Bioflex plates, Flexcell International, McKeesport, PA) and incubated at 37˚C in an incubator maintained at 5% CO_2 until 90% myotube population was visualized. Immediately prior to the initiation of stretch, the medium was aspirated and changed to differentiation medium supplemented with or without 5 mM L-NAME. The cells were subjected to cyclic strain at 1-0.1 Hz (1 s of 4-18% stretch alternating with 1-10 s of relaxation) for 1-4 h using a computer-controlled vacuum stretch apparatus (FX-4000T Tension Plus System, FlexCell International) with a vacuum pressure that is sufficient to generate to predetermined percentage of mechanical strain. Replicate control samples and cells undergoing cessation of stretch were maintained under static conditions with no applied cyclic strain.

The Flexcell system used for our stretch apparatus employed equibiaxial deformations to the membranes on the bottom of each culture plate. Equibiaxial stretch is the preferred model of *in vitro* deformation because a myotube adhered in any direction is subject the same shape

change. Although the Flexcell Bioflex software uses percentile stretch to calibrate the vacuum necessary to deform the elastic membrane, each cell is not exposed to the same percent of stretch. The percent stretch would depend on the orientation and length of the myotube. Larger myotubes would be stretched a smaller percent than those of a lesser size. Specifically, the 12% stretch used in aims one and two corresponded to a 4.2 mm stretch equal in all directions, and the 18% stretch used in aim three referred to 6.3 mm deformation. While the orientation of the myotube on the membrane would still affect the direction of deformation, the myotubes had a tendency to align in the same plane with maturation and exposure to stretch as observed previously (39). In addition, the myotubes adhered to the section of the membrane that was forced over the loading post during stretch experienced greater stress and often detached from the plate in comparison to myotubes at the center of the well. Thus, these peripheral myotubes were excluded from all images and immunostaining.

Immunohistochemistry

Myotubes were fixed in 2% paraformaldehyde for 10 min, washed twice with PBS, and membranes were permeabilized for 15 min with 0.2% Triton-X. Myotubes were blocked in 5% goat serum for 30 min, followed by incubation in primary antibody diluted in 0.5% BSA for dystrophin (Lab Vision Corporation), MHC type IIa (1:50; N2.261 Developmental Studies Hybridoma Bank) , nNOS (1:133; BD Transduction Labs), eNOS (1:133; BD Transduction Labs), or iNOS (1:133; BD Transduction Labs) for 1 h. Myotubes were then incubated in secondary antibody diluted in 5% Pierce Super Blocker (Pierce Biotechnology) for Rhodamine (1:40, Invitrogen) or Alexa 488 IgG (1:133, Invitrogen) for 1 hour and stained with DAPI-containing mounting media (Vector Laboratories). All cultures were viewed on a Zeiss microscope with rhodamine, FITC, and DAPI filters.

Image Analysis

Three digital images per culture were captured using a Zeiss microscope. The images were analyzed for myotube length, diameter and area using ImageJ imaging software (NIH).

Nuclear and Cytosolic Fractionation

Cells were harvested in cytosolic extraction reagent (CERI; Pierce Biotechnology) containing 0.05% vol/vol protease inhibitors and 0.5% vol/vol phosphatase inhibitors from Sigma and centrifuged, and the resulting pellets was treated with NE-PER nuclear and cytosolic extraction reagents according to the manufacturer's procedures (Pierce Biotechnology, Rockford, IL). The nuclear fraction was confirmed by western blot for histone H2B (Upstate; Lake Placid, NY) and cytosolic fraction for β-actin (Abcam; Cambridge, MA).

Whole Cell Lysate

Cells were harvested in ice-cold non-denaturing lysis (NDL) buffer containing 30mM Tris-HCL (pH 7.5), 0.7% Triton-X, 150 mM NaCl, 3.5 mM EDTA, 10 mg/ml NaN_3, 1 μM Na_3VO_4, 0.05% vol/vol protease inhibitors and 0.5% vol/vol phosphatase inhibitors (Sigma, St. Louis). Lysates were then centrifuged at 4°C for 10 minutes at 1000 x g.

Western Blot Analysis

Protein concentrations were measured using the D_C Protein Assay Kit (Bio-Rad Laboratories, Richmond, CA). Aliquots of whole cell lysate or nuclear and cytosolic samples were ran on SDS-PAGE gels and proteins were transferred to nitrocellulose membranes and blocked with Odyssey blocking buffer for 1 h. The membranes were incubated at 4°C overnight in primary antibody diluted with Odyssey blocking buffer (LI-COR Biosciences, Lincoln, NE), TBS, and 0.01% Tween-20 for phospho-GSK-3β (Santa Cruz; Santa Cruz, CA), total GSK (Santa Cruz; Santa Cruz, CA), phospho-AKT (Santa Cruz; Santa Cruz, CA), total AKT (Santa Cruz; Santa Cruz, CA), p65 (Abcam; Cambridge, MA), p50 (Abcam; Cambridge, MA), IκB-

α (Santa Cruz; Santa Cruz, CA), Bcl-3 (Santa Cruz; Santa Cruz, CA), β-actin (Abcam; Cambridge, MA), and histone H2B (Upstate; Lake Placid, NY). Membranes were washed with TBS-T three times and incubated for 35 min in secondary antibody, Odyssey blocking buffer, and TBS-T. The secondary antibodies were IR Dye conjugated secondaries obtained from LICOR detectable at wavelengths of 680 or 800 nm. Membranes were washed three times with TBS-T and once with TBS before being scanned and detected using the Odyssey infrared imaging system (LI-COR).

Isolation of RNA and Real-Time RT PCR

Myotubes were washed in ice-cold PBS and harvested in TRizol® (Invitrogen; Carlsbad, CA) for RNA isolation. Quantification of mRNAs were performed with specific primer and probes using TaqMan® technology designed by Applied Biosystems for quantitative real-time PCR. Briefly, concentration and purity of the extracted RNA were measured spectrophotometrically at 260 and 280 nm absorbance in 1X Tris-EDTA buffer (Promega, Madison, WI). RT was performed using the SuperScript III First-Strand Synthesis System for RT-PCR according to the manufacturer's instructions (Life Technologies, Carlsbad, CA). Reactions were carried out using 1–5 μg of total RNA and 2.5 M oligo(dT)20 primers. First-strand cDNA was treated with two units of RNase H and stored at −80°C. Primers and probes were obtained from Applied Biosystems: iNOS (GenBank NM_010927.3, assay Mm0040485_m1); GAPDH (GenBank NM_008084.2, assay Mm99999915_g1). Primer and probe sequences from this service are proprietary and therefore are not reported. Quantitative real-time PCR for the target genes were performed in the ABI Prism 7700 Sequence Detection System (ABI, Foster City, CA), using the $2^{-\Delta\Delta}$CT method, where CT is threshold cycle, and glyceraldehyde-3-phosphate dehydrogenase (GAPDH) as the control gene.

Nuclear Factor of κB-Dependent Transcriptional Activity

NF-κB activity was assessed using a transient transfection of a reporter plasmid. Myoblasts were transfected with either a reporter plasmid containing the firefly luciferase gene driven by a promoter sequence containing five repeats of a consensus NF-κB binding site or a negative control plasmid (pNF-κB-luc or pCIS-CK, Stratagene; 2 μg/well). Cells were cotransfected with a second plasmid (pRL-CMV, 0.04 μg/well; Promega, Madison, WI) to control for transfection efficiency. Plasmids were complexed with Lipofectamine reagent (Invitrogen) and exposed to myoblasts in Opti-MEM for 6 h. After transfection, cells were placed in 6% HoS in Opti-MEM for 18 h before being switched to differentiation media (DMEM supplemented with 2% HoS and 1% penicillin-streptomycin). Differentiation medium was refreshed every 48 h until confluent myotubes were formed (5 days).

Dual Luciferase Assay

Immediately following treatment, myotube cultures were washed with ice-cold PBS and lysed by addition of 500 μl passive lysis buffer (Promega). Plates were rocked at room temperature for 15 min. The lysate was then transferred to microcentrifuge tubes and centrifuged for 30 s at 400 x g to sediment cellular debris. Firefly luciferase (originating from transcriptional activity of the pNF-κB-luc or pCIS-CK vectors) and renilla luciferase activities were measured sequentially in the same 10 μl volume of cell lysate using the dual luciferase assay kit (Promega) according to the manufacturer's instructions and a luminometer (model FB12, Berthold) set to measure average light intensity in relative light units (RLU) over a 10-s measurement period. NF-κB-dependent transcriptional activity for each sample was taken as the raw firefly luciferase activity (RLU) divided by the renilla luciferase activity (RLU). For each experiment, all values are expressed relative to the average of the control group.

Nitric Oxide Production

Intracellular NO was monitored with DAF-FM diacetate (Invitrogen, Carlsbad,CA), a pH-insensitive fluorescent dye that emits increased fluorescence after reaction with an active intermediate of NO formed during the spontaneous oxidation of NO to NO_2. Myotubes were incubated at 37°C for 30 min in phenol red-free, serum-free DMEM containing 10 μM of DAF-FM diacetate. After loading is completed, cells were rinsed three times with phenol red-free, serum-free DMEM and subjected to 1 h of mechanical strain. Cells were harvested in deionized water, centrifuged at 12,000 x g and aliquots of 100 μl were quantified on a microplate fluorometer (Molecular Devices) using excitation and emission wavelengths of 488 and 520 nm, respectively. NO production in the medium was assessed with the Nitrate/Nitrite Fluorometric Assay Kit from Cayman Chemical (Ann Arbor, MI). This assay measures the sum of nitrate and nitrite, the final products of nitric oxide metabolism, in a two-step process. First, nitrate is converted to nitrite using nitrate reductase. This is followed by reaction of nitrite with 2,3-diaminoaphthalene to produce the fluorescent compound, 1(H)-naphthotriazole, which is quantified on a microplate fluorometer (Molecular Devices) using excitation and emission wavelengths of 360 and 430 nm, respectively.

Statistical Analysis

Group sample size was determined with power analysis of our preliminary data. Comparisons between groups were made by a 3-way full factorial ANOVA, and when appropriate, Tukey's HSD test was performed post-hoc. Significance was established at $p<0.05$.

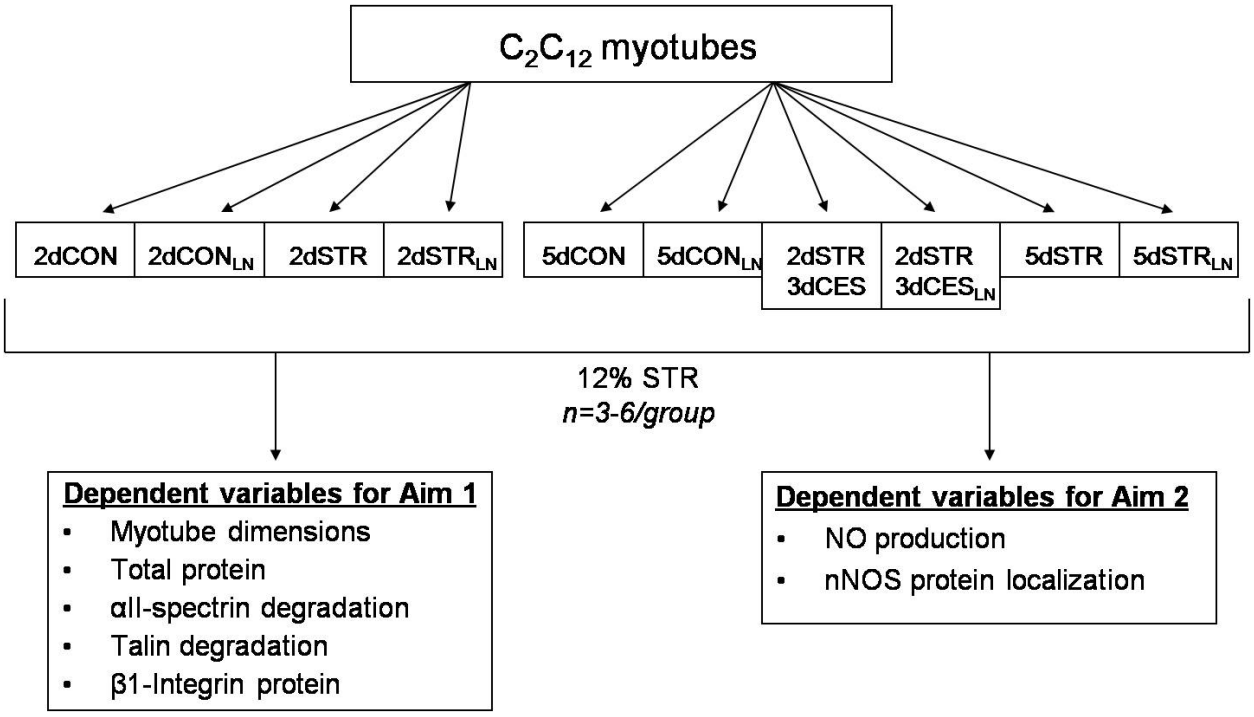

Figure 3-1. Experiment 1 design for Aims 1 and 2. Purpose was to develop an *in vitro* model of disuse skeletal muscle atrophy with cyclic stretch and test whether NOS inhibition prevented the progression of atrophy.

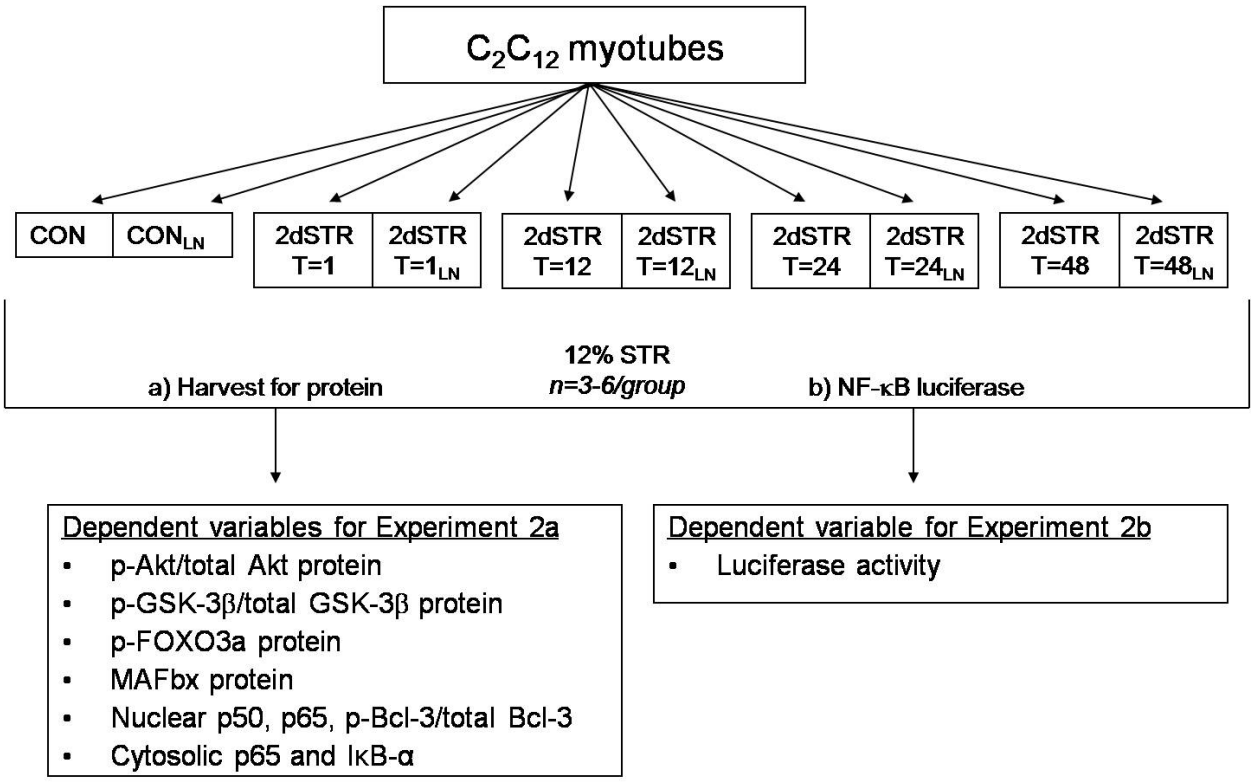

Figure 3-2. Experiment 2a and 2b designs for Aim 2. Purpose was to monitor the activity of members of the Akt and NF-κB pathways during cessation of stretch and test whether NOS inhibition prevented their activity.

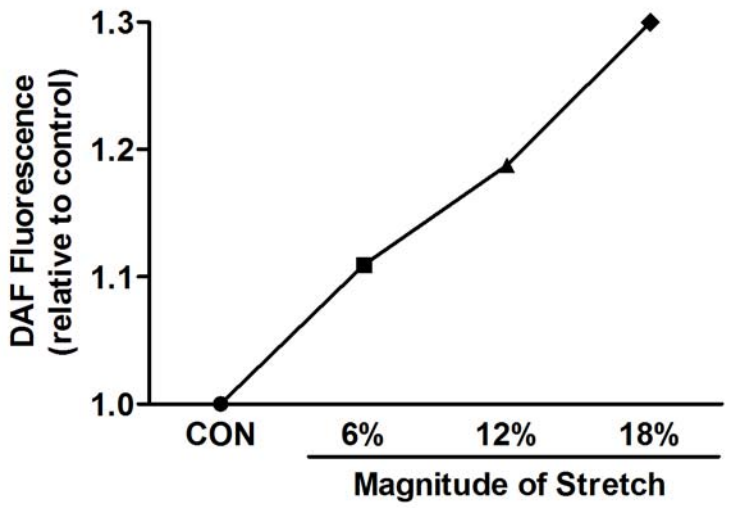

Figure 3-3. Average 4-amino-5-methylamino-2',7'-difluorofluorescein (DAF-FM) diacetate fluorescence in C_2C_{12} myotubes after 1 h of cyclic stretch at various magnitudes.

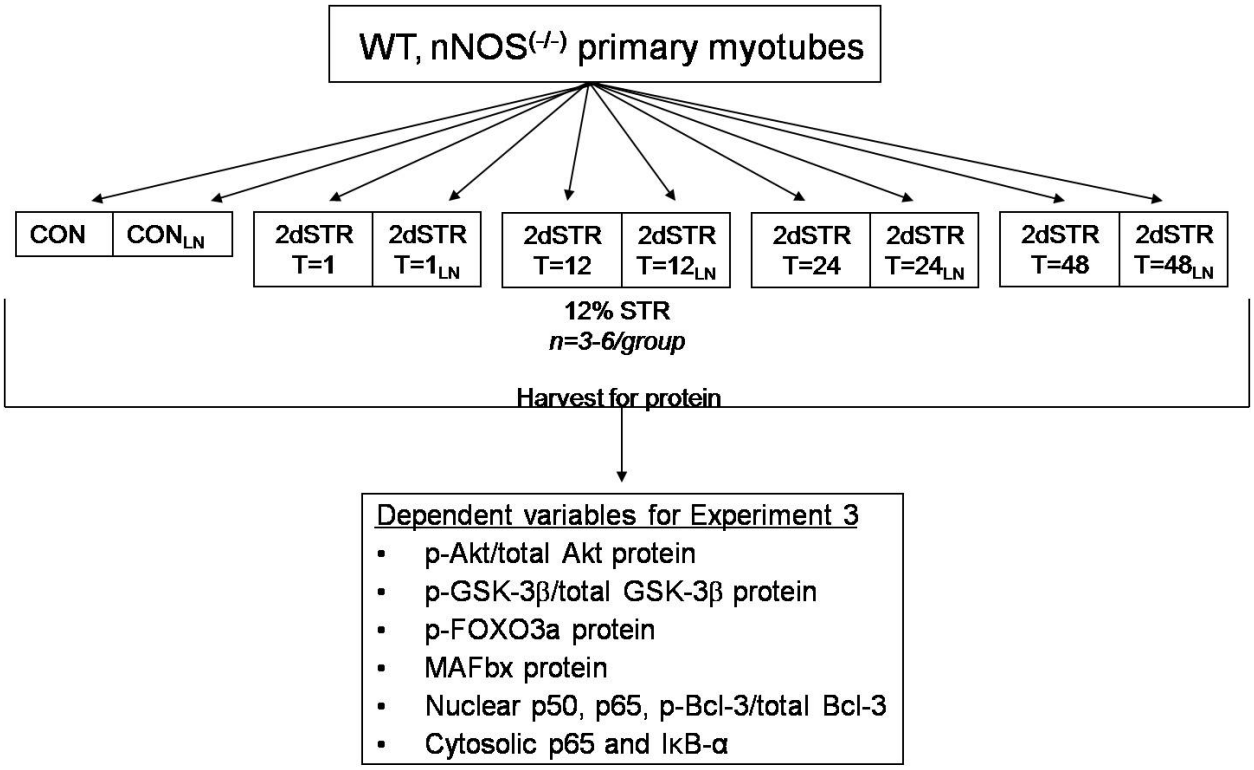

Figure 3-4. Experiment 3 design for Aim 2. Purpose was to monitor the activity of members of the Akt and NF-κB pathways during inactivity using genetic and pharmacological inhibition of nNOS in primary cultured myotubes.

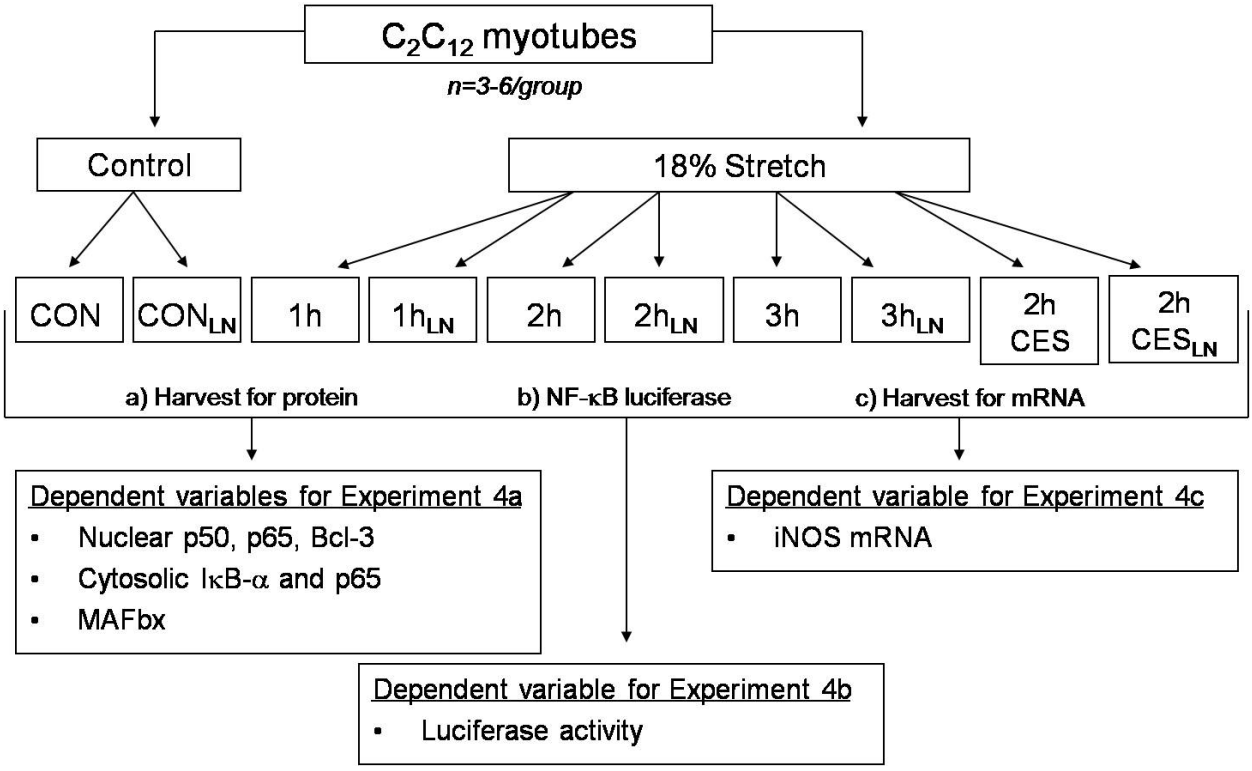

Figure 3-5. Experiment 4 design for Aim 3. Purpose was to monitor activity of the classical NF-κB pathway during high magnitudes of stretch and test whether NOS inhibition altered its activity.

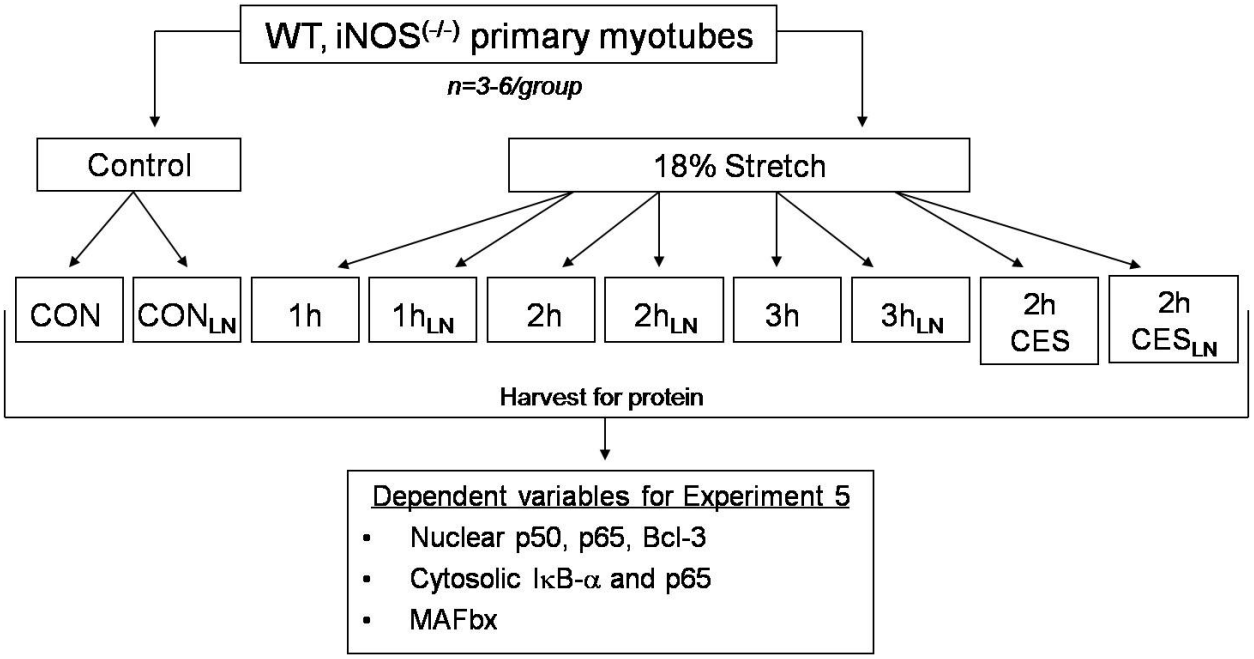

Figure 3-6. Experiment 5 design for Aim 3. Purpose was to monitor activity of the classical NF-κB pathway during high magnitudes of stretch using genetic and pharmacological inhibition of iNOS in primary cultured myotubes.

CHAPTER 4
RESULTS

Skeletal Muscle Myotube Atrophy Model

The purpose of Specifc aim 1 is to develop models of atrophy *in vitro* using skeletal muscle myotubes. The hypothesis that cessation of a daily cyclic stretch will cause myotube atrophy is based on the concept that daily repetitive stretching of the muscle membrane induces protein synthesis (81), muscle metabolism (86, 155, 178), NO production (178, 212), and muscle integrity (213) via mechanotransduction pathways. Withdrawal of the stretching stimulus is sufficient to cause significant remodeling, protein degradation, and myotube atrophy. Our protocol used the Flexcell TensionPlus© system by which skeletal muscle myotubes are plated on flexible bottom plates and submitted to a vacuum generated stretch for 1 h/d for 2 d at a 12% strain (0.7 Hz). The 2 d of a cyclic stretch is a mimic of skeletal muscle activity. Following the 2 d of repetitive stretch, the myotubes were removed from the Flexcell baseplate and remain inactive (i.e. no stretch) for three subsequent days. Three days of inactivity is sufficient to cause visual myotube atrophy (Figure 4-1 and Figure 4-2) and cytoskeletal protein degradation (Figure 4-3 and Figure 4-4). In order to compare treatments, cells were divided into five groups. Two groups were non-stretched controls at the 2 d and 5 d timepoints to control for myotube maturation (2dCON and 5dCON, respectively). One group was stretched for 2 days only with no inactivity period (2dSTR). One group was stretched for the entire 5 day period (5dSTR). The final group encountered 2 d of cyclic stretch and 3 d of inactivity (2dSTR3dCES).

An elevation in NO production due to dissociation of nNOS from the dystrophin-glycoprotein complex has been implicated as a cause for skeletal muscle atrophy during disuse (169). To study the effect of NOS activity in our *in vitro* model, L-NAME was administered in the culture medium to subgroups of myotubes at each timepoint.

Myotube Atrophy

Two days of 12% cyclic stretch for one hour per day did not alter average length, diameter, and area in C_2C_{12} myotubes (Figure 4-2). Importantly, cessation of the stretch for three sequential days thereafter caused a significant reduction in myotube diameter and area in comparison to all control and stretched groups, representing skeletal muscle myotube atrophy. Cells undergoing five days of consecutive stretch experienced a significant increase in diameter and area. However, treatment with the NOS inhibitor L-NAME in all groups led to diameter and area measurements similar to those of atrophied myotubes, which were significantly lower than non-treated cells.

Protein Degradation

Skeletal muscle atrophy is predominately due to increased proteolysis leading to a loss of mass. With our *in vitro* model of atrophy, muscle protein degradation increased in cells undergoing a three-day cessation of activity (Figure 4-3 and Figure 4-4). AlphaII-spectrin is a cytoskeletal protein that is susceptible to proteolysis by calpain (generating a 150/145 kDa product) and caspase-3 (generating a 120 kDa product) (171). Western blotting for these cleavage products demonstrated that following three days of withdrawal of mechanical activity *in vitro*, there was significant activation of calpain (Figure 4-3A-B). Caspase-3 may also be active and participate in αII-spectrin degradation during the atrophy protocol employed in our study although the elevation of the 120 kDa cleavage product did not reach statistical significance (Figure 4-3C).

Another cytoskeletal protein, talin, interacts with the DGC and focal adhesion proteins, such as integrin and vinculin (53, 193), to generate a transmembrane connection involved in mechanotransduction of skeletal muscle. Calpain is known to cleave the intact 235-kDa talin into 190- and 47-kDa fragments (13), thus calpain-induced protein degradation was also measured as

the ratio of concentrations of the 190- and the 235-kDa bands by western blot (Figure 4-4). Myotubes withdrawn from stretch for three days showed significantly greater talin proteolytic ratio than all untreated control and stretched cells. Inhibition of NOS also increased talin cleavage in 2 d cultures which is in agreement with other studies that NO can prevent calpain-mediated talin proteolysis and cytoskeletal breakdown in C_2C_{12} muscle cells (99).

The integrins, specifically the β1-integrin subunit found in skeletal muscle, provide strength to the linkage between the cytoskeleton and extracellular matrix and may enable muscle to sense changes in the mechanical environment (14). Further, a decrement in β1-integrin expression is linked to reduced NO production (213). Thus we measured β1-integrin in stretched and atrophied myotubes in our model. Five days of 12% cyclic stretch induced a dramatic and significant increase in β1-integrin protein, whereas two days of stretch was not sufficient to cause any change (Figure 4-5). Beta1-integrin levels in myotubes atrophied for 3 d did not differ from 5dCON but were significantly lower than 5dSTR cells. Treatment of myotubes with the NOS inhibitor L-NAME showed a trend toward reduced β1-integrin expression in stretched myotubes, but this effect did not reach statistical significance.

Although our data provides evidence for an increase in proteolysis with cessation of stretch, there was no decrement in protein content in myotubes after withdrawal from activity (Figure 4-6) and no change in protein concentrations with stretch. Treatment of myotubes with L-NAME only significantly reduced protein content in the 2dSTR3dCES+LN group. This result is surprising considering that, collectively, our data indicates that two days of stretch followed by three days of inactivity is sufficient to induce cytoskeletal protein degradation and visual atrophy of C_2C_{12} myotubes.

Cellular Signaling during Disuse

The purpose of Specifc aim 2 was to test if cessation of repetitive daily activity of skeletal muscle myotubes causes elevation of NO production (>20%) and activation of skeletal muscle disuse atrophy signaling pathways. Specifc aim 2 had three hypotheses. First, we hypothesized that 12% cyclic stretch in C_2C_{12} myotubes would maintain nNOS localization, low levels of NO, and opposes skeletal muscle atrophy. Secondly, cessation of stretch would cause dissociation of nNOS from the sarcolemma, elevated NO production and initiation of skeletal muscle disuse atrophy signaling. Lastly, our final hypothesis was that NOS inhibition with L-NAME in C_2C_{12} or genetic knockout of nNOS in primary myotubes would prevent the upregulation of atrophy signaling pathways following cessation of cyclic stretch.

To test Specifc aim 2, myotubes were differentiated for 4-5 d before enduring 2 d of 12% cyclic strain for 1 h/d at 0.7 Hz. To determine the time course for upregulation of atrophying signaling pathways, samples were taken immediately after the second bout of stretch (Stretched) and at timed intervals of 12, 24, and 48 h during cessation of stretch. The non-specific NOS inhibitor L-NAME was administered to subcultures of each group throughout the entire protocol.

Measurements in C_2C_{12} Cell Culture during Disuse

Myosin heavy chain and dystrophin

The resemblance of C_2C_{12} myotubes to adult skeletal muscle is unclear. Thus we sought to determine if C_2C_{12} myotubes contain the cytoskeletal and contractile proteins, dystrophin and myosin heavy chain as well as all isoforms of the NOS enzyme. After 6 d of differentiation, immunohistochemistry revealed that C_2C_{12} myotubes do express type IIa myosin heavy chain (Figure 4-7A). This is in agreement with other studies in C_2C_{12}s demonstrating that myotubes begin expressing all isoforms of MHC after 3 d of differentiation (40). We did not perform immunostaining on primary cultured myotubes, but they are also capable of expressing all MHC

isoforms. Primary myotubes from rat immunostain for embryonic, neonatal, and type II MHC after 7 d of culture whereas slow isoforms were detected at 12-13 d after plating (182).

Dystrophin staining is also evident throughout the C_2C_{12} myotubes (Figure 4-7A). Dystrophin and the glycoprotein complex with which it is associated play a fundamental role in mechanotransduction during stretch and provide structural integrity for the cell. Thus the presence of dystropin in normally differentiated C_2C_{12} myotubes was critical for testing our hypotheses of myotube adaptation to cyclic strain and inactivity. Negative controls for each secondary antibody (with no primary antibody) reveal no visible background fluorescence (Figure 4-7B).

Nitric oxide synthase isoforms

The presence and localization of the nitric oxide synthases in C_2C_{12}s were also unknown. Immunostaining for nNOS, iNOS, and eNOS after 6 d of differentiation revealed that all three isoforms exist *in vitro* (Figure 4-8). Both nNOS and iNOS appear to be localized in clusters near the cell membrane whereas eNOS is expressed more diffusely throughout the cytosplasm.

Localization of nNOS

In normal adult skeletal muscle, nNOS is localized at the sarcolemma associated with the dystrophin-glycoprotein complex. Evidence indicates that nNOS is dislocated from the sarcolemma during hindlimb unloading and contributes to skeletal muscle atrophy (169). Immunostaining for nNOS in C_2C_{12} myotubes shows nNOS localized in clusters at the cell membrane in all control and stretched groups (Figure 4-9). However, cessation of activity for 3 d causes nNOS localization to become more diffuse throughout the myotube potentially indicating its dissociation from the sarcolemma and migration to the cytoplasm. Treatment of myotubes with L-NAME does not appear to alter nNOS localization during the first 2 d of treatment;

however, after 5 d, nNOS appears to lose its clustering effect and becomes more diffuse throughout the cell (5dLN, 5dSTR+LN, 2dSTR3dCES+LN).

Nitric oxide production

The final products of nitric oxide *in vivo* are nitrate (NO_3^-) and nitrite (NO_2^-) (125). The relative proportion of these products is variable and cannot be predicted with certainty. Thus, the best index of total NO production is the sum of both nitrate and nitrite. To test for changes in nitric oxide concentrations in stretched and atrophied myotubes, we measured total nitrate plus nitrate content in the culture medium. Although nitrate concentrations did not reach statistical significance, there was a trend for an increase in NO levels with stretch (Figure 4-10). NOS inhibition by addition of L-NAME to the culture medium was successful in attenuating the stretch-induced NO production, but did not alter basal levels. NO release in the 2dSTR3dCES group was not significantly different than that of the 5dSTR cells but showed trends to be higher than 5dCON cells and comparable to cells stretched for 2 d. This suggests that NO production remains elevated during cessation of activity for up to 72 h and may contribute to the signaling events occurring during inactivity. Myotubes stretched for 5 d had higher NOS activity than the remaining groups demonstrating that an increase in NO production with stretch is maintained with continued activity but can be blunted with L-NAME administration.

Components of the Akt pathway

The Akt (or protein kinase B) pathway is known to regulate muscle protein synthesis and has recently been implicated as a master controller of skeletal muscle size by also playing a role in skeletal muscle atrophy (111, 154). We sought to determine if the activity of Akt and its downstream targets were altered with 2 d of cyclic stretch followed by 3 d of inactivity.

Akt protein expression. Akt activity, as indicated by its phosphorylation status, was increased 5-fold following the second bout of cyclic stretch (Figure 4-11). This elevation was

transient as it returned to baseline after 48 h. Notably, NOS inhibition significantly blunted activation of Akt at all time points indicating that phosphorylation of Akt in C_2C_{12} myotubes is NOS-dependent.

GSK-3β protein expression. GSK-3β is activated by its dephosphorylation and translocation to the nucleus where is known to trigger numerous transcription factors. Many of its targets are thought to promote transcription of atrophy-related genes (214); thus, we sought to determine if GSK-3β activity was altered in our stretch model. Two days of 12% cyclic stretch was successful in inhibiting GSK-3β activity (Figure 4-12). However, the ratio of phosphorylated to total GSK-3β decreased over time with cessation of stretch. Interestingly, L-NAME administration to the media completely prevented phosphorylation of GSK-3β until 48 h post-stretch, suggesting that NO is an important signaling molecule for GSK inhibition *in vitro*.

Phosphorylated FOXO3a protein expression. The FOXO family of transcription factors is involved in the transcription of many genes regulating ubiquitin-proteasome pathway. FOXO3a is thought to specifically induce gene expression of the muscle specific E3 ligases, MAFbx and MuRF1 which are essential for muscle protein degradation (154). FOXO3a is phosphorylated and inactivated by Akt, and upon dephosphorylation can translocate to the nucleus to bind to DNA. Next, we sought to determine if FOXO3a was activated in our atrophy protocol. Immediately after stretch, phosphorylated FOXO3a was significantly elevated (Figure 4-13) and tapered off as time elapsed. Nitric oxide synthase inhibition completely abrogated the increase in FOXO3a phosphorylation, again demonstrating the importance of NO in this signaling pathway.

MAFbx protein expression. Protein degradation by the 26S proteasome is dependent on ubiquitination by E3 ligases. MAFbx is a muscle-specific E3 ligase that has been deemed

essential for skeletal muscle atrophy through activation of the FOXO transcription factors (154). In an attempt to correlate Akt and FOXO3a activity with MAFbx expression, we measured MAFbx protein levels using our atrophy model in C_2C_{12}s. Immediately after stretch, levels of MAFbx protein were not altered but tended to continually increase through 48 h of inactivity, which does mimic the decrease in Akt activity and FOXO3a phosphorylation although this trend was not statistically significant (Figure 4-14). Treatment of the myotubes with L-NAME did not affect MAFbx upregulation in comparison to untreated controls.

Altogether, the anabolic effects of the Akt pathway are upregulated after 2 d of moderate magnitude cyclic stretch. Cessation of activity for up to 48 h is sufficient to upregulate atrophic signals through activation of GSK-3β, FOXO3a, and MAFbx.

Alternative NF-κB pathway

Various subunits of NF-κB have been implicated in atrophy models to be essential for skeletal muscle loss. The primary NF-κB proteins operating during inflammation and oxidative stress models are p65 and p50 (59, 202); however, with disuse, genetic knockout of p65 was not effective in attenuating atrophy, whereas mice null for the p50 or Bcl-3 gene suffered minimal muscle loss during hindlimb unloading (83). Thus we measured all of these subunits to distinguish those involved in our *in vitro* model of disuse atrophy.

Nuclear p50. The NF-κB member p50 undergoes nuclear translocation following partial processing of its cytoplasmic precursor molecule, p105, and after forming a homodimer, can bind to DNA. We found that following two bouts of 12% cyclic stretch, nuclear p50 protein levels were significantly and transiently elevated but returned to baseline after 12 h cessation of stretch (Figure 4-15). NOS inhibition did not affect p50 translocation until after 48 h where it caused a significant augmentation of nuclear p50.

Bcl-3. Generally, homodimers of NF-κB p50, which lack transactivation domains, function as transcriptional repressors. However, upon binding with B cell lymphoma 3 (Bcl-3), these complexes can activate transcription through the Bcl-3 transactivation domain (22, 57, 133). Bcl-3 activity largely depends on is phosphorylation status (25, 129), and phosphorylation of, the $p50_2$/Bcl-3 complex can occur via GSK-3β (190). Thus we tested how Bcl-3 phosphorylation and protein expression were affected by cyclic stretch and NOS inhibition. The ratio of phosphorylated to total Bcl-3 was not affected with mechanical stimulation or cessation of stretch (Figure 4-16A). However, L-NAME treatment significantly increased Bcl-3 phosporylation. This correlates with GSK-3β activity data in L-NAME-treated myotubes (Figure 4-12), suggesting that NO may inhibit GSK-3β and thereby attenuate phosphorylation of Bcl-3.

Levels of total Bcl-3 protein were significantly greater after stretch and throughout 24 h of inactivity but returned to baseline after 48 h (Figure 4-16B). Inhibition of NOS increased Bcl-3 expression following 24 h cessation of stretch but did not affect protein levels at any of the other time points measured.

Nuclear and cytosolic p65. In agreement with the literature (84), p65 levels were not altered with moderate stretch or disuse atrophy as indicated by nuclear and cytosolic p65 measurements (Figure 4-17A-C). Interestingly, translocation of p65 to the nucleus was significantly elevated by NOS blockade immediately and up to 24 h after stretch.

Cytosolic IkB-α. The NF-kβ subunit p65 maintains its cytosolic residence through its binding to IκB-α. Upon phosphorylation by IκB kinase (IKK), IκB is ubiquitinated and degraded by the proteasome which frees p65 to translocate to the nucleus. Western blotting for IκB-α demonstrates that NOS inhibition caused a reduction in cytosolic IκB-α immediately following and 12 h post-stretch (Figure 4-18). IκB-α levels returned to control levels after 24 h. This trend

correlates with the appearance of p65 in the nuclear fraction of C_2C_{12} myotubes after stretch (Figure 4-17A). Further, stretched but untreated cells experienced an increase in IκB-α at all time points. Our data suggests that nitric oxide may be protective against IκB-α phosphorylation/degradation and p65 release after moderate magnitudes of stretch, which may occur through regulation of an upstream kinase.

Nuclear factor of κ-B transcriptional activity during disuse

Nuclear translocation and binding of NF-κB subunits to κB sites on DNA does not always correspond to increased gene transcription since both p50 and p52 homodimers can act as transcriptional repressors due to lack of a transactivation domain. In order to determine if moderate cyclical strain and withdrawal of stretch results in NF-κB-dependent transcriptional activity, C_2C_{12} myotubes were transfected with either a reporter plasmid containing the firefly luciferase gene driven by a promoter sequence containing consensus NF-κB binding sites (pNF-κB-luc) or a negative control plasmid (pCIS-CK). No significant differences were detected with any treatment most likely due to our small sample size (Figure 4-19). However, there was a trend for an increase in NF-κB activity with stretch that declined back to baseline over time. Conversely, L-NAME treatment attenuated this rise immediately after 12% stretch, but induced an upward tendency in NF-κB-dependent transcription as time progressed.

The trends demonstrated by NF-κB transcriptional activity follow the pattern of p50 translocation to the nucleus (Figure 4-15), which suggests that p50 is most likely involved in gene regulation using our model of atrophy. However, whether or not p65 and/or Bcl-3 are involved in this model remains to be determined.

Myotubes transfected with the negative control vector, pCIS-CK, which contains the luciferase gene but lacks the NF-kB-responsive promoter sequence, did not respond to any of the treatments in any of our transfection experiments (Figures 4-19 and 4-25).

Neuronal NOS Knockout Primary Satellite Cell Culture

To elucidate which NOS isoform is involved in the stretch-induced changes of Akt and NF-κB signaling, we proposed to isolate satellite cells from mice null for the nNOS gene. However, our technique proved unsuccessful in maintaining these satellite cells in culture. From observation only, fewer myogenic cells were present after isolation, and these cells did not demonstrate the proliferative qualities seen in other primary cultured myoblasts. Therefore, we were unable to collect data for the final hypothesis in Specifc aim 2, and we cannot determine if nNOS is the key isoform responsible for atrophy signaling *in vitro*. Although iNOS is expressed in low levels in skeletal muscle myotubes, it is unlikely that iNOS is active at such low strain. From our results, we remain speculative that nNOS is responsible for the adaptations seen in Akt activation and NF-κB signaling during our *in vitro* model of disuse atrophy.

Cellular Signaling during High Strain

Specific aim 3 tested if excessive load applied to skeletal muscle myotubes causes production of high amounts of NO via iNOS and activation of proteolysis. Skeletal muscle injury leads to inflammation and upregulation of iNOS (140, 147), which is associated with the classical pathway of NF-κB (IκB-α/p50/p65) (102) to induce protein degradation (11).

We examined the translocation or degradation of NF-κB family members as well as iNOS mRNA that are associated with inflammation and injury in the classical pathway of atrophy. We isolated nuclear and cytosolic fractions to probe for the nuclear localization of the NF-κB members, p50, p65, Bcl-3, and cytosolic content of IκB-α and MAFbx. MAFbx was measured as

an indirect measure ubiquitin-proteasome activity and protein degradation. Lastly, we used a reporter plasmid to measure NF-κB-dependent transcriptional activity as a function of time at high magnitude cyclic strain.

Measurements in C_2C_{12} Cell Culture during High Strain

C_2C_{12} myotubes were subjected to a high magnitude stretch (18%; 0.1 Hz) for 1, 2, or 3 h. One group remained inactive for 2 h following the stretch protocol (2hCES). These time points were chosen to test for a time course of up/downregulation of iNOS mRNA and NF-κB activity previously shown in other cell types (5). The non-specific NOS inhibitor L-NAME was also administered to subcultures of each group throughout the entire protocol.

Classical NF-κB pathway

The classical NF-κB pathway involves the nuclear transport of p65/p50 heterodimers by degradation of IκB-α triggered by its phosphorylation by IKKβ. NO production by iNOS has been shown to induce this classic pathway (5, 12). We hypothesized that high magnitudes of stretch induce large amounts of NO (via iNOS) and lead to activation of NF-κB through the classical pathway.

Nuclear p50. Western blot of C_2C_{12} myotubes subjected to high strain revealed that nuclear translocation of p50 significantly peaked after 1 h of 18% stretch (Figure 4-20), and then drifted back toward baseline with continued stretch. Treatment of myotubes with L-NAME was only effective in attenuating nuclear p50 at the 2 h time point.

Nuclear Bcl-3. In accord with the accepted cachexia model of atrophy, we were not able to detect Bcl-3 protein in the nuclear fractions of myotubes subjected to 18% stretch for 3 h. The classical pathway suggests that the p50/p65 heterodimer is sufficient to induce transcription of

atrophy related genes, and that this pathway does not involve Bcl-3. Thus, high cyclic strain appears to activate the classical pathway rather than the alternative pathway of atrophy signaling.

Nuclear and cytosolic p65. The localization of p65 tends to be primarily cytosolic as its nuclear transport sequence is blocked by its inhibitor IκB-α. Following IκB-α phosphorylation and degradation, p65 is free to translocate to the nucleus. In order to follow this progression we attempted to measure nuclear p65 and cytosolic p65 and IκB-α protein content. Cytosolic levels of p65 did not vary considerably throughout the protocol (Figure 4-21B). However, nuclear amounts of p65 significantly increased with 1 and 2 h of stretch (Figure 4-21A and C). L-NAME was overall ineffective at preventing p65 nuclear transport.

Cytosolic IκB-α. Although statistical significance was not reached, there was a trend for a reduction in cytosolic IκB-α protein content during the progression of stretch (Figure 4-22). However, administration of L-NAME to the culture medium increased the loss of IκB-α protein after 2 and 3 h of stretch suggesting that NO may actually inhibit phosphorylation and degradation of IκB-α during high strain. NOS inhibition demonstrated this same effect on IκB-α expression during moderate stretch (Figure 4-18) suggesting that NO may be protective against IκB-α phosphorylation independent of stretch magnitude and NO concentration.

MAFbx. Protein degradation by the 26S proteasome is dependent on their ubiquitination by E3 ligases. MAFbx is one such muscle-specific ligase that has been deemed essential for skeletal muscle atrophy. It is also thought to be involved in the ubiquitination of IκB-α. MAFbx protein expression increased in a time-dependent manner through 3 h of 18% cyclic strain (Figure 4-23). Two hours of inactivity was sufficient to return MAFbx levels to baseline. Most interestingly, L-NAME treatment completely abrogated the increase in MAFbx at all time points

measured indicating that the nitric oxide produced during high strain is necessary for protein degradation in C_2C_{12} myotubes.

Inducible NOS gene expression

During cachexia and injury, micromolar concentrations of NO are thought to be produced by iNOS leading to further injury and inflammation. We sought to determine if iNOS was activated in our model of inflammation/injury during high cyclic strain. C_2C_{12} myotubes were stretched for 2, 3, or 4 h with one group resting for 2 h following stretch (2hCES). L-NAME was administered in parallel at each time point. Although not significantly different, there was a trend for an increase in iNOS mRNA expression with stretch (Figure 4-24). L-NAME significantly blunted the upregulation of iNOS at every time point. This suggests that iNOS gene expression is regulated by a positive feedback loop such that inhibition of NO production can prevent transcription of the iNOS gene.

Nuclear factor of κ-B transcriptional activity during high strain

To determine if high-magnitude cyclic strain results in NF-κB-dependent transcriptional activity, C_2C_{12} myotubes were transfected with either a reporter plasmid containing the firefly luciferase gene driven by a promoter sequence containing consensus NF-κB binding sites (pNF-κB-luc) or a negative control plasmid (pCIS-CK). No significant differences were detected with any treatment most likely due to our small sample size (Figure 4-25). However, there was a trend for an increase in NF-κB activity through 2 h of high strain that declined back to baseline over time. In addition, L-NAME treatment attenuated any rise in NF-κB-dependent transcription after 1 h.

The trends demonstrated by the NF-κB reporter plasmid at 18% stretch follow the pattern of both the p65 and p50 subunit translocation to the nucleus (Figures 4-20 and 4-21), which

suggests that the p65/p50 heterodimer is most likely involved in gene regulation using our model of injury.

Inducible NOS Knockout Primary Satellite Cell Culture

To test which isoform of NOS is involved in the stretch-induced changes in the classical pathway of NF-κB signaling, we isolated satellite cells from mice null for the iNOS gene. After differentiation, the primary myotubes were stretched for 3 h followed by 2 h of cessation of stretch in accordance with the high strain protocol used for the C_2C_{12}s. Subgroups were also treated with L-NAME in an effort to distinguish the effects of iNOS from that of eNOS and nNOS. Visually, the myogenic cells isolated from the $iNOS^{-/-}$ mice showed enhanced proliferation rates in comparison to wildtype myoblasts; however, both cultures achieved full differentiation after 5 d.

After implementing the 18% cyclic stretch protocol, myotubes from the wildtype mice demonstrated very similar results for NF-κB protein expression as seen in the C_2C_{12} myotubes (Figures 4-20 through 4-22). The cytosolic proteins, p65 and IκB-α, did not change in wildtype or knockout myotubes (Figures 4-27B and 4-28); however, nuclear levels of p65 and p50 varied considerably with treatment. Wildtype myotubes exposed to stretch experienced a time-dependent increase in nuclear p50 which was attenuated with NOS inhibition (Figure 4-26). Inducible NOS knockout myotubes had a similar response to stretch although the increase in p50 was significantly reduced. Further, L-NAME completely abrogated p50 protein expression in $iNOS^{-/-}$ myotubes at all time points (Figure 4-26) Wildtype and iNOS null mice both showed a progressive increase in nuclear p65 with stretch over 2 h (Figure 4-27A and C), and once again, L-NAME completely prevented any increase of nuclear p65 in $iNOS^{-/-}$ myotubes during stretch.

We also attempted to measure MAFbx and Bcl-3 expression in both wildtype and iNOS knockout myotubes. However, neither of these proteins could be detected by western blot.

Altogether, these results demonstrate that 18% cyclic strain is sufficient to induce iNOS production of NO which activates the classical pathway of NF-κB signaling. Concomitant administration of L-NAME to $iNOS^{(-/-)}$ myotubes further inhibited the pathway suggesting that either nNOS or eNOS may also contribute to the production of nitric oxide involved in this signal.

Figure 4-1. Representative images of C_2C_{12} myotubes using the atrophy protocol. Top row indicates cells cultured for 2 d with no stretch (2dCON) and with L-NAME (2dLN). Second row shows cells exposed to 2 d of 12% cyclic strain for 1 h/d (2dSTR) in the presence of L-NAME (2dSTR+LN). Third row represents cells after 2 d of stretch and 3 subsequent days of no stretch (2dSTR3dCES) and with L-NAME in the medium (2dSTR3dCES+LN). Fourth row denotes myotubes after 5 d of no stretch (5dCON) and with L-NAME (5dLN). Bottom row indicates cells subjected to 5 d of continuous stretch (1 h/d) (5dSTR) in the presence of L-NAME (5dSTR+LN).

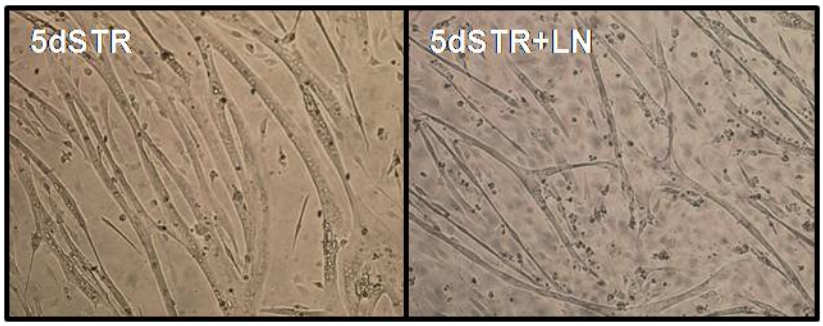

Figure 4-1 Continued.

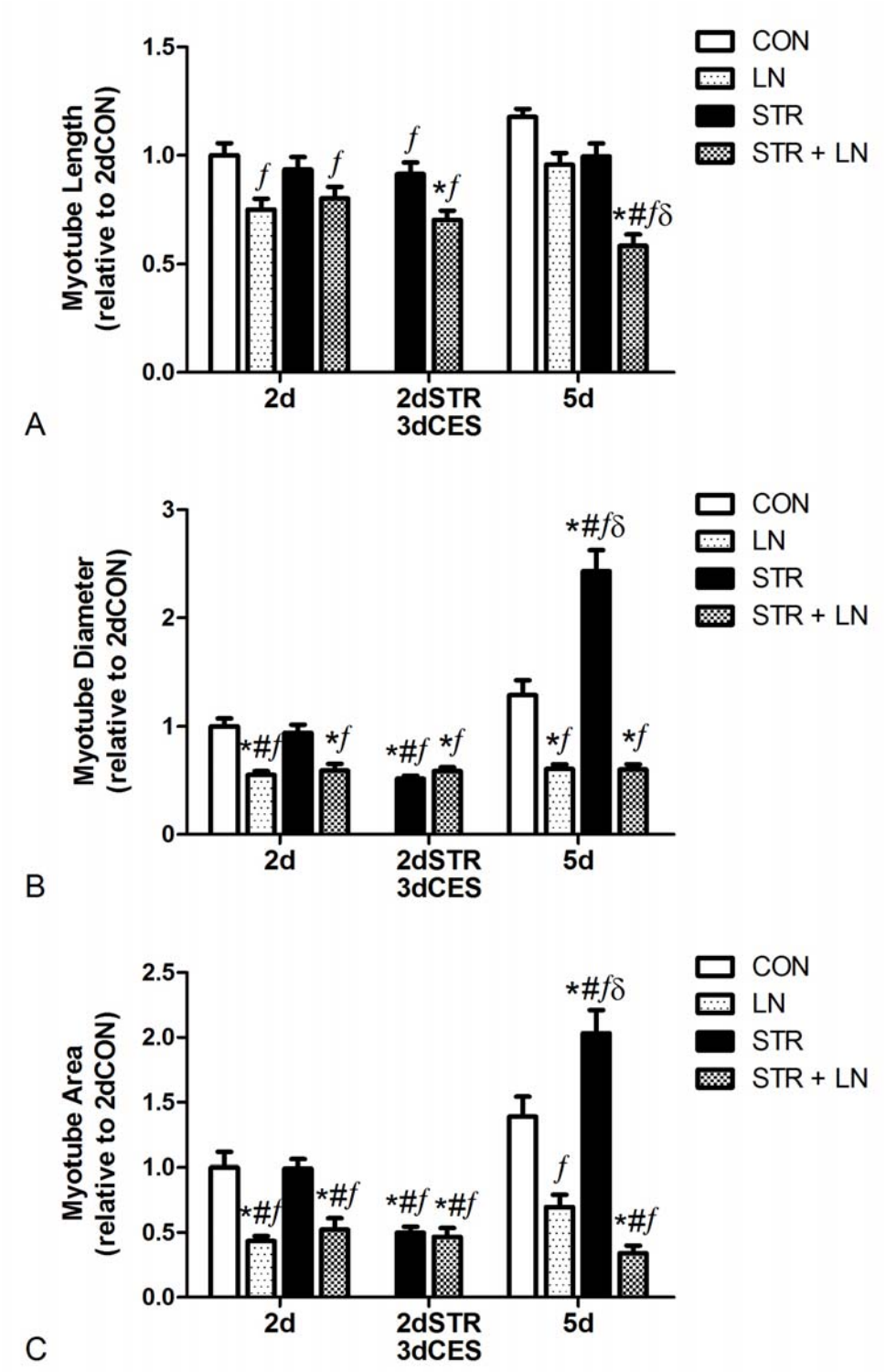

Figure 4-2. Image analysis of C_2C_{12} myotubes using the atrophy protocol. A) Average myotube length. B) Average myotube diameter. C) Average myotube area. Values represent the mean ± SEM. (n=35) *Significantly different from 2dCON. $^{\#}$ Significantly different from 2dSTR. ^{f} Significantly different from 5dCON.$^{\delta}$ Significantly different from 2dSTR3dCES. ($p<0.05$)

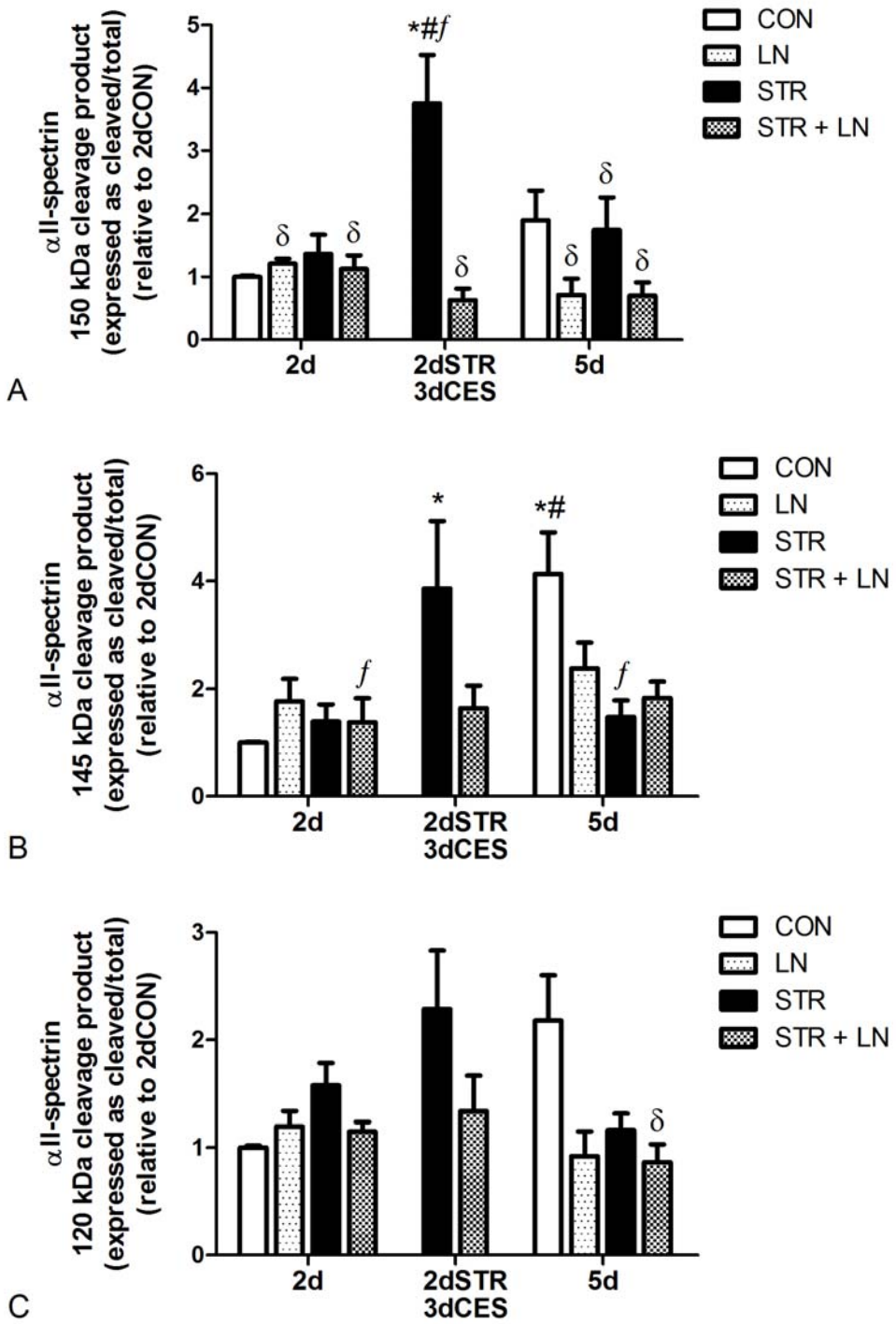

Figure 4-3. AlphaII-spectrin protein degradation of C_2C_{12} myotubes using the atrophy protocol. Graphs represent ratio of cleaved to intact αII-spectrin protein. A) Calpain-specific 150 kDa αII-spectrin cleavage product. B) Calpain-specific 145 kDa αII-spectrin cleavage product. C) Caspase-3-specific 120 kDa αII-spectrin cleavage product. Values represent the mean ± SEM. (n=5) *Significantly different from 2dCON. $^{\#}$ Significantly different from 2dSTR. ^{f} Significantly different from 5dCON.$^{\delta}$ Significantly different from 2dSTR3dCES. ($p<0.05$)

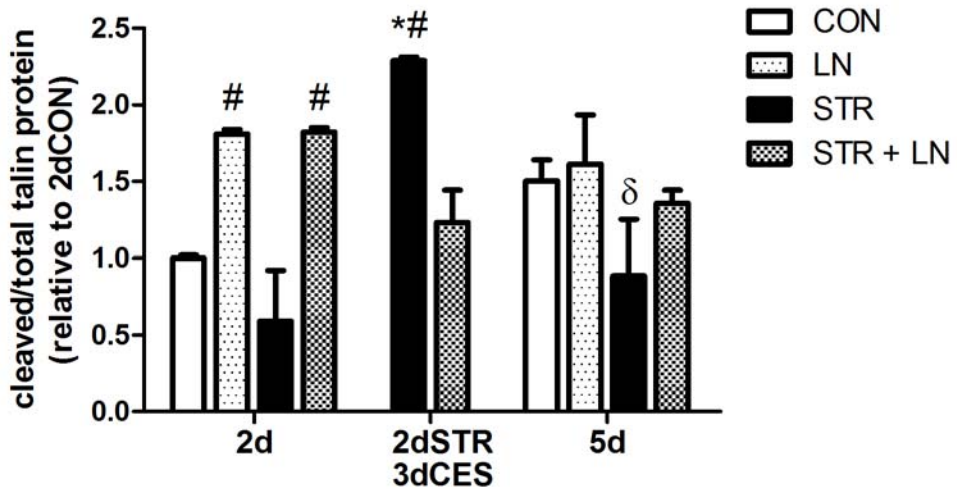

Figure 4-4. Talin protein degradation of C_2C_{12} myotubes using the atrophy protocol. Graphs represent ratio of the 190-kDa cleavage product to the 235-kDa intact talin protein. Values represent the mean ± SEM. (n=3) *Significantly different from 2dCON. $^{\#}$ Significantly different from 2dSTR.$^{\delta}$ Significantly different from 2dSTR3dCES. ($p<0.05$)

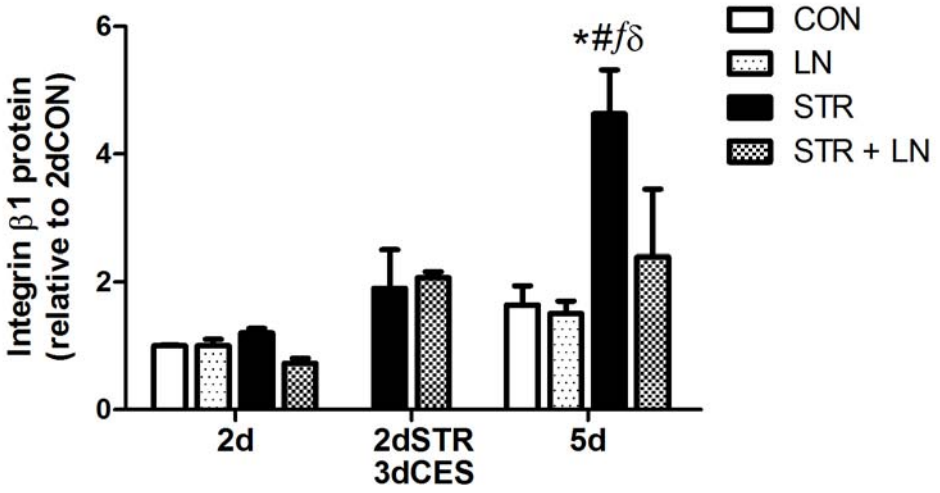

Figure 4-5. Integrin β1 protein expression in C_2C_{12} myotubes using the atrophy protocol. Graph represents integrin β1 normalized to β-actin. Values represent the mean ± SEM. (n=4) [*]Significantly different from 2dCON. [#] Significantly different from 2dSTR. [f] Significantly different from 5dCON.[δ] Significantly different from 2dSTR3dCES. ($p<0.05$)

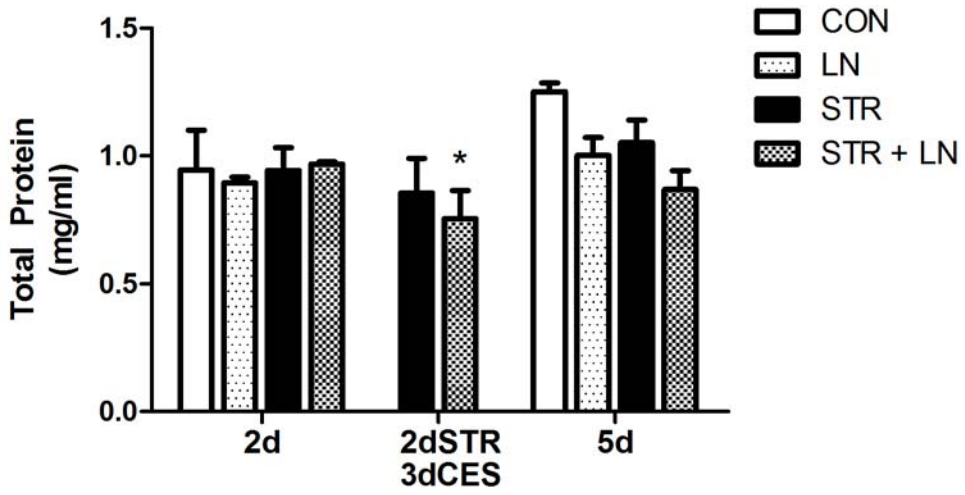

Figure 4-6. Total protein content of C_2C_{12} myotubes using the atrophy protocol. Graph represents total protein content in whole cell lysate. Values represent the mean ± SEM. (n=3) * Significantly different from 5dCON. ($p<0.05$)

A

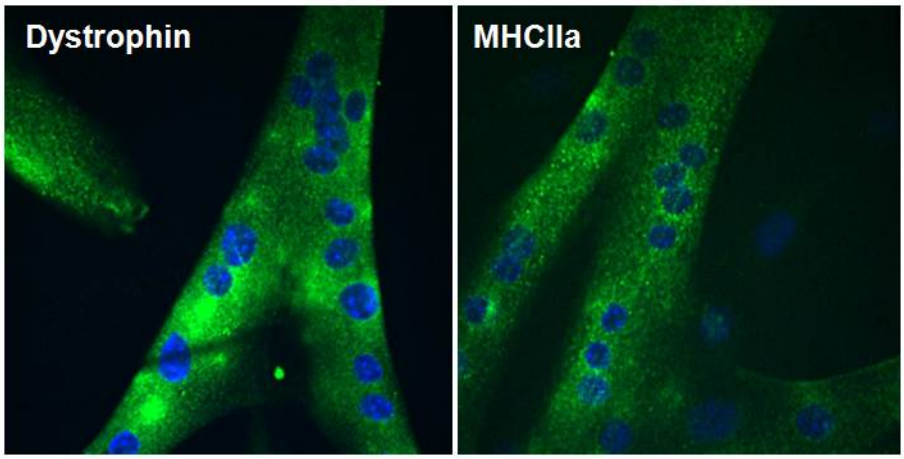

B

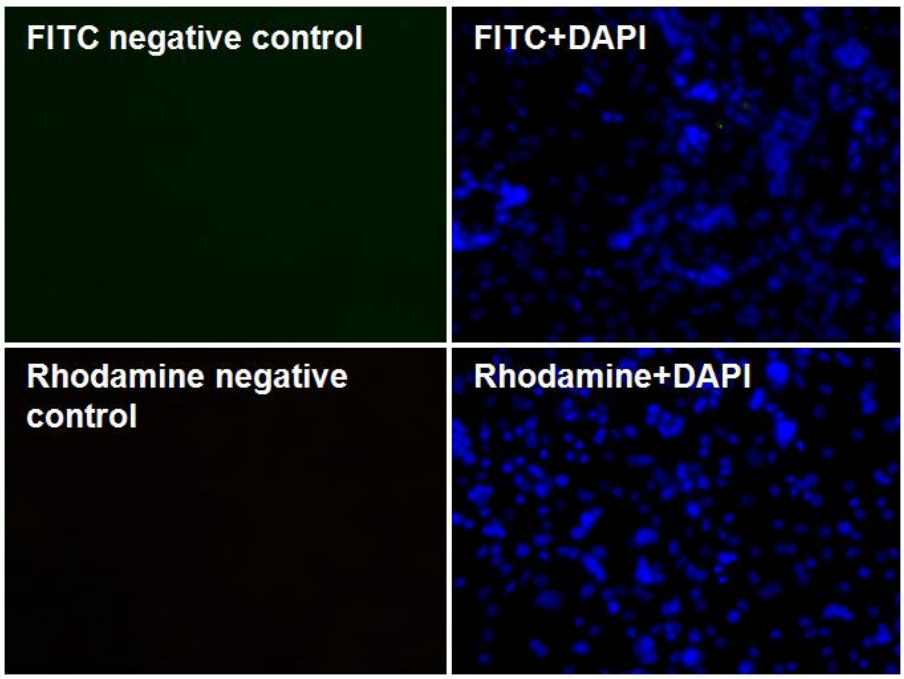

Figure 4-7. Representative images of C_2C_{12} myotubes immunostained for dystrophin and MHC type IIa and corresponding negative controls after 6 d of differentiation. A) Immunostain of dystrophin and myosin heavy chain type IIa. B) Negative control for MHCIIa (FITC) and dystrophin (Rhodamine).

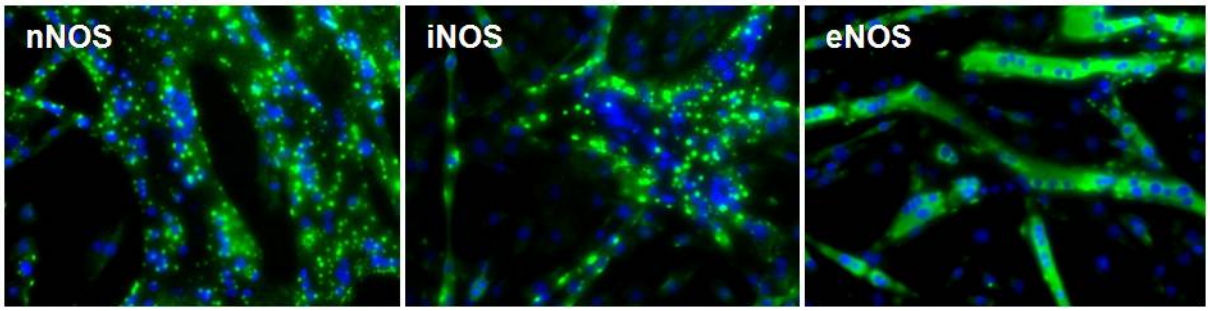

Figure 4-8. Representative images of C_2C_{12} myotubes immunostained for nNOS, iNOS, and eNOS after 6 d of differentiation.

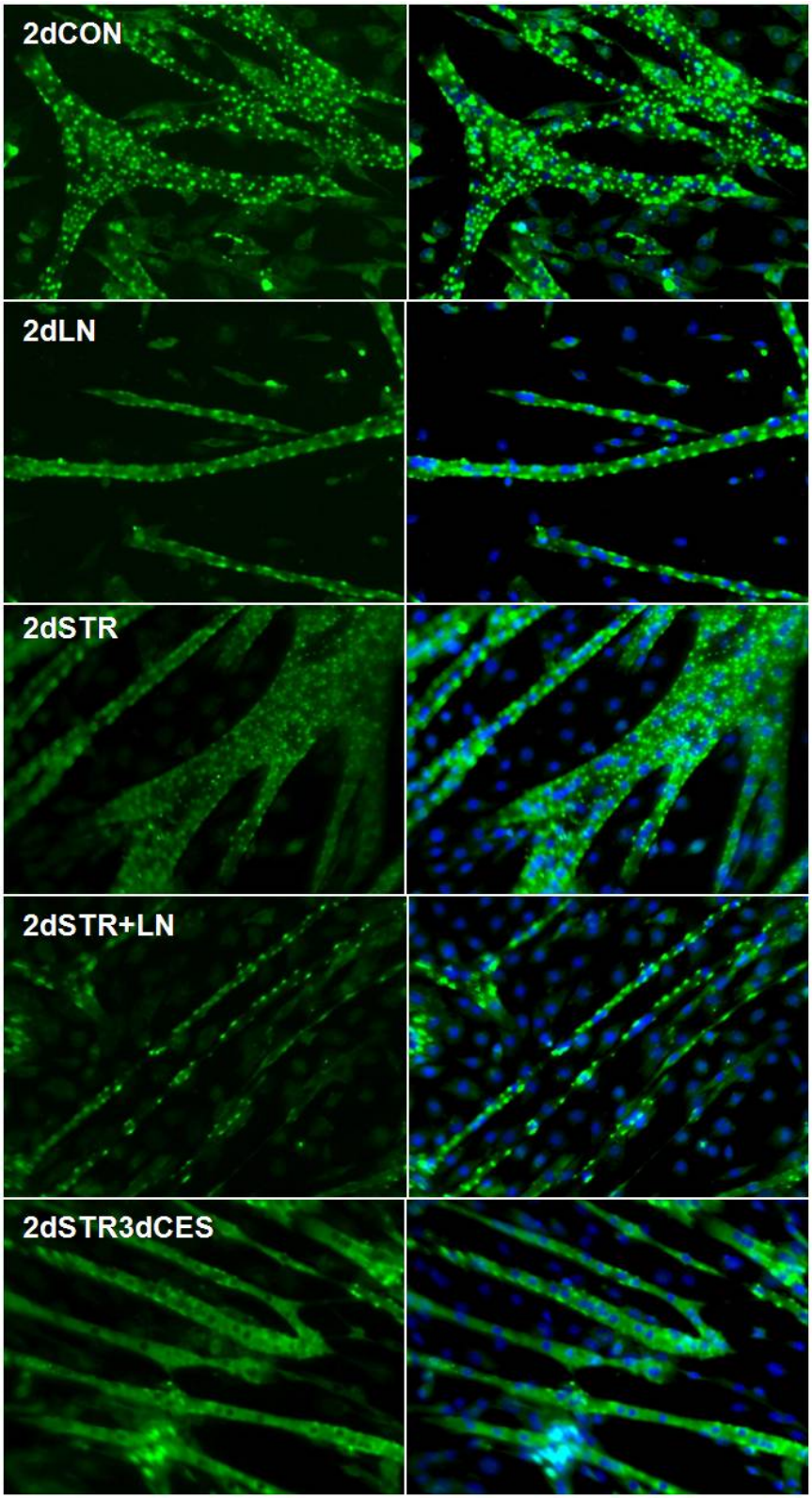

Figure 4-9. Representative images of C_2C_{12} myotubes immunostained for nNOS using the atrophy protocol.

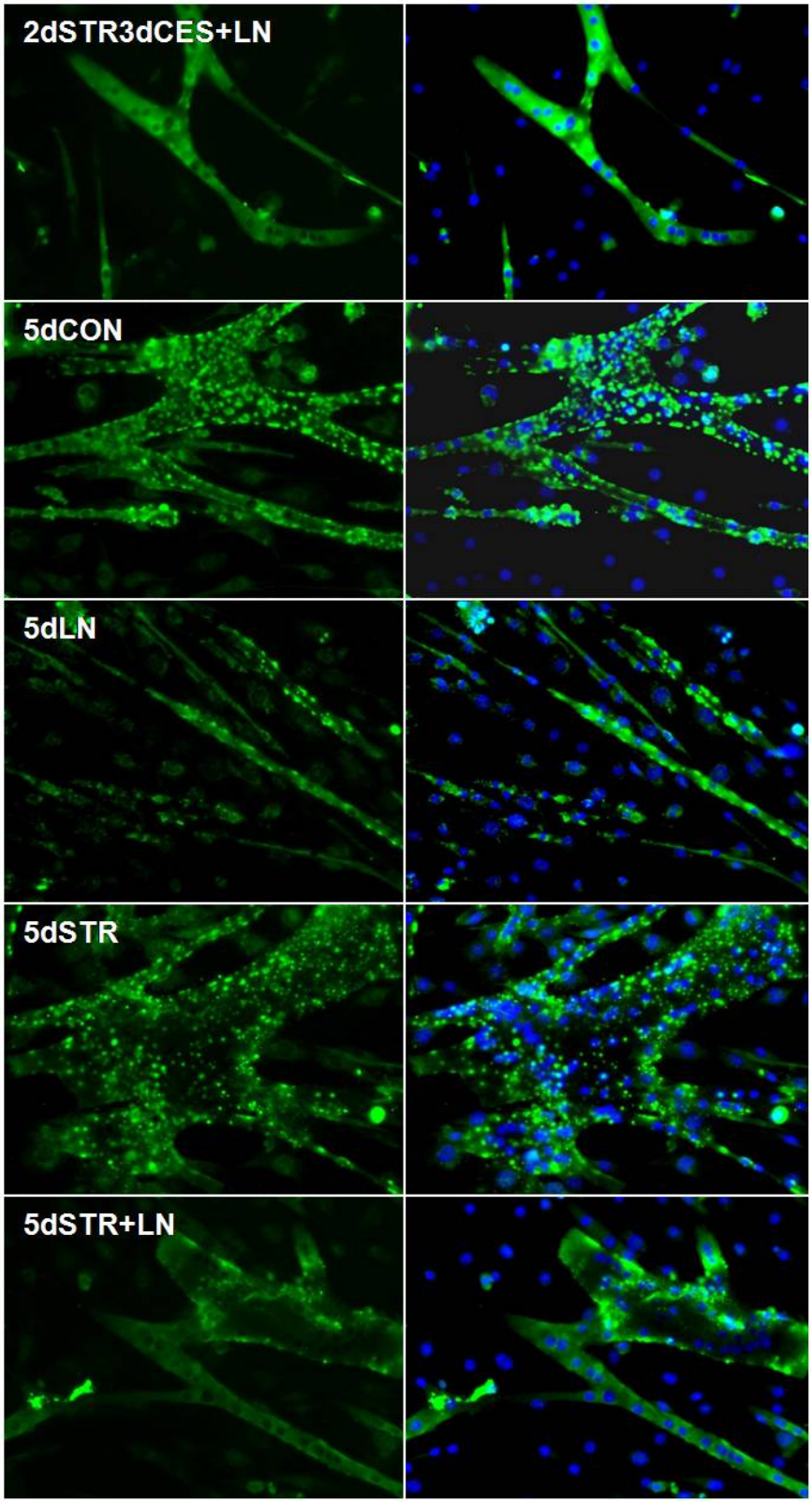

Figure 4-9 Continued.

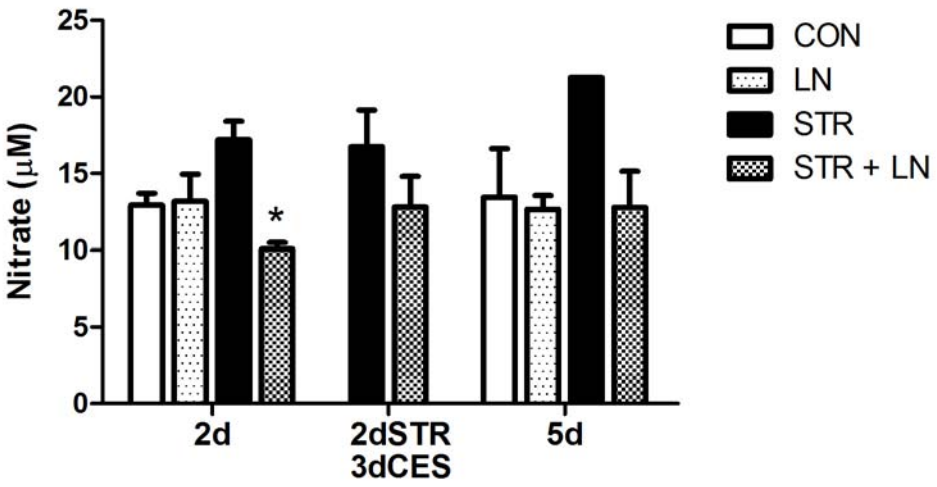

Figure 4-10. Total nitrate plus nitrite concentrations throughout the atrophy protocol. Culture medium was collected during the final 48 h of treatment. Values represent the mean ± SEM. (n=6) * Significantly different from 5dSTR. ($p<0.05$)

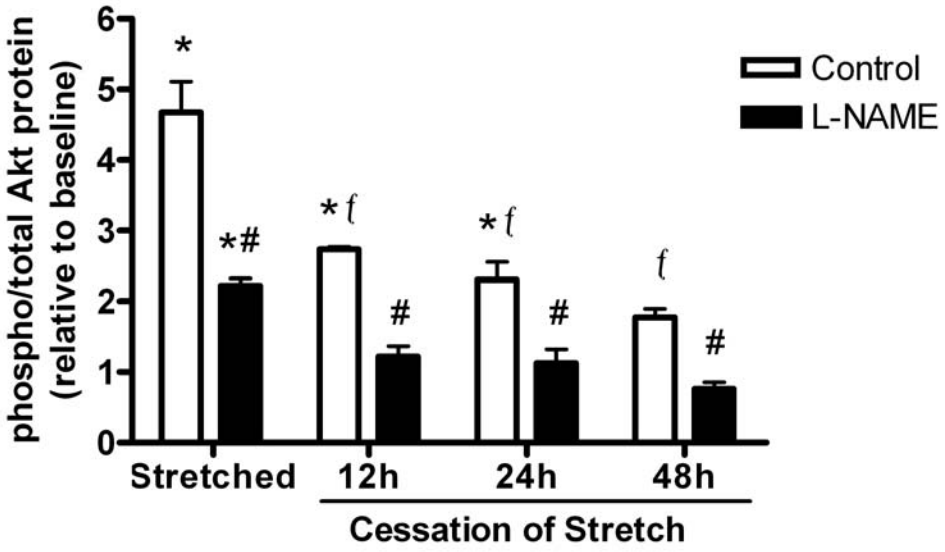

Figure 4-11. Ratio of phosphorylated to total Akt protein expression in C_2C_{12} myotubes 12, 24, and 48 h after 12% stretch. Values represent the mean ± SEM. (n=3) * Significantly different from baseline. # Significantly different from Control. f Significantly different from Stretched Control. Significant main effect of time, L-NAME, and interaction. ($p<0.05$)

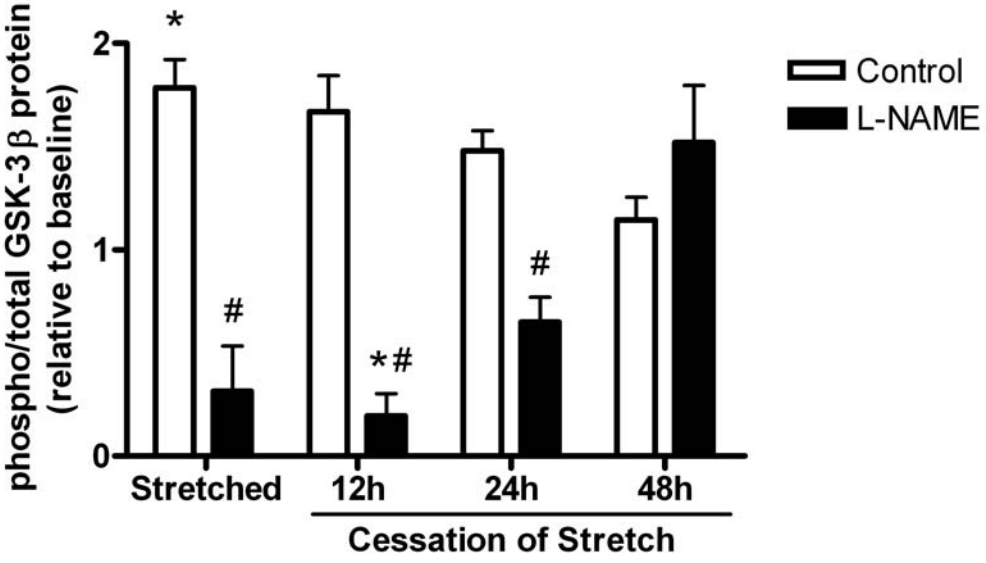

Figure 4-12. Ratio of phosphorylated to total GSK-3β protein expression in C_2C_{12} myotubes 12, 24, and 48 h after 12% stretch. Values represent the mean ± SEM. (n=3) * Significantly different from baseline. # Significantly different from Control. Significant main effect of L-NAME and interaction. ($p<0.05$)

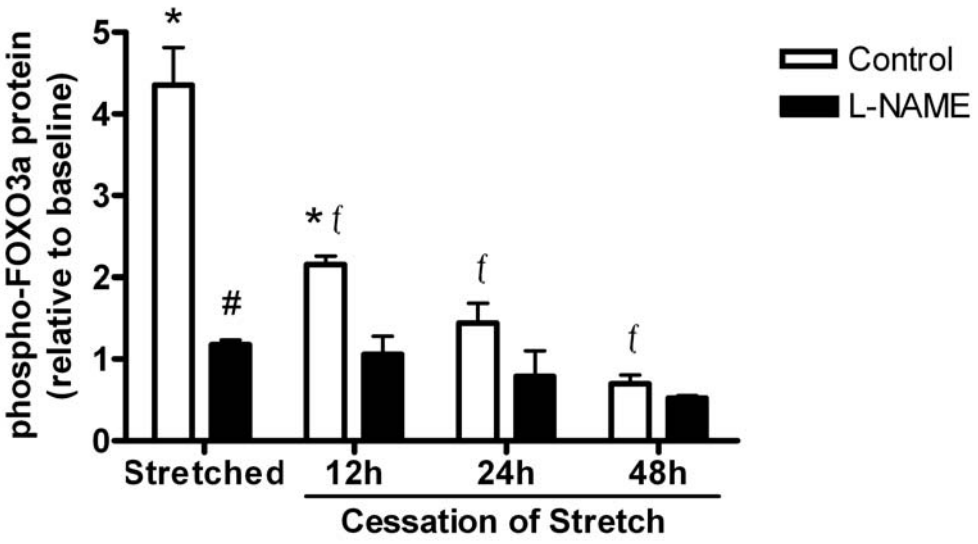

Figure 4-13. Phosphorylated FOXO3a protein levels in C_2C_{12} myotubes 12, 24, and 48 h after 12% stretch. Values represent the mean ± SEM. (n=3) * Significantly different from baseline. # Significantly different from Control. f Significantly different from Stretched Control. Significant main effect of time, L-NAME, and interaction. ($p<0.05$)

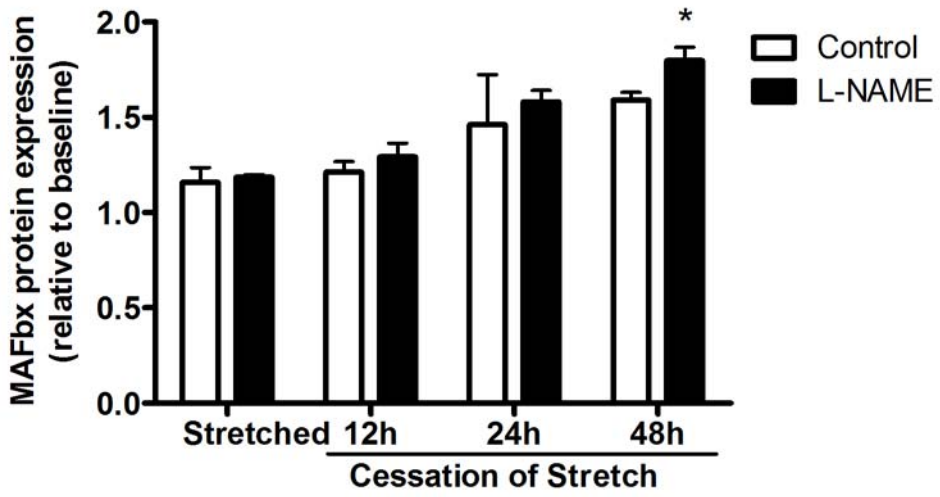

Figure 4-14. Muscle atrophy F-box (MAFbx) protein expression in C_2C_{12} myotubes 12, 24, and 48 h after 12% stretch. Values represent the mean ± SEM. (n=3) * Significantly different from baseline. Significant main effect of time. ($p<0.05$)

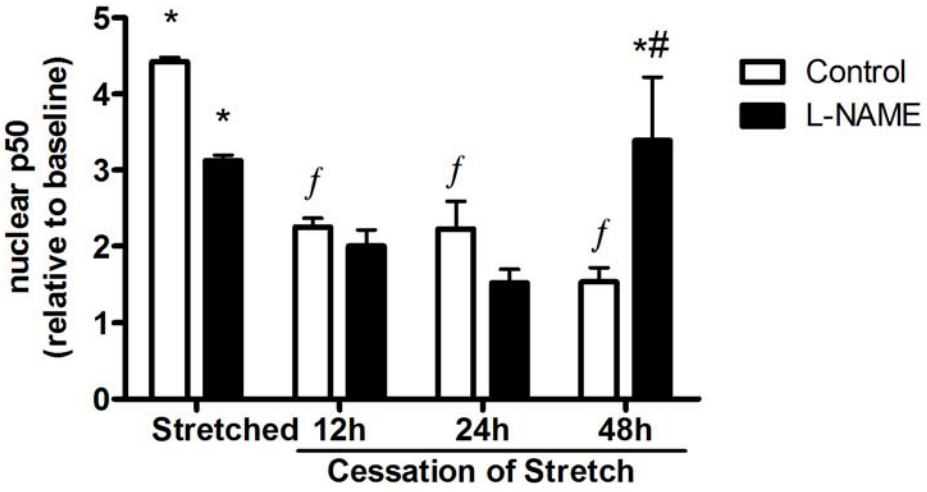

Figure 4-15. Nuclear p50 protein levels in C_2C_{12} myotubes 12, 24, and 48 h after 12% stretch. Values represent the mean ± SEM. (n=3) * Significantly different from baseline. # Significantly different from Control. f Significantly different from Stretched Control. Significant main effect of time and interaction. ($p<0.05$)

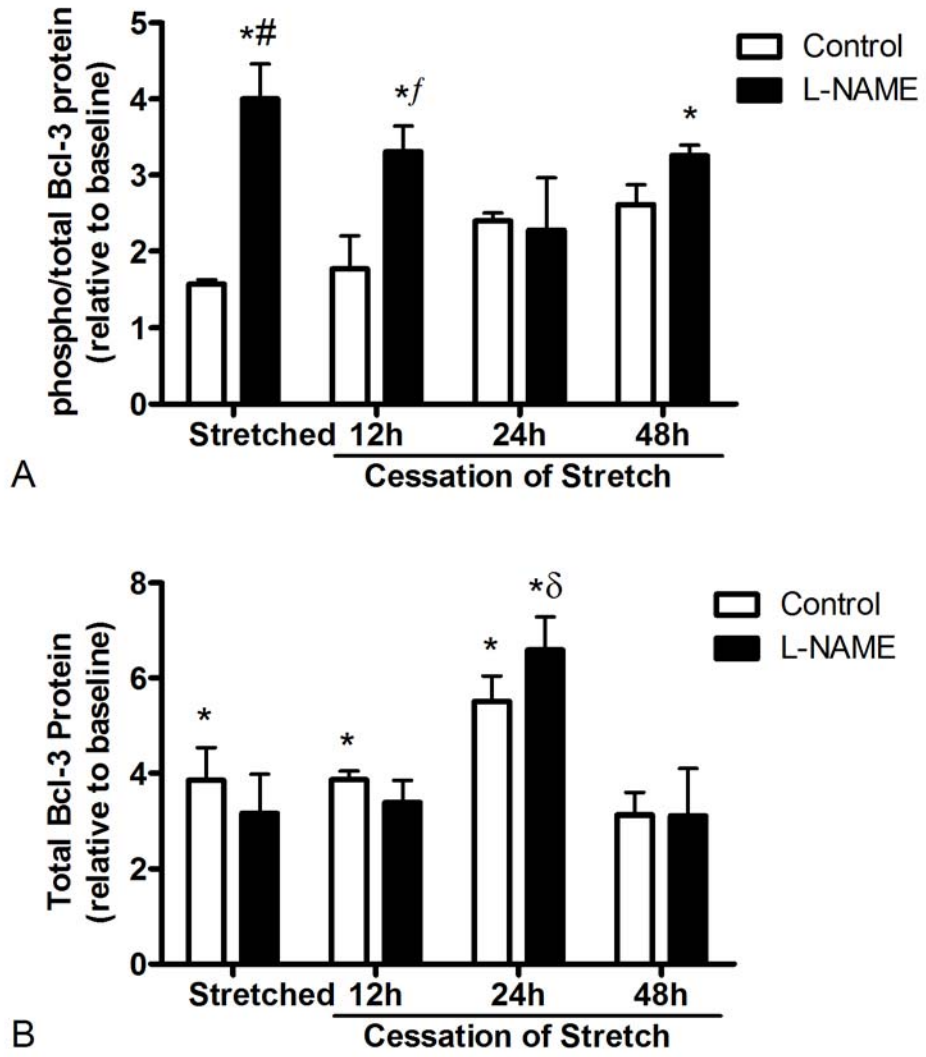

Figure 4-16. Nuclear Bcl-3 protein expression in C_2C_{12} myotubes 12, 24, and 48 h after 12% stretch. A) Ratio of phosphorylated to total Bcl-3 protein. (Significant main effect of L-NAME and interaction.) B) Total Bcl-3 protein. (Significant main effect of time.) Values represent the mean ± SEM. (n=3) * Significantly different from baseline. $^{\#}$ Significantly different from Control. ^{f} Significantly different from Stretched Control. $^{\delta}$ Significantly different from Stretched L-NAME. ($p<0.05$)

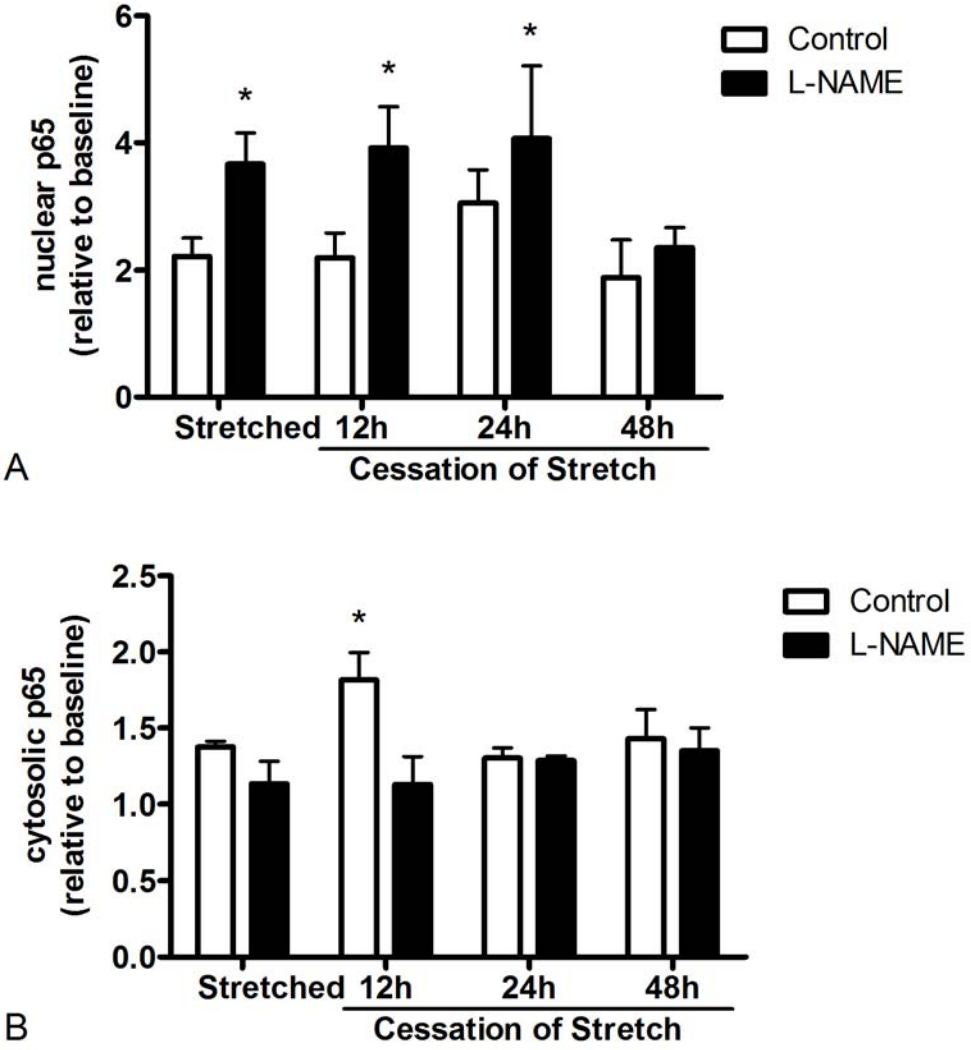

Figure 4-17. Nuclear and cytosolic p65 protein levels in C_2C_{12} myotubes 12, 24, and 48 h after 12% stretch. A) Nuclear p65 levels. (Significant main effect of drug.) B) Cytosolic p65 levels. (Significant main effect of drug.) C) Ratio of nuclear to cytosolic p65. (Significant main effect of drug, time, and interaction.) Values represent the mean ± SEM. (n=3) * Significantly different from baseline. $^{\#}$ Significantly different from Control. ^{f} Significantly different from Stretched Control. $^{\delta}$ Significantly different from Stretched L-NAME. ($p<0.05$)

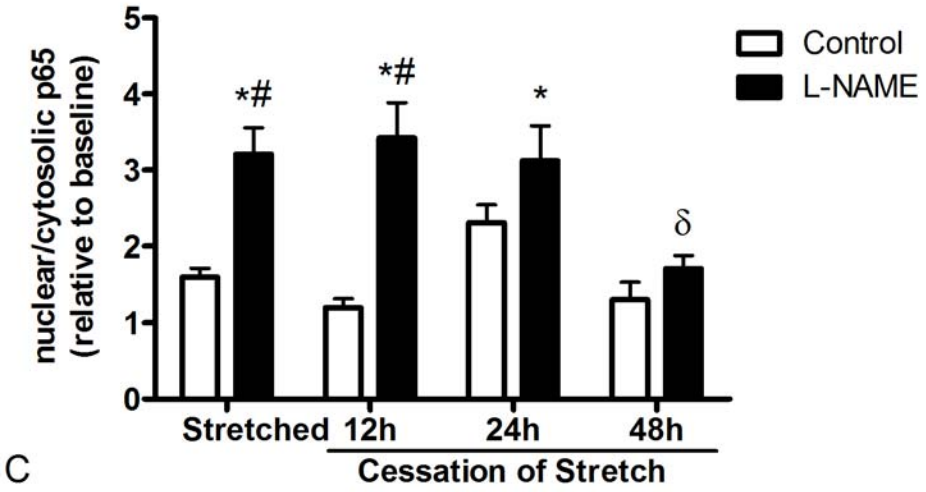

Figure 4-17 Continued.

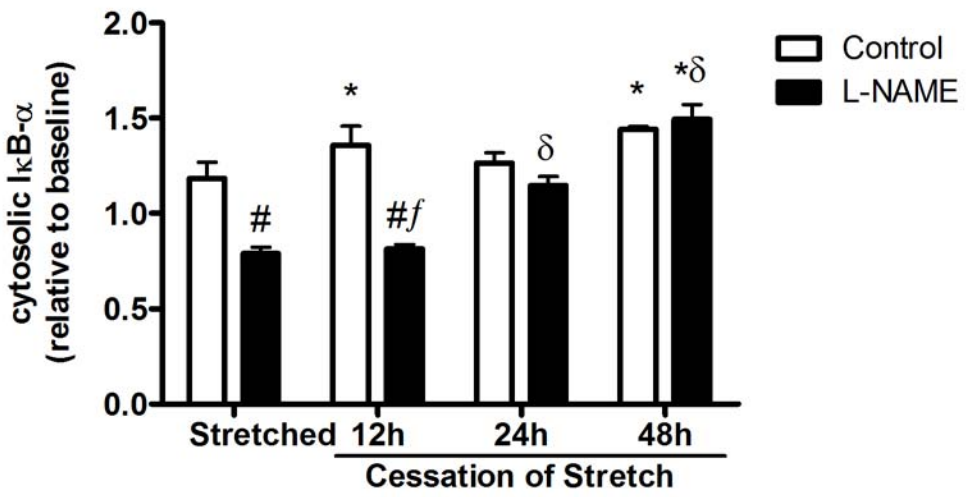

Figure 4-18. Cytosolic IκB-α protein expression in C_2C_{12} myotubes 12, 24, and 48 h after 12% stretch. Values represent the mean ± SEM. (n=3) * Significantly different from baseline. $^{\#}$ Significantly different from Control. ^{f} Significantly different from Stretched Control. $^{\delta}$ Significantly different from Stretched L-NAME. Significant main effect of time, drug, and interaction. ($p<0.05$)

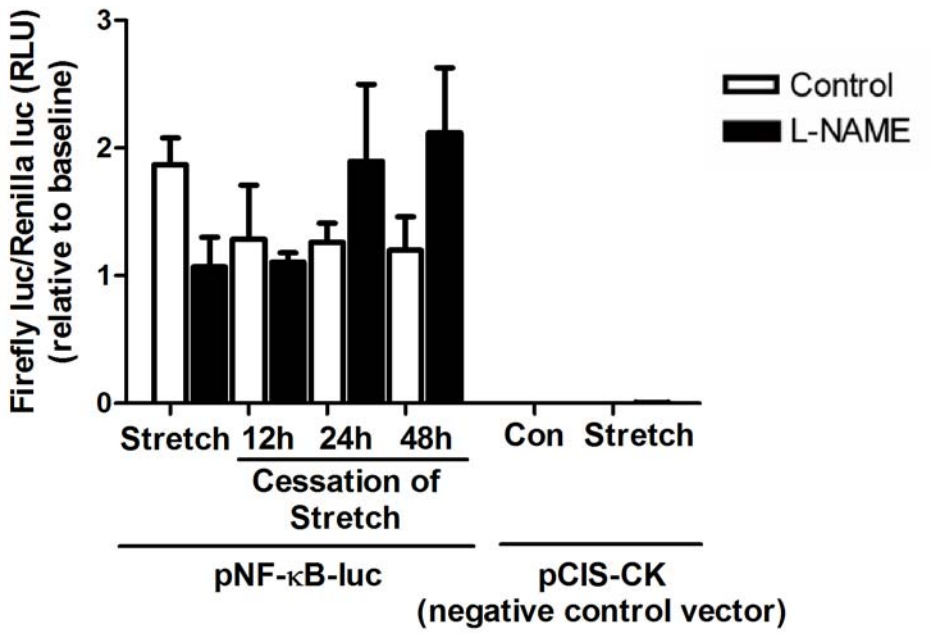

Figure 4-19. Nuclear factor of κB (NF-κB) transcriptional activity in C_2C_{12} myotubes 12, 24, and 48 h after 12% stretch. Graph represents NF-κB-dependent transcriptional activity (NF-κB reporter plasmid indicated by pNF-κB-luc) or empty vector activity (pCIS-CK) relative to uptake control (pRL-CMV). Values represent the mean ± SEM. (n=3) No statistical differences.

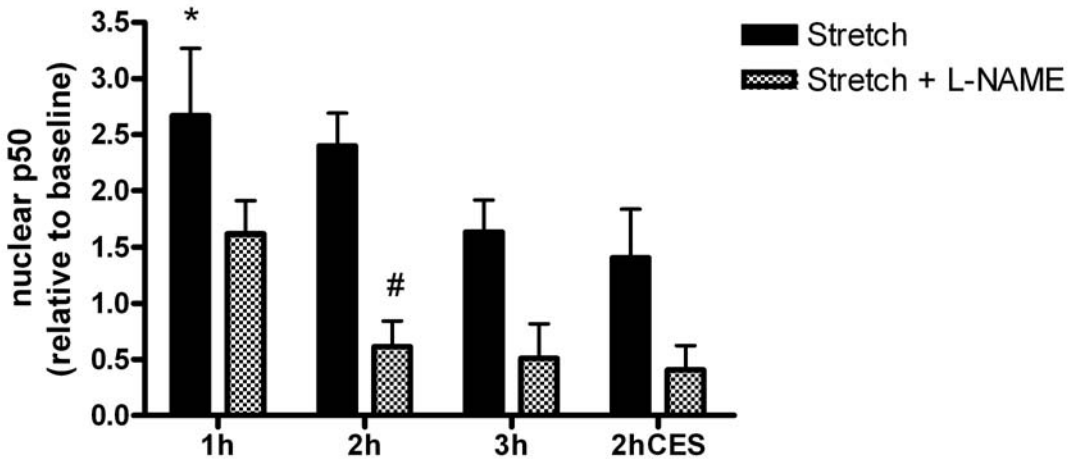

Figure 4-20. Nuclear p50 protein expression in C_2C_{12} myotubes subjected to high cyclic strain for 3 h. Values represent the mean ± SEM. (n=3) * Significantly different from baseline. # Significantly different from Stretch. Significant main effect of time and L-NAME. ($p<0.05$)

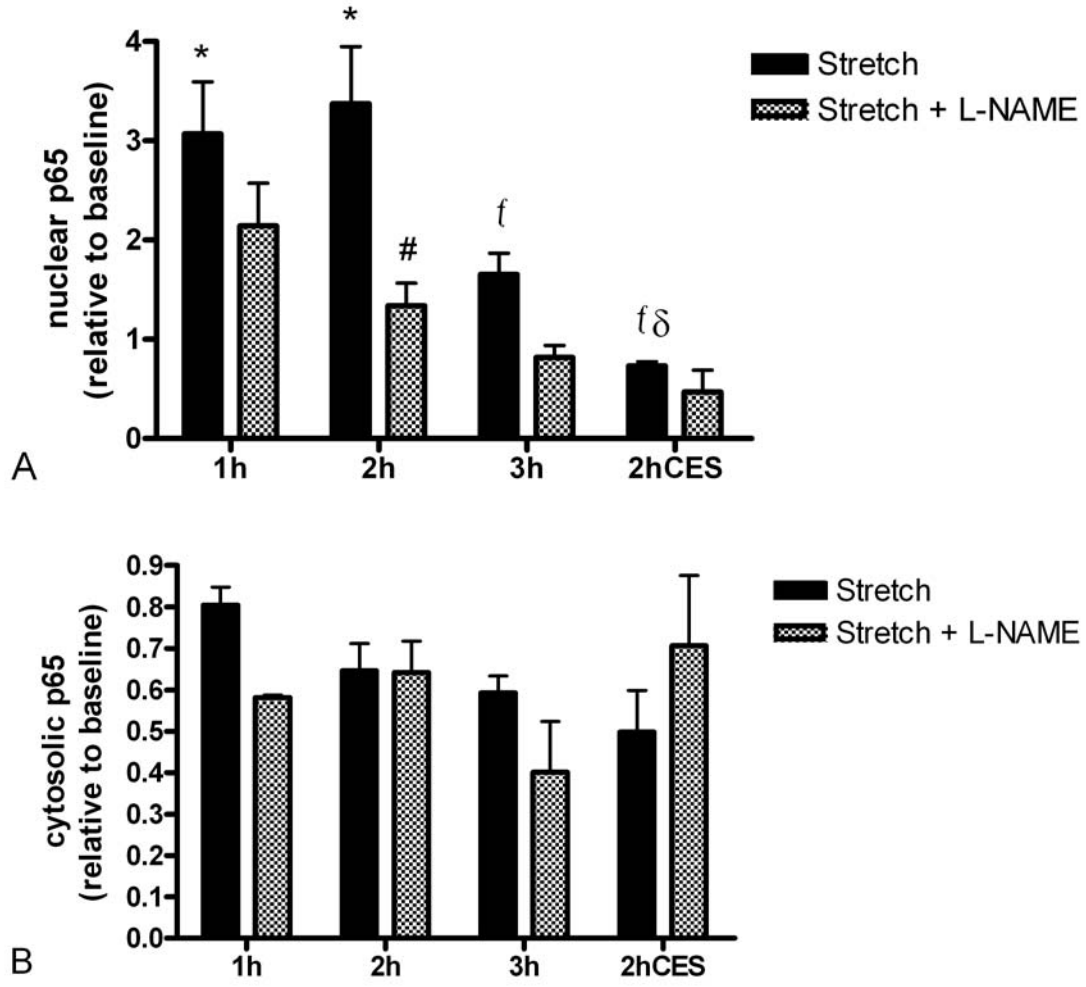

Figure 4-21. Nuclear and cytosolic p65 protein expression in C_2C_{12} myotubes subjected to high cyclic strain for 3 h. A) Nuclear p65 levels. (Significant main effect of L-NAME, time, and interaction). B) Cytosolic p65 levels. (Significant main effect of time.) C) Ratio of nuclear to cytosolic p65. (Significant main effect of L-NAME and time.) Values represent the mean ± SEM. (n=3) * Significantly different from baseline. # Significantly different from Stretch. f Significantly different from 2hSTR. δ Significantly different from 1hSTR. ($p<0.05$)

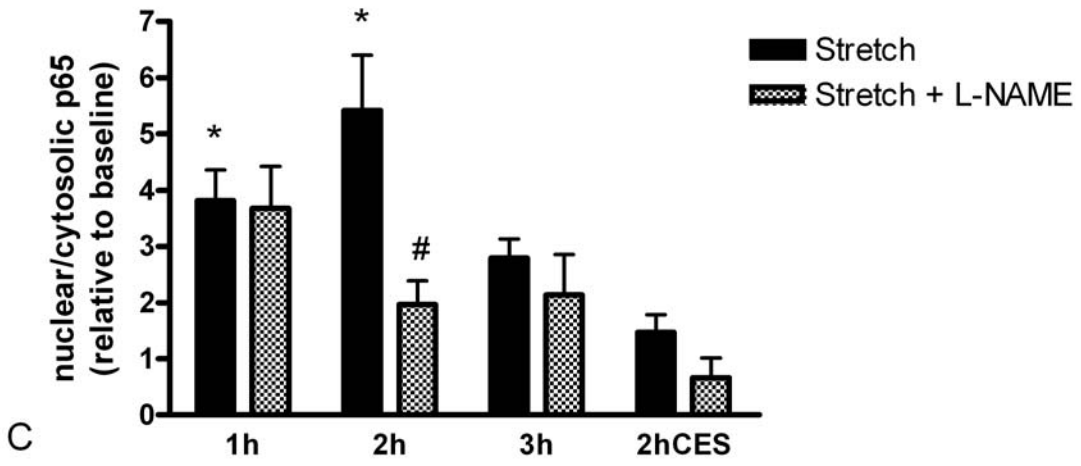

Figure 4-21 Continued.

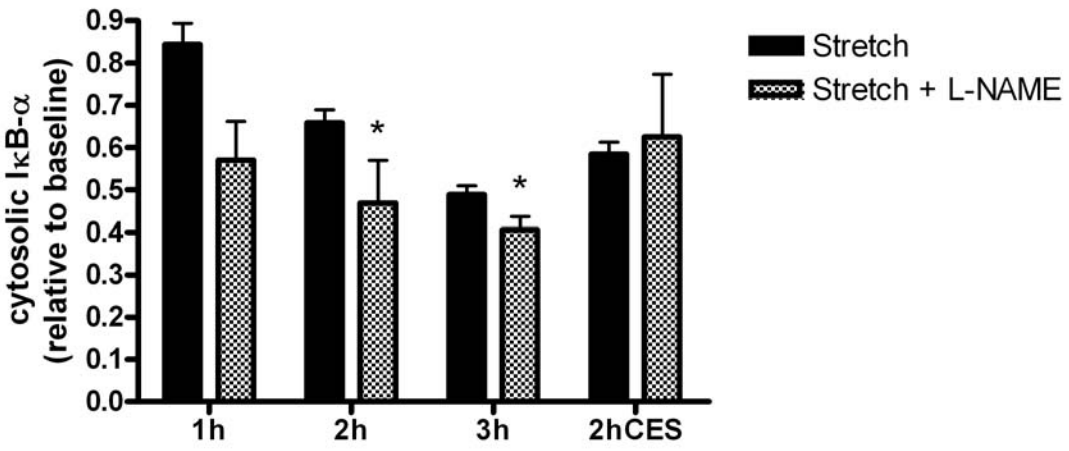

Figure 4-22. Cytosolic IκB-α protein expression in C_2C_{12} myotubes subjected to high cyclic strain for 3 h. Values represent the mean ± SEM. (n=3) * Significantly different from baseline. Significant main effect of time. ($p<0.05$)

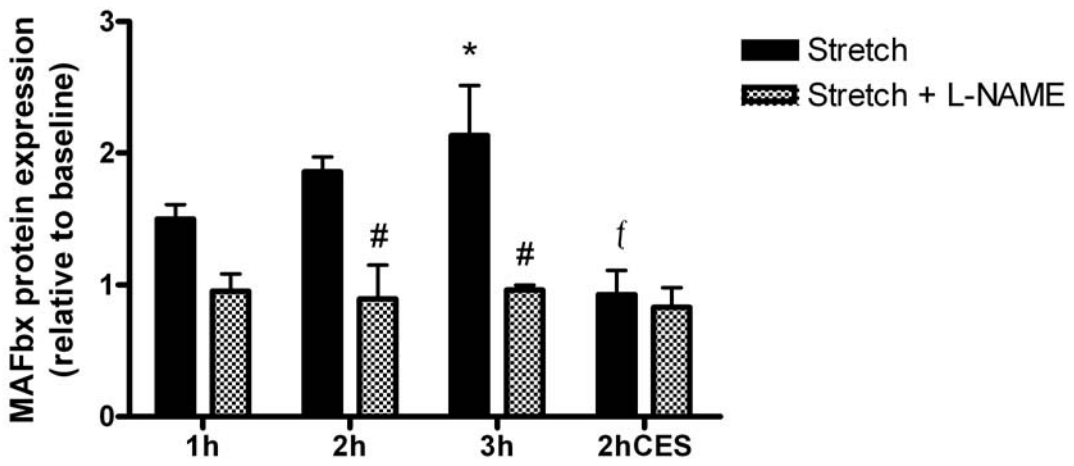

Figure 4-23. Muscle atrophy F-box (MAFbx) protein expression in C_2C_{12} myotubes subjected to high cyclic strain for 3 h. Values represent the mean ± SEM. (n=3) * Significantly different from baseline. # Significantly different from Stretch. *f* Significantly different from 3hSTR. Significant main effect of L-NAME, time, and interaction. ($p<0.05$)

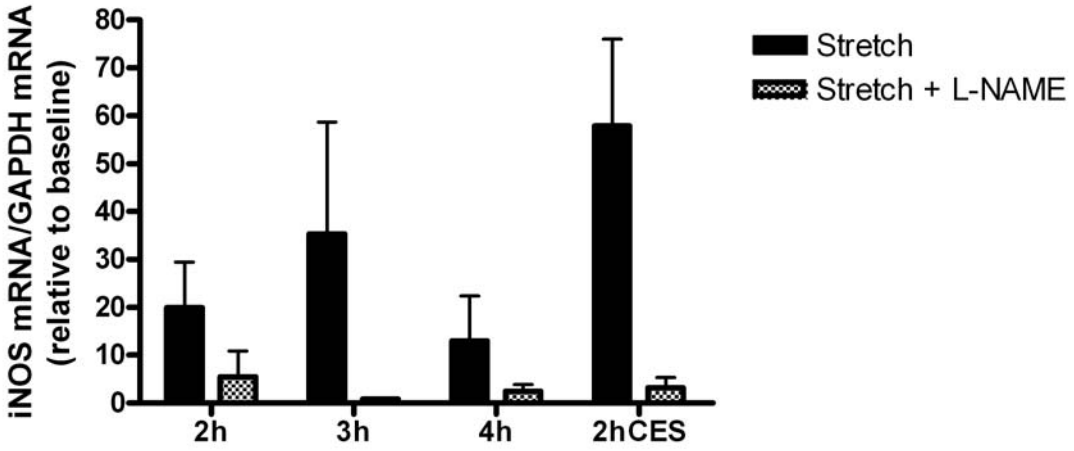

Figure 4-24. Inducible NOS (iNOS) mRNA levels in C_2C_{12} myotubes during 4 h of high cyclic strain. Values represent the mean ± SEM. (n=3) Significant main effect of L-NAME treatment. ($p<0.05$)

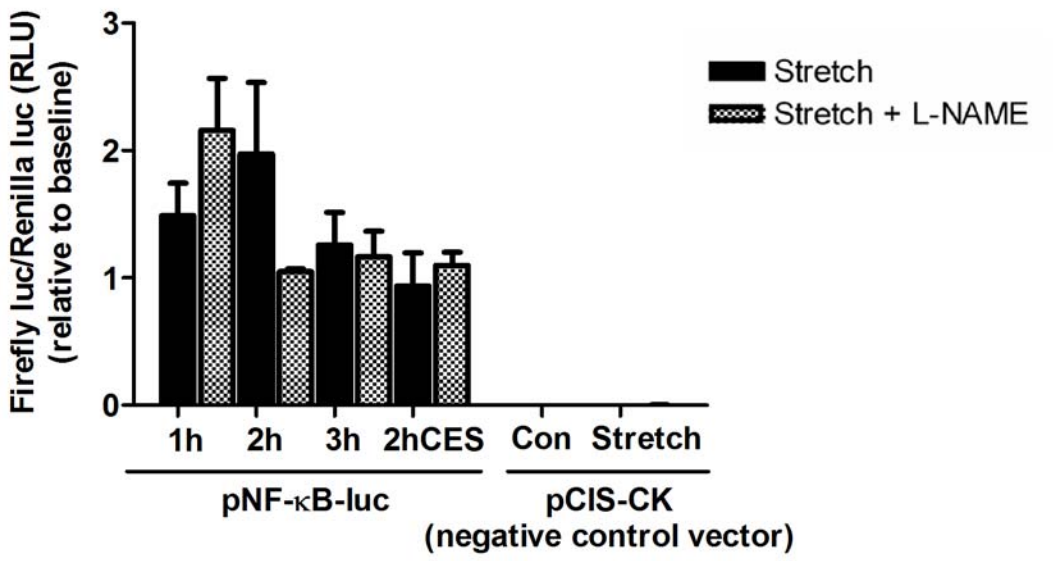

Figure 4-25. Nuclear factor of κB (NF-κB) transcriptional activity in C_2C_{12} myotubes subjected to high cyclic strain for 3 h. Graph represents NF-κB-dependent transcriptional activity (NF-κB reporter plasmid indicated by pNF-κB-luc) or empty vector activity (pCIS-CK) relative to uptake control (pRL-CMV). Values represent the mean ± SEM. (n=3) No statistical differences.

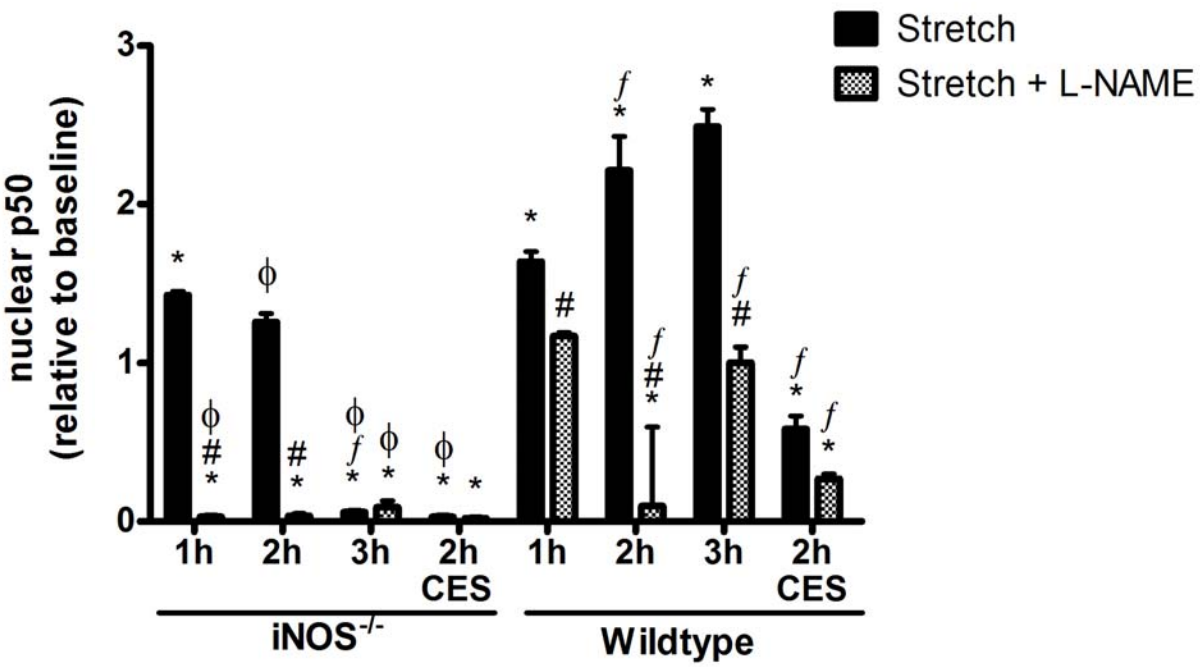

Figure 4-26. Nuclear p50 protein expression in primary cultured myotubes from iNOS$^{-/-}$ and wildtype mice subjected to high cyclic strain for 3 h. Values represent the mean ± SEM. (n=3) * Significantly different from baseline. # Significantly different from Stretch. . f Significantly different from previous hour treatment. □ Significantly different from Wildtype. Significant main effect of L-NAME, time, and interaction. ($p<0.05$)

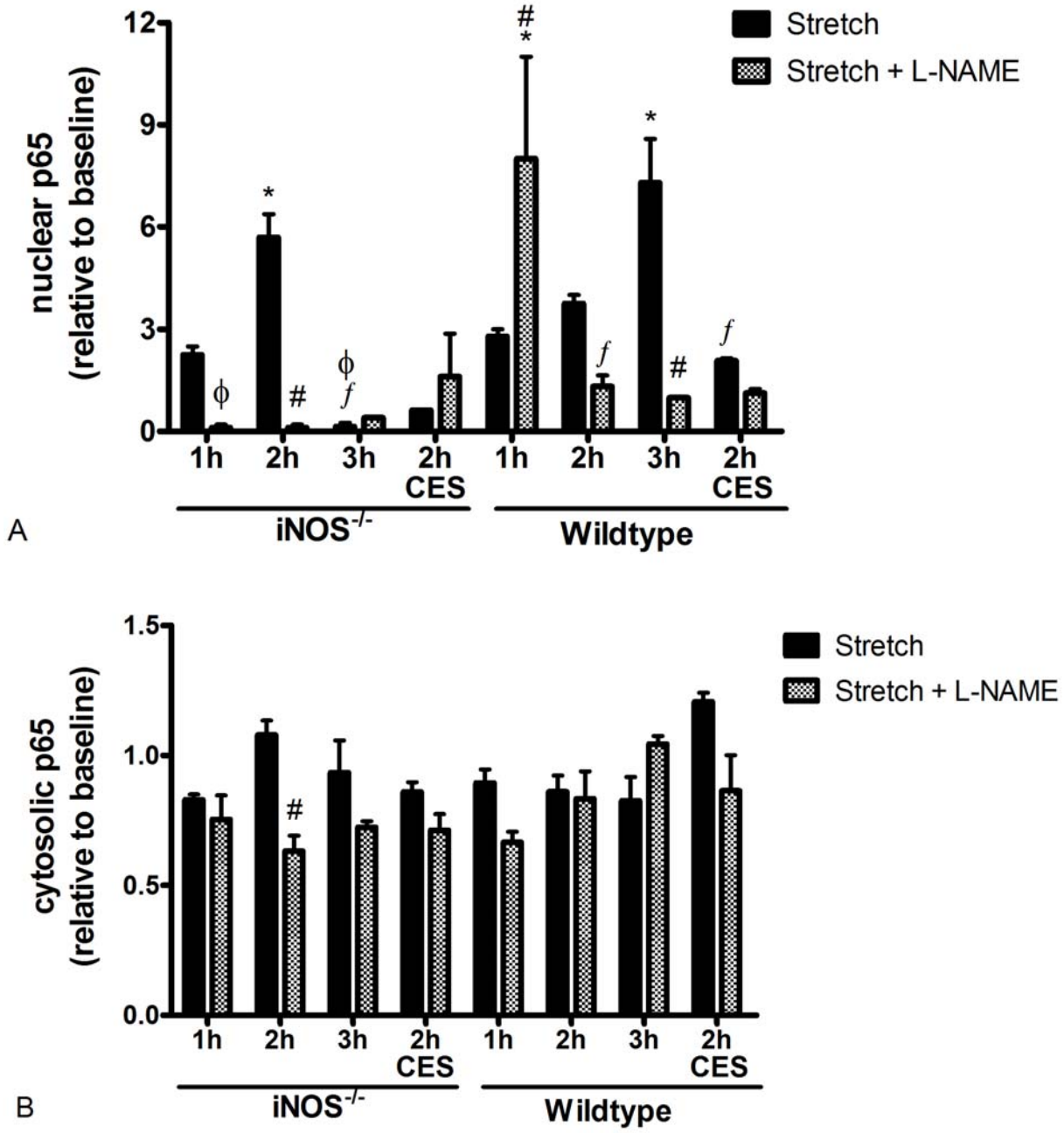

Figure 4-27. Nuclear and cytosolic p65 protein expression in primary cultured myotubes from iNOS$^{-/-}$ and wildtype mice subjected to high cyclic strain for 3 h. A) Nuclear p65 levels. (Significant main effect of L-NAME, time, and interaction.) B) Cytosolic p65 levels. (Significant main effect of L-NAME, time, and interaction.) C) Ratio of nuclear to cytosolic p65. (Significant main effect of time and interaction.) Values represent the mean ± SEM. (n=3) * Significantly different from baseline. # Significantly different from Stretch. . f Significantly different from previous hour treatment. Significantly different from Wildtype. ($p<0.05$)

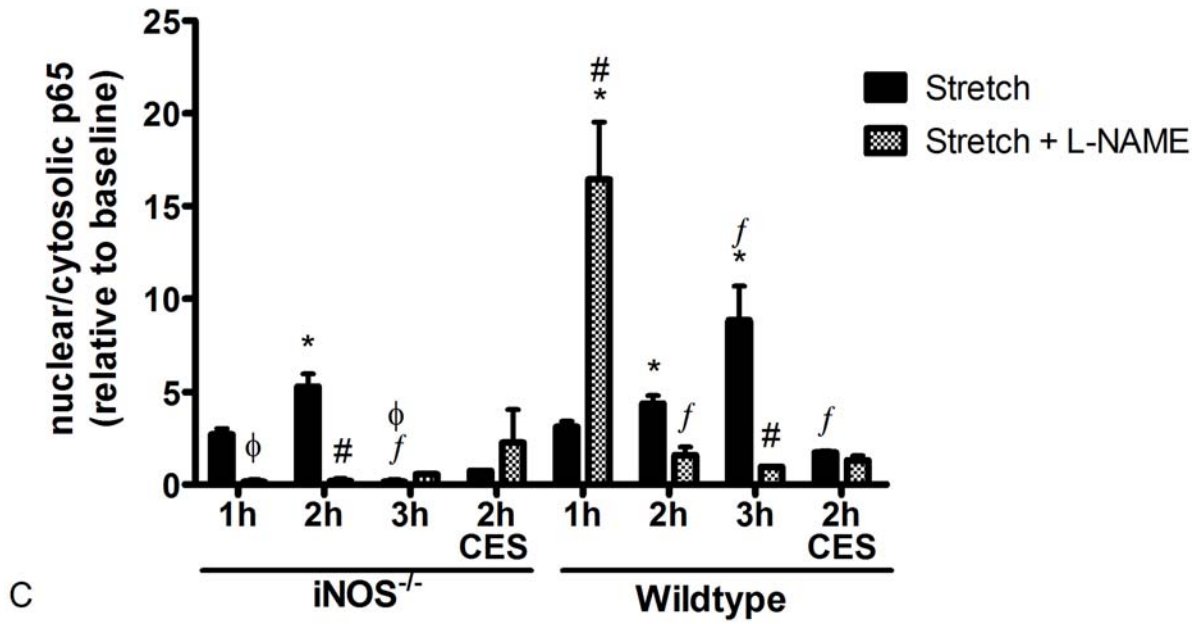

C

Figure 4-27 Continued.

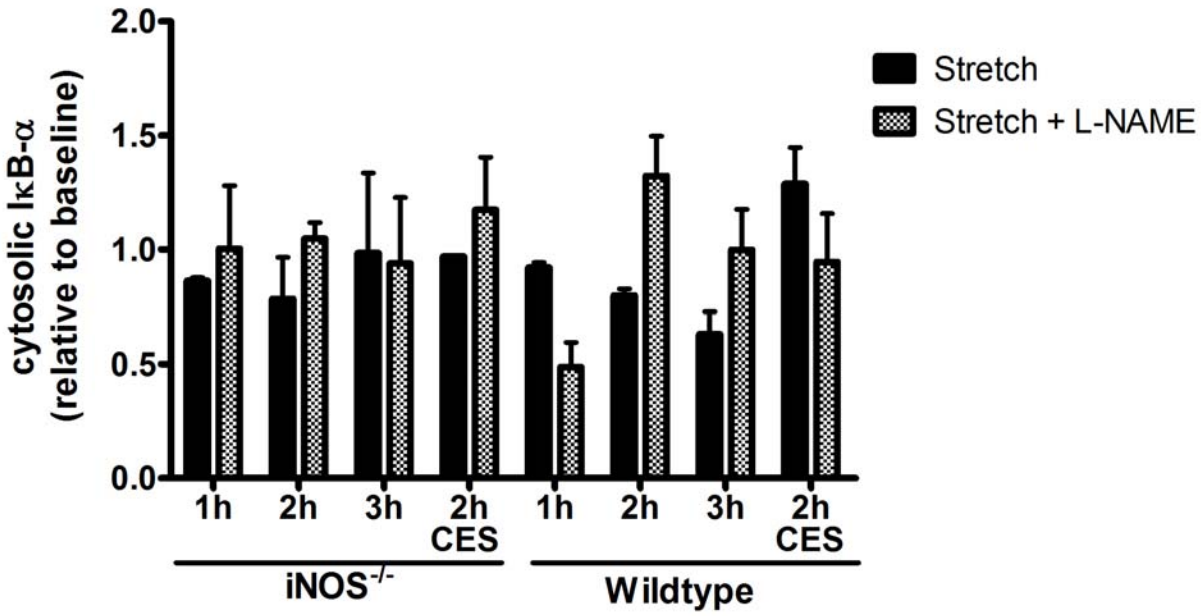

Figure 4-28. Cytosolic IκB-α protein expression in primary cultured myotubes from iNOS$^{-/-}$ and wildtype mice subjected to high cyclic strain for 3 h. Values represent the mean ± SEM. (n=3) No statistical differences.

CHAPTER 5
DISCUSSION

Main Findings

This is the first study to our knowledge to develop two completely intrinsic models of skeletal muscle atrophy *in vitro*: 1) withdrawal from moderate cyclic stretch, and 2) high magnitude cyclic strain. First, moderate cyclic mechanical stretch can be used as a model of activity in cultured skeletal muscle myotubes, and increases myotube size through NOS-dependent induction of Akt signaling. Cessation of this type of moderate stretch causes protein degradation, altered nNOS localization, and a reduction in myotube size via downregulation of Akt, which may contribute to NF-κB signaling through an alternative pathway. Secondly, high magnitude cyclic strain can induce the classical pathway of NF-κB signaling and upregulate iNOS in cultured skeletal muscle myotubes. These data demonstrate *in vitro* models of atrophy independent of external factors and provide evidence to better understand the signaling pathways involved during skeletal muscle loss.

Disuse Atrophy Model

Cessation of Cyclic Stretch Causes Skeletal Muscle Myotube Atrophy

In vivo, skeletal muscle atrophy is defined as a loss in skeletal muscle mass, and can be measured as a reduction in fiber cross-sectional area and protein content, reduced force and power output, increased fatigability and increased insulin resistance. We define skeletal muscle myotube atrophy as a decrease in myotube size, increased protein degradation and protein loss.

Cyclic mechanical stretch in culture elicits the acute effects similar to muscle activity *in vivo* such as membrane deformation (28), increased glucose uptake (86), protein synthesis (81), and free radical production (102), as well as some of the chronic adaptations associated with exercise, including myotube hypertrophy (188), increased cytoskeletal stability (212), and

reduced fast myosin heavy chain composition (122). Thus, cyclic mechanical stretch to skeletal muscle myotubes can be used as a denervated model of skeletal muscle activity *in vitro*. In our model, we demonstrated that five days of a 12% cyclic stretch applied to C_2C_{12} myotubes was sufficient to cause myotube hypertrophy through an increase in myotube diameter and area (Figures 4-1 and 4-2) although no change in total protein content was evident (Figure 4-6).

Passive stretch of mature muscle leads to an increase in muscle tension which plays an important role in cell proliferation, differentiation, metabolism, remodeling, and survival (30, 46, 94, 104, 143). Many of these processes are dependent on activation of integrin-mediated signaling pathways (93, 124, 156). This notion is supported by an *in vivo* study that showed impaired fusion and defective cytoskeleton in β1D-integrin-deficient myoblasts (158). Thus, it is conceivable that the expression of β1-integrin is required to strengthen the linkage between cytoskeleton and extracellular matrix in the developing myotube. Localization of β1-integrin at the sarcolemma in skeletal myotubes may enable it optimally to sense changes in the mechanical environment, where it serves an important role in sensing and transducing mechanical signals from the external environment to the cytoplasm (14). In agreement with the literature (213), we showed that multiple days of 1-h bouts of cyclic stretch increased the mechanotransduction signaling protein β1-integrin in C_2C_{12} myotubes (Figure 4-5).

Beta1-integrin may also interact with Rho GTPases, and the activity of Rho GTPases is critical for integrin clustering and partial phosphorylation of FAK (35, 37, 54). Similar to FAK, Rho GTPases play an important role in myodifferentiation. These Rho family proteins also regulate the organization of the actin cytoskeleton. In C_2C_{12}s, a 10% cyclic stretch successfully activated RhoA, GTP-binding proteins, FAK, and Z-line formation (36, 213), as well as RhoA

protein expression (120). Thus, repetitive stretch of myotubes *in vitro* can initiate cytoskeletal formation and mechanotranduction pathways associated with skeletal muscle activity.

On the other hand, inactivity of skeletal muscle causes fiber atrophy. Removal of mechanical stretch caused myotubes to respond as if they had been forced to an inactive state. Here, we demonstrated that C_2C_{12} myotubes experience cytoskeletal protein degradation (Figures 4-3 and 4-4) and a decrease in size after three days of no stretch (Figures 4-1 and 4-2). Thus, forced inactivity of skeletal muscle myotubes through cessation of daily repetitive stretch is sufficient to induce visible and measurable myotube atrophy.

Skeletal muscle atrophy is predominately due to increased proteolysis leading to a loss of mass. Evidence indicates that the rate-limiting step in protein degradation during skeletal muscle atrophy is the actomyosin disassociation by calpain and/or caspase-3. The cleavage products of two cytoskeletal proteins, αII-spectrin and talin, that are known to be substrates of calpain and caspase were increased during the inactivity period of our protocol (Figures 4-3 and 4-4).

Evidence that ubiquitous calpains are key players in atrophy is based on expression analysis, detection of activity of calpain and the use of calpain inhibitors. Several studies have established that calpains are elevated in atrophic conditions like disuse, denervation, glucocorticoid treatment and sepsis (72, 79, 172, 192, 199). Calpain substrates include proteins that are important to sarcomeric structural integrity, such as Z-disk proteins, myofibrillar proteins and structural cytoskeletal proteins (65, 198) including, talin, vinculin, αII-spectrin, nebulin and titin (82, 116). Ca^{2+} spikes, removal of the N-terminus region by autolysis, calpastatin and nitric oxide, all seem to be involved in the regulation of ubiquitous calpain activity (66, 123).

Interestingly, the inhibition of nitric oxide synthase with L-NAME in C_2C_{12} myotubes induced talin degradation independent of stretch (Figure 4-4). Nitric oxide has been shown to

inhibit calpain activity via S-nitrosylaton of an active site cysteine, and the NO donor sodium nitroprusside was sufficient to prevent vinculin and talin degradation after calcium ionophore-treatment in C_2C_{12} myoblasts (99). Thus, endogenous nitric oxide production may be protective against calpain-induced proteolysis. Since nitric oxide production is enhanced by cyclic stretch (Figure 3-3), this may partly explain why cytoskeletal proteolysis by calpain was reduced by mechanical activity in our model.

Localization and Activity of NOS after Stretch

Skeletal muscle contains all three isoforms of nitric oxide synthase, neuronal NOS (nNOS), inducible NOS (iNOS) and endothelial NOS (eNOS), and the localization of each NOS isoform in skeletal muscle varies (Figure 4-8) (18, 148).

Endothelial NOS is mainly expressed in the cytoplasm of all fibers, but mostly types I and IIa (76), where it is colocalized with mitochondrial markers within rat diaphragm, EDL, gastrocnemius, and soleus muscles (98). Immunostaining of eNOS in C_2C_{12}s demonstrated its diffuse location throughout the myotubes (Figure 4-8). We cannot ascertain if eNOS is associated with mitochondria in these cells or merely maintained a cytosolic residence.

Inducible NOS is present at very low levels in healthy skeletal muscle of humans (135) and rodents (177) but is enhanced in normal C_2C_{12} myotubes (18) and in response to endotoxin (177). The presence of iNOS is normally cytosolic or concentrated at the neuromuscular junction (206); however, our C_2C_{12} immunohistochemical analyses showed spotty staining similar to that of nNOS (Figure 4-8) suggesting a membrane-bound locality. Inducible NOS is constitutively expressed in skeletal muscle fibers of pathogen-free guinea pigs (61) where it copurified with a pooled particulate protein fraction and showed a spotty intracellular appearance in type I fibers of the diaphragm and gastrocnemius muscles (61). Others reported that iNOS coimmunoprecipates with the sarcolemmal caveolae membrane protein, caveolin-3, thus providing a molecular basis

for a sarcolemmal localization of iNOS (62). Further, in muscle fibers of patients with autoimmune inflammatory myopathies, an intense immunocytochemical labeling was observed along large stretches of the sarcolemma, in contrast to small spots seen in normal muscle (174). In human vastus lateralis and soleus muscle, iNOS is associated with subsarcolemmal caveolin-3 primarily in Type I fibers; however, after 90 d of bed rest, iNOS is no longer detectable at the membrane is seen only in the sarcoplasm (148). All together, the evidence suggests that in healthy tissue iNOS may be localized at the membrane in relatively low levels in most mammals and more highly expressed in C_2C_{12} myotubes and guinea pigs. However, iNOS localization differs in response to unloading, endotoxin, or disease where it may become upregulated and maintained throughout the sarcoplasm.

Neuronal NOS is associated with the dystrophin-glycoprotein complex which determines its sarcolemmal positioning in normal adult myofibers (4). This prominent molecular association of nNOS to the sarcolemmal DGC is reflected by the "ring-like" immunostaining patterns (60, 69). We also witnessed this "ring-like" appearance in C_2C_{12} myotubes after 6 d of differentiation (Figure 4-8) and was enhanced after repeated bouts of cyclic stretch (Figure 4-9). Disruption of the NOS dystrophin complex in mdx mice and human Duchenne musclular dystrophy results in displacement of NOS protein from the sarcolemma to the cytosolic compartment in myofibers (23). Also, in human atropic and necrotic muscle fibers, nNOS displayed an enhanced cytoplasmic nNOS distribution (174). More recently, Suzuki and colleagues demonstrated nNOS becomes dislocated from DGC during hindlimb unloading and becomes cytoplasmic where it facilitates activation of FOXO3a, MuRF-1, and MAFbx leading to skeletal muscle atrophy (169).

Athough we did not co-stain for nNOS and dystrophin, we did demonstrate that C_2C_{12} myotubes are capable of expressing dystrophin after 6 d of differentiation (Figure 4-7A). The

literature endorses the association of nNOS and the DGC as well as its dissociation during disuse and disease. Thus the lack of "spottiness" in myotubes subjected to a 3 d withdrawal of stretch is likely due to nNOS dissociation from the DGC in response to atrophic cytoskeletal degradation and release of structural proteins located at the sarcolemma.

Long term (5 days) exposure to L-NAME was also capable of causing sarcolemmal dislocation and nNOS diffusion throughout the cytoplasm (Figure 4-8). L-NAME has been shown to inhibit increased nNOS protein expression after stretch as well as levels of desmin, vinculin and talin in C_2C_{12} myotubes (212) Further, nNOS overexpression is sufficient to increase mRNA and protein levels of integrin, vinculin, talin, dystrophin, dystroglycans, and syntrophins (180). Renormalization of NO production in mdx muscle was sufficient to reduce membrane damage (197) possibly due to increased expression of structural proteins at the cell membrane (51) such as talin (179), vinculin (179), and utrophin (34). Altogether, it appears that nitric oxide production is essential for expression and maintenance of cytoskeletal and DGC-associated proteins. Inhibition of NOS with L-NAME may cause the cytoskeleton to be more susceptible to calpain-stimulated degradation (99), thereby releasing nNOS into the cytoplasm.

NOS activity did not significant change during our disuse atrophy model; however levels of NO production did highly correlate with stretch and β1-integrin protein concentrations (Figures 4-10 and 4-5). Genetic knockout of the β1-integrin gene completely eliminated NO production following 10% stretch in C_2C_{12}s, but β1-integrin reincorporation into the muscle membrane restored normal NO levels (213). This suggests that nNOS association with β1-integrin is necessary for the stretched-induced NOS activity seen in our model. Loss of integrin and its membrane-associated proteins during atrophy may disrupt mechanotransduction pathways and influence NO production during atrophy or other pathologies.

Stretch-Induced Activation of Akt is NOS-Dependent

The mechanisms by which growth factors, such as insulin and IGF, simulate protein synthesis in skeletal muscles have been well characterized. This includes activation of Akt, which occurs through a PI3K-dependent mechanism (96). In turn, activated Akt phosphorylates GSK-3β, resulting in an inhibition of GSK-3β activity (152, 187). The decrease in GSK-3β activity is linked to a decrease in phosphorylation of eIF2B at Ser535, an event that is linked to enhanced eIF2B activity and protein synthesis (141, 195). Insulin also induces an increase in $p70^{S6k}$ phosphorylation through a PI3K- and mTOR-dependent pathway (29, 44, 85). Activated $p70^{S6k}$ is known to phosphorylate the S6 subunit of the 40 S ribosome, an event that has been implicated in the translational control of RNAs (88, 95). Thus, after insulin/IGF1 stimulation, both GSK-3β and $p70^{S6k}$ contribute to the PI3K- and mTOR-dependent pathways that regulate protein synthesis.

Similar to insulin, mechanically-induced increases in protein synthesis were found to be both PI3K- and mTOR-dependent, and highly correlated with the changes in GSK-3β and $p70^{S6k}$ phosphorylation (81). However, in both the co-incubation and conditioned-media experiments, the release of locally acting factors was not sufficient for the activation of mTOR-dependent signaling events, thus suggesting that mechanotransduction (e.g., mechanoreceptor) rather than ligand binding of autocrine/paracrine growth factors as the cause for the induction of the mTOR-dependent signaling events (81).

The PI3K-Akt signaling pathway is now one of the most recognized mechanosensitive signaling pathways in skeletal muscles. Several reports have convincingly shown the activation of Akt by increased skeletal muscle contraction or passive muscle stretch (81, 146, 151, 152, 185). Akt signaling contributes to muscle mass growth and maintenance by two independent mechanisms: one involves stimulation of protein synthesis (as previously discussed), and the

other includes inhibition of protein degradation. Akt inhibition of protein degradation acts through downregulation of the family of FOXO transcription factors, which are responsible for expression of the muscle atrophy-induced ubiquitin ligases MuRF1 and MAFbx (154, 166). Regulation of FOXO factor activity is mainly controlled by a shuttling system that modulates its cellular localization by phosphorylation sites located in the COOH-terminal domain. Phosphorylation of these sites by Akt provokes their nuclear export (186).

Four members of the FOXO subfamily of forkhead transcription factors have been identified in the mouse; and in C_2C_{12} myotubes, the expression of constitutively active Foxo3a is enough to induce atrophy, with a concomitant activation of MAFbx expression (154). Further, passive stretch of the diaphragm was sufficient to induce PI3K-Akt and inhibited DNA binding of FOXO1 and FOXO3a (134), suggesting that a stretch stimulus is sufficient to suppress the signals leading to protein degradation.

In agreement with the literature, our model of cyclic mechanical stretch in C_2C_{12} myotubes induced a large and transient increase in Akt activity, which was complimented by phosphorylation of GSK-3β and inhibition of FOXO3a (Figures 4-11 through 4-13). Thus, membrane deformation via mechanical stretch of myotubes is sufficient to activate mechanosensitive pathways necessary to enhance protein synthesis and prevent proteolysis.

Likewise, cessation of mechanical stretch for 12-48 h caused a significant reduction in Akt activity and a concomitant increase in FOXO3a (Figures 4-11 and 4-13). However, this length of time was not sufficient to induce significant MAFbx expression. In spite of this, protein degradation and myotube atrophy did occur within 72 h withdrawal of stretch (Figures 4-2 through 4-4), and we can speculate that perhaps the other muscle-specific E3-ligase MuRF1, and not MAFbx, was involved in tagging proteins for degradation in our model. Others have shown

MuRF1 to be associated with sarcomeric proteins in skeletal muscle (121), and thus MuRF1 may play a larger role in myofibrillar ubiquitination during myotube atrophy than MAFbx.

Most interestingly, the Akt response to stretch was completely dependent on nitric oxide synthase activity, as L-NAME blocked both phosphorylation of Akt and GSK-3β and led to increased activity of FOXO3a. Our lab was the first to demonstrate the ability of nitric oxide to augment Akt activity in skeletal muscle cells. Low doses of the NO donors SNAP and PAPA-NO (1 and 10 μM) were sufficient to induce phosphorylation of Akt; whereas, higher concentrations (100-1000 μM) inhibited Akt phosphorylation (48), presumably via S-nitrosylation of cysteine 224 independent of PI3K signaling (207). Thus, the nitric oxide regulation of Akt is dose-dependent and may be altered during various magnitudes of strain (80). The mechanism for how NO facilitates activation Akt is unknown, but it is thought that NO may influence upstream targets such as PI3K or protein phosphatases (48).

Moderate Stretch and Pathways of NF-κB Signaling

The NF-κB family of transcription factors is well documented as being involved in both cachexia and disuse forms of skeletal muscle atrophy. However, NF-κB has also been shown to increase with exercise and stretch. Our data shows that NF-κB-dependent transcription and the NF-κB subunits p50, Bcl-3 and p65 become temporarily elevated in the nucleus following repetitive bouts of 12% cyclic strain in C_2C_{12} myotubes (Figures 4-15 through 4-17, 4-19). Acute bouts of treadmill exercise, muscle contraction, and passive stretch transiently induce IκB kinase-α and –β (IKKα/β) and IκBα phosphorylation, nuclear import of p65/p50, and enhanced NF-κB binding that peaks within 2 h of exercise in mice (77, 102, 103) and rats (89). The elevated NF-κB activity following stretch was prevented by the antioxidant NAC (103), and the exercise-induced NF-κB binding to DNA was associated with binding domains of antioxidant genes (i.e., MnSOD) and was accompanied by an elevation of endogenous antioxidant enzyme

RNA and protein content (78). Thus, NF-κB activation may be stimulated by ROS production following exercise or stretch and may be an underlying mechanism for training adaptations and increased expression of antioxidant enzymes. Further, the upregulation of NF-κB binding following exercise training stimulates cellular protection against apoptosis and reduction of the pro-apoptotic proteins (1, 64, 90).

The induction of NF-kB subunits p50/p65 immediately after stretch in our model is likely due to phosphorylation of IKK by Akt. Of the several kinases known to activate IKK, Akt is the most prominent (173, 181), and we show that Akt phosphorylation increases ~5 fold after stretch (Figure 4-11). IKK activation leads to subsequent phosphorylation of the NF-κB inhibitory protein IκBα causing its ubiquitination and degradation by the proteasome. This results in translocation of NF-κB dimers to the nucleus and initiation of gene expression (105). Mechanical stretch has been shown to activate NF-κB transcription factors in myofibers through a PI3K/Akt-dependent pathway. Inhibition of PI3K and Akt abrogated IKKα activity and prevented degradation of the inhibitory subunit IκBα (47). Thus, this suggests that activation of NF-κB transcription may be due to increased IKK activity by phosphorylation of Akt.

Although the p65/p50 heterodimer release by IκBα degradation follows the classical NF-κB pathway induced with stress, we cannot rule out the possibility of an alternative pathway, which involves the DNA binding of p50 homodimers in combination with Bcl-3, since nuclear levels of all three subunits were elevated in our model of stretch (Figures 4-15 through 4-17). The Akt-induced IKK activation has also been shown to phosphorylate p105, which is the inhibitory subunit of p50 (153). Phosphorylation of p105 involves ubiquitination and subsequent degradation by the 26 S proteasome (132). However, a glycine-rich region in the C-terminal half of the p50 moiety acts as a physical barrier to the proteasome and causes limited proteolysis

(117, 130). This process reveals a nuclear translocation sequence allowing p50 to bind to DNA. However, p50 lacks a transactivation domain and cannot initiate gene transcription on its own. The IκB family member Bcl-3 has a high affinitiy for p50 homodimers, and p50/Bcl-3 complexes can activate transcription through the Bcl-3 transactivation domain (22, 57, 133). This agrees with our model in C_2C_{12} myotubes which showed a 4-fold increase in both nuclear p50 and Bcl-3 after a 1-h bout of cyclic stretch (Figure 4-15 and 4-16B).

Another link between Akt signaling and the alternative pathway of NF-κB signaling may contribute to myotube atrophy during cessation of stretch. Along with the decrease in Akt activity 12-48 h post-stretch, we saw a concomitant increase in GSK-3β activity (Figures 4-11 and 4-12). GSK-3β is a kinase known to phosphorylate Bcl-3, and the NF-κB p50/Bcl-3 complex becomes more transcriptionally active when Bcl-3 is phosphorylated (25, 129). The increased ratio of phosphorylated-to-total Bcl-3 followed the same trend as GSK-3β activity (Figure 4-16A) suggesting that the alternative pathway of NF-κB is activated during cessation of stretch in our model. Also, similar to Akt, both Bcl-3 and GSK-3β appear to be regulated by nitric oxide production, since the activities of both were significantly augmented with NOS inhibition after stretch. Thus, the skeletal muscle myotube atrophy witnessed during 3 d of stretch withdrawal may be due in part by reduced Akt activity, increased activation of GSK-3β, and enhanced phosphorylation of the NF-κB complex p50/Bcl-3 to induce atrophy related genes.

Lastly, the fact that NOS inhibition induced nuclear levels of p65 and NF-κB-dependent transcriptional activity during cessation of stretch was unexpected (Figures 4-17 and 4-19); however, they may be interconnected. Nitric oxide has been shown to induce and stabilize IκBα (137), which would contribute to maintenance of p65 in the cytosol. By inhibiting NO

production, IκBα may be more susceptible to degradation, less abundant, and allow for p65 nuclear translocation to contribute to enhanced NF-κB transcription.

Inflammation-Associated Atrophy Model

High Magnitude Stretch Induces iNOS and NF-κB

Cachexia and muscle injury are known to cause a robust increase in various cytokines, iNOS, and NF-κB pathways which lead to skeletal muscle breakdown and atrophy (56, 147). High strain applied to skeletal muscle myotubes *in vitro* is sufficient to induce myotube injury, superoxide production (184) as well as upregulate cytokines and NF-κB signaling through mechanosenstive pathways (211). Therefore, high magnitude cyclic stretch of C_2C_{12} myotubes is an appropriate model in which to study the intrinsic signaling pathways involved in cachexia and inflammation-associated atrophy.

Mechanotransduction pathways are sensitive to load, velocity and magnitude of the stress imposed upon the muscle, and the signal that is tranduced from the muscle membrane to the interior of the cell will regulate the downstream pathways (27). Moderate stretch, as discussed in the previous section, can elicit anabolic, adaptive, and protective signals within skeletal muscle. Conversely, higher magnitudes of stretch may be deleterious to muscle, and the subsequent response is to induce mediators of injury and inflammation which leads to muscle breakdown and degradation. In general, 10-12% stretch of muscle cells in culture, which causes cell deformation without significant injury, is considered to be a model for mechanical activity; whereas stretch of 17-20% or greater is considered an injury model (157, 189). Thus, we chose to stretch C_2C_{12} myotubes by 18% as a model for inflammation-induced atrophy.

The proinflammatory cytokine TNF-α, a potent activator of NF-κB in muscle cells (113) plays a pathological role in mediation of such disorders as cachexic muscle wasting, inflammatory myopathies, and insulin resistance (119, 144). Although, as a regulator of immune

and inflammatory response, TNF-α is primarily synthesized by macrophages and other immune cells (183), but it is also synthesized by skeletal muscle in a highly regulated manner. Myoblasts constitutively synthesize TNF-α (150), and this activity increases transiently upon differentiation (115). Myofibers respond to various types of injury with dramatically increased expression of TNF-α and its receptors (38, 42, 175, 196, 210). In addition, strenuous exercise elevates the level of circulating TNF-α (131, 165), which originates from skeletal muscle (128, 165). TNF-α is synthesized as a 26 kDa pro-TNF-α, which is then anchored to the plasma membrane. The membrane-bound pro-TNF-α is cleaved and released as a 17 kDa secreted form of TNF-α by TNF-α converting enzyme (TACE). TACE, also known as ADAM17, is a ubiquitous enzyme that belongs to the ADAM family of disintegrin metalloproteinases (16, 17) and is key regulator of the availability of autocrine TNF-α in mechanotransduction (211).

Tumor necrosis factor-α is one of the main activators of the NF-κB pathway (24, 71, 92), and it is well established that cachexic muscle atrophy requires the activation of transcription factors including NF-κB (31) and Foxo3a (154), leading either to the rapid decrease of MyoD mRNA (71) or to the overexpression of the ubiquitin ligase, MAFbx (154). NF-κB regulates the expression of a wide variety of genes, including those encoding cytokines, chemokines, adhesion molecules, and inducible enzymes (e.g., iNOS and COX-2) (63). It was previously shown that TNF-α induces the expression of iNOS, leading to the production and release of NO and, oxidative stress in the skeletal muscles of cachexic animals and C_2C_{12} myocytes (24, 200). The release of NO by iNOS depends on the transcription of the NOS gene. The murine and human iNOS promoters contain several binding sites for transcription factors such as NF-κB (6). Regulation of iNOS via the NF-κB pathway is an important mechanism in the inflammatory process and constitutes a potential target to combat inflammation-related disease.

In our *in vitro* model of inflammation-associated atrophy, we demonstrated that 18% cyclic stretch to C_2C_{12} myotubes significantly increases NF-κB nuclear translocation and NF-κB-dependent transcription leading to the upregulation of iNOS and MAFbx expression (Figures 4-20 through 4-25). The IκB member, Bcl-3, was undetectable in all samples suggesting that the classical pathway of NF-κB signaling (i.e., IκB-α/p50/p65) was exclusively activated in our model. This agrees with the observation that TNF-α-induced activation of NF-κB activates the prototypical p65-p50 heterodimer in skeletal muscle (127).

The inflammation-associated, TNF-α-dependent pathway of NF-κB signaling has been shown to initiate degradation of intrinsic muscle proteins as well as inhibit myogenesis through a complex list of target genes (70). Using dominant negative inhibition of NF-κB, investigators have shown that TNF-induced NF-κB activation is responsible for an increase in ubiquitin-conjugating activity and upregulation of the ubiquitin-conjugating E2 enzyme, called UbcH2 (114). Another target gene of NF-κB in muscle cells is the C3 proteasome subunit (49), which again implicates NF-κB's involvement in the ubiquitin-proteasome pathway of protein degradation. Additionally, treatment of C_2C_{12} cells with TNF-α, leads to the lost expression of MyoD, myogenin, CDK, myosin heavy chain, and tropomyosin proteins, resulting in the eventual inhibition of myotube formation (3, 70). TNF-α inhibits skeletal muscle differentiation via the induction of iNOS and NO production in a NF-κB dependent manner, which subsequently leads to MyoD mRNA degeneration (45, 71). Furthermore, several genetic approaches have demonstrated that TNF-α and its downstream effectors negatively regulate the process of myogenesis *in vitro* (71, 106). Therefore, inflammation-associated atrophy through NF-κB and iNOS is likely due to downregulation of myogenesis and increased proteolysis of skeletal muscle cells.

Nitric Oxide Synthase Inhibition Prevents NF-κB Nuclear Translocation, iNOS and MAFbx Expression during High Strain

The inhibition of NOS during 1-3 h of 18% cyclic mechanical strain in C_2C_{12} myotubes significantly abrogated the degradation of IκB-α, nuclear translocation of NF-κB subunits p50 and p65, and the upregulation of MAFbx expression (Figures 4-20 through 4-23). Thus, it appears that NOS inhibition can prevent inflammation-associated atrophy signaling *in vitro*. This is in agreement with the literature as an isoform-specific iNOS inhibitor was shown to prevent the onset of cachexia in nude mice injected with TNF-α (24).

Further, L-NAME also completely prevented the upregulation of iNOS mRNA with stretch (Figure 4-24). The explanation for these results can be two fold. First, we know that nitric oxide concentrations increase with high magnitudes of stretch, so, elevated NO levels may be responsible for the initial activation and propagation of NF-κB signaling leading to transcription of the iNOS gene. This would suggest that either iNOS is constitutively expressed in C_2C_{12}s (which we did show with immunostaining in Figure 4-9) and was functional during strain prior to transcriptional regulation by NF-κB, or that the initial burst of NO following stretch was not due to increased iNOS activitiy but rather to that of nNOS or eNOS. Second, the TNF-α converting enzyme (TACE) is mechanosensitive and may initiate activation of TNF-α and subsequently, NF-κB after stretch, either independently or in combination with NO. The ensuing iNOS transcription and NO production would contribute to a positive feedback loop to propagate the signal as long as the cyclic strain continues. However, because we did not manipulate TACE or measure TNF-α levels, we cannot be certain of their contribution in our model.

Inducible NOS Is Not Solely Responsible for NO Production during High Strain

Genetic knockout of the iNOS gene in primary cultured myotubes showed blunted NF-κB nuclear translocation during 18% cyclic strain, but concomitant administration of L-NAME to

iNOS$^{(-/-)}$ myotubes further inhibited the pathway (Figures 4-26 through 4-28). This suggests that either nNOS or eNOS may also contribute to the production of nitric oxide involved in inflammation-associated signaling. It is logical to implicate nNOS here, since it is located within the DGC and susceptible to activation during changes in muscle length. On the other hand, non-isoform specific NOS inhibition did not completely eliminate the stretch-induced NF-κB activity with stretch in C_2C_{12} myotubes, indicating that another pathway must play a role in NF-κB induction during high strain. Altogether, it is likely that two mechanosensitive enzymes, TACE and NOS, initiate the cellular events (via NO and TNF-α) leading to the production of iNOS and subsequently more NO which has been deemed necessary for cachexia and inflammation-associated atrophy (24).

Limitations and Future Directions

Deformation induced signaling through stretch is unquestionably different than signaling associated with active force generation. Active force generation induces metabolic, calcium, and likely more oxidative stresses than mechanical stretch alone. The varied aspects of the cellular environment have synergistic actions. Thus, it is important to consider the entire milieu when evaluating skeletal muscle responses to stress. We are aware that our culture model does not include innervation. In fact, nerve activity and many other potential extraneous variables were controlled by excluding them from study and manipulating only cell loading or stretch. We are confident that our findings are due to loading differences. Future studies should examine the interaction of these load-specific effects with other changes, such as denervation and hindlimb unloading or immobillization.

Conclusions

In conclusion, cyclic mechanical stretch can be used as a model of activity and strain in cultured skeletal muscle myotubes. First, cyclic stretch increases myotube size through induction

of Akt signaling that is dependent on NOS activity. Cessation of stretch causes protein degradation, altered nNOS localization, and a reduction in myotube size via downregulation of Akt, which may contribute to NF-κB signaling through an alternative pathway (Figure 5-1). Secondly, high magnitude cyclic strain can induce the classical pathway of NF-κB signaling and upregulate iNOS and MAFbx expression in cultured skeletal muscle myotubes (Figure 5-2). This study provides evidence that altered loading conditions *in vitro* can be used to gain a better understanding of skeletal muscle atrophy signaling as it occurs *in vivo* and may provide hope for finding potential remedies for this debilitating disease.

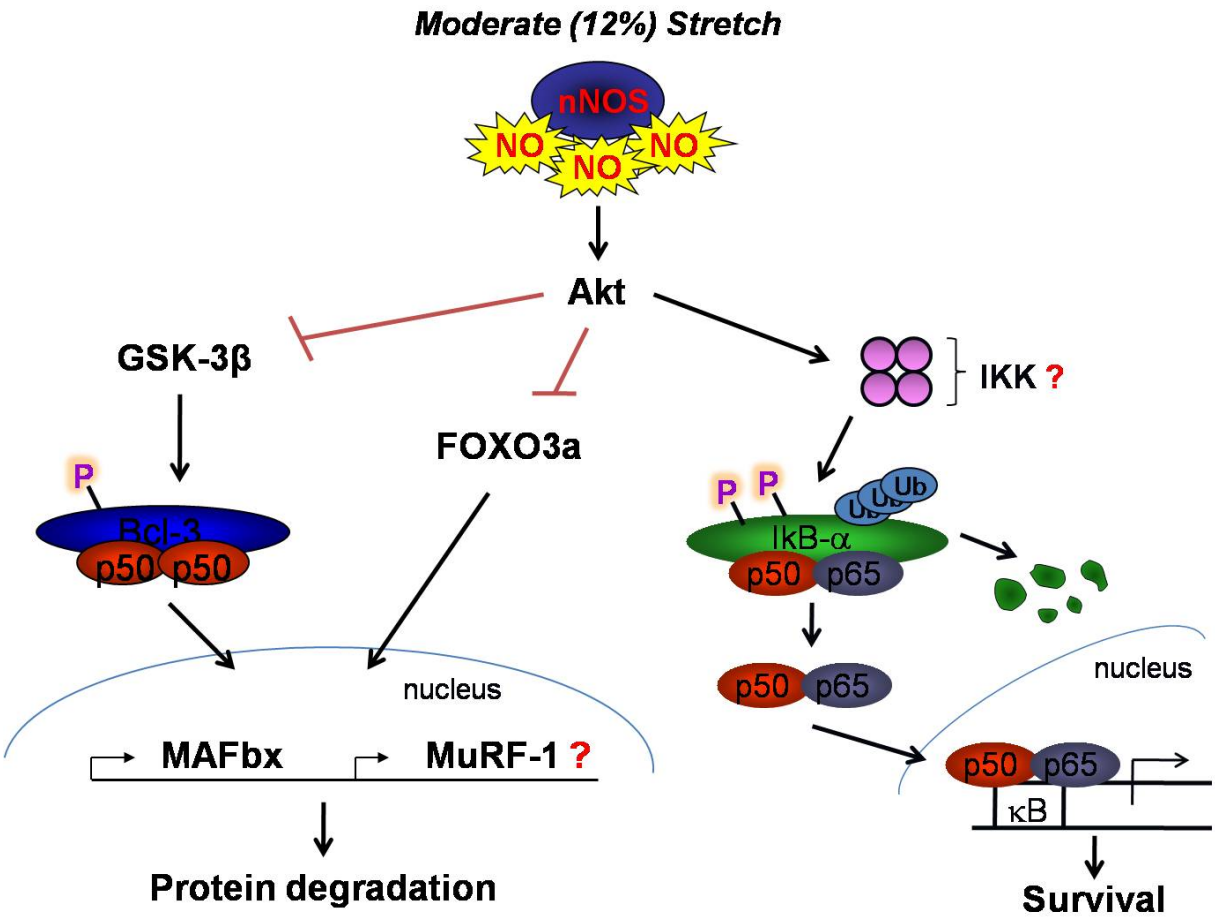

Figure 5-1. Proposed mechanism of nNOS contribution to skeletal muscle disuse atrophy signaling. The release of low levels of nitric oxide after moderate stretch of C_2C_{12} myotubes activates anabolic signaling through Akt and NF-κB survival pathways. Cessation of moderate stretch removes the Akt inhibition of GSK-3β and FOXO3a and promotes protein degradation via the alternative pathway of NF-κB signaling.

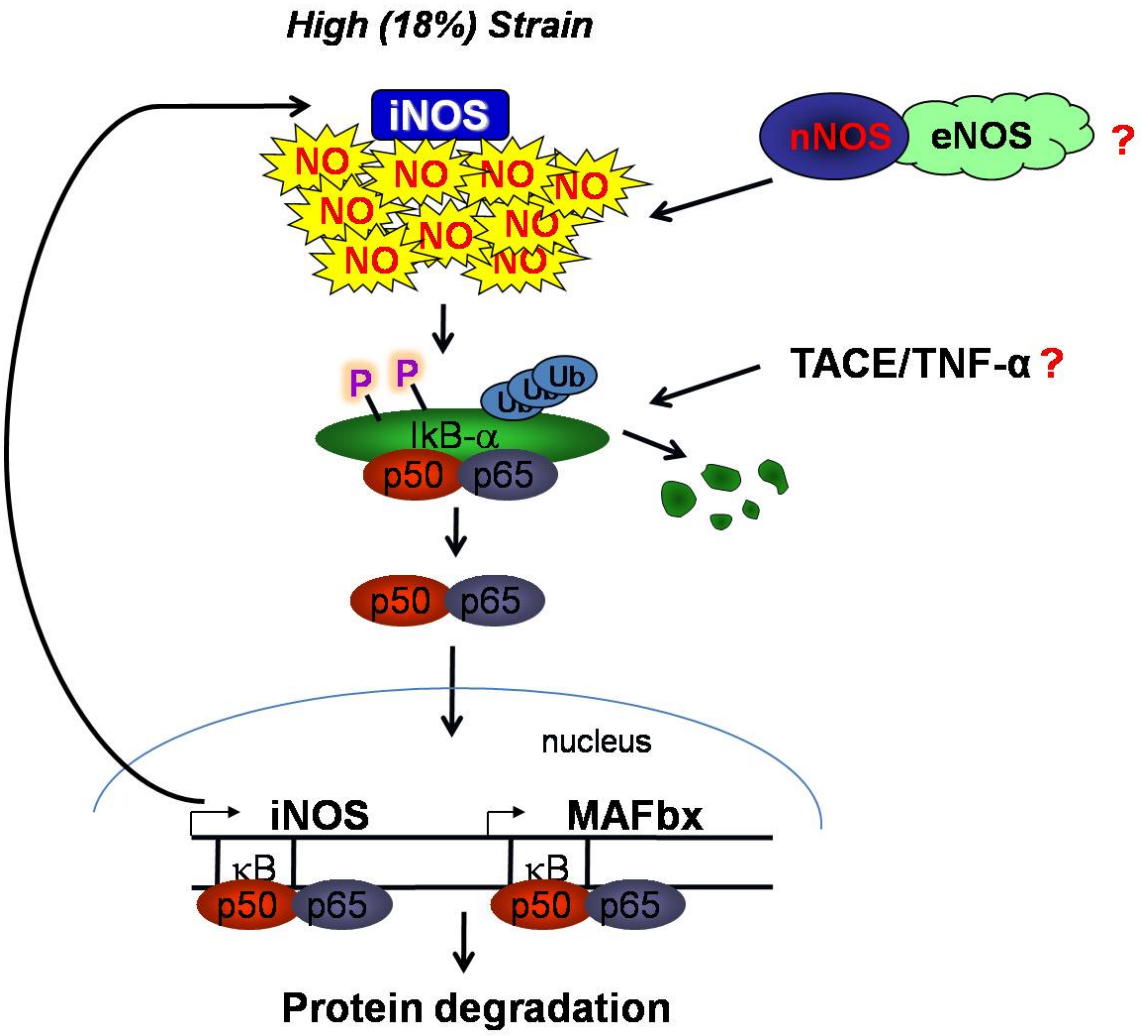

Figure 5-2. Proposed mechanism of NOS involvement in inflammation-associated atrophy during high strain. An 18% stretch of C_2C_{12} myotubes activates the classical pathway of NF-κB signaling by mechanosensitive stimulation of NOS and TNF-α converting enzyme (TACE). NF-κB binding to promoter sites of iNOS and E3 ligases contributes to protein degradation and a positive feedback loop of iNOS activation if high stretch is sustained.

LIST OF REFERENCES

1. **Abbas S and Abu-Amer Y**. Dominant-negative ikappab facilitates apoptosis of osteoclasts by tumor necrosis factor-alpha. *J Biol Chem* 278: 20077-20082, 2003.

2. **Acharyya S, Butchbach ME, Sahenk Z, Wang H, Saji M, Carathers M, Ringel MD, Skipworth RJ, Fearon KC, Hollingsworth MA, Muscarella P, Burghes AH, Rafael-Fortney JA and Guttridge DC**. Dystrophin glycoprotein complex dysfunction: A regulatory link between muscular dystrophy and cancer cachexia. *Cancer Cell* 8: 421-432, 2005.

3. **Acharyya S, Ladner KJ, Nelsen LL, Damrauer J, Reiser PJ, Swoap S and Guttridge DC**. Cancer cachexia is regulated by selective targeting of skeletal muscle gene products. *J Clin Invest* 114: 370-378, 2004.

4. **Adams SA, Robson SC, Gathiram V, Jackson TF, Pillay TS, Kirsch RE and Makgoba MW**. Immunological similarity between the 170 kd amoebic adherence glycoprotein and human beta 2 integrins. *Lancet* 341: 17-19, 1993.

5. **Agarwal S, Deschner J, Long P, Verma A, Hofman C, Evans CH and Piesco N**. Role of nf-kappab transcription factors in antiinflammatory and proinflammatory actions of mechanical signals. *Arthritis Rheum* 50: 3541-3548, 2004.

6. **Aktan F**. Inos-mediated nitric oxide production and its regulation. *Life Sci* 75: 639-653, 2004.

7. **Anderson JE**. A role for nitric oxide in muscle repair: Nitric oxide-mediated activation of muscle satellite cells. *Mol Biol Cell* 11: 1859-1874, 2000.

8. **Arnold WP, Mittal CK, Katsuki S and Murad F**. Nitric oxide activates guanylate cyclase and increases guanosine 3':5'-cyclic monophosphate levels in various tissue preparations. *Proc Natl Acad Sci U S A* 74: 3203-3207, 1977.

9. **Baldwin AS, Jr.** The nf-kappa b and i kappa b proteins: New discoveries and insights. *Annu Rev Immunol* 14: 649-683, 1996.

10. **Balon TW and Nadler JL**. Evidence that nitric oxide increases glucose transport in skeletal muscle. *J Appl Physiol* 82: 359-363, 1997.

11. **Bar-Shai M, Carmeli E and Reznick AZ**. The role of nf-kappab in protein breakdown in immobilization, aging, and exercise: From basic processes to promotion of health. *Ann N Y Acad Sci* 1057: 431-447, 2005.

12. **Bar-Shai M and Reznick AZ**. Reactive nitrogen species induce nuclear factor-kappab-mediated protein degradation in skeletal muscle cells. *Free Radic Biol Med* 40: 2112-2125, 2006.

13. **Beckerle MC, Burridge K, DeMartino GN and Croall DE**. Colocalization of calcium-dependent protease ii and one of its substrates at sites of cell adhesion. *Cell* 51: 569-577, 1987.

14. **Belkin AM, Retta SF, Pletjushkina OY, Balzac F, Silengo L, Fassler R, Koteliansky VE, Burridge K and Tarone G**. Muscle beta1d integrin reinforces the cytoskeleton-matrix link: Modulation of integrin adhesive function by alternative splicing. *J Cell Biol* 139: 1583-1595, 1997.

15. **Bevington A, Poulter C, Brown J and Walls J**. Inhibition of protein synthesis by acid in l6 skeletal muscle cells: Analogies with the acute starvation response. *Miner Electrolyte Metab* 24: 261-266, 1998.

16. **Black RA**. Tumor necrosis factor-alpha converting enzyme. *Int J Biochem Cell Biol* 34: 1-5, 2002.

17. **Blobel CP**. Metalloprotease-disintegrins: Links to cell adhesion and cleavage of tnf alpha and notch. *Cell* 90: 589-592, 1997.

18. **Blottner D and Luck G**. Nitric oxide synthase (nos) in mouse skeletal muscle development and differentiated myoblasts. *Cell Tissue Res* 292: 293-302, 1998.

19. **Bodine S, Latres E, Baumhueter S, Lai V, Nunez L, Clarke B, Poueymirou W, Panaro F, Na E, Dharmaranjan K, Pan Z, Valenzuela D, DeChiara T, Stitt T, Yancopoulos G and Glass D**. Identification of ubiquitin ligases required for skeletal muscle atrophy. *Science* 294: 1704-1708, 2001.

20. **Booth F**. Effect of limb immobilization on skeletal muscle. *J Appl Physiol* 52: 1704-1708, 1982.

21. **Booth F and Seider M**. Early change in skeletal muscle protein synthesis after limb immobilization. *J Appl Physiol* 47: 974-977, 1979.

22. **Bours V, Franzoso G, Azarenko V, Park S, Kanno T, Brown K and Siebenlist U**. The oncoprotein bcl-3 directly transactivates through kappa b motifs via association with DNA-binding p50b homodimers. *Cell* 72: 729-739, 1993.

23. **Brenman JE, Chao DS, Xia H, Aldape K and Bredt DS**. Nitric oxide synthase complexed with dystrophin and absent from skeletal muscle sarcolemma in duchenne muscular dystrophy. *Cell* 82: 743-752, 1995.

24. **Buck M and Chojkier M**. Muscle wasting and dedifferentiation induced by oxidative stress in a murine model of cachexia is prevented by inhibitors of nitric oxide synthesis and antioxidants. *Embo J* 15: 1753-1765, 1996.

25. **Bundy DL and McKeithan TW**. Diverse effects of bcl3 phosphorylation on its modulation of nf-kappab p52 homodimer binding to DNA. *J Biol Chem* 272: 33132-33139, 1997.

26. **Burgering B and Coffer P**. Protein kinase b (c-akt) in phosphatidylinositol-3-oh kinase signal transduction. *Nature* 376: 599-602, 1995.

27. **Burkholder TJ**. Mechanotransduction in skeletal muscle. *Front Biosci* 12: 174-191, 2007.

28. **Burkholder TJ**. Permeability of c2c12 myotube membranes is influenced by stretch velocity. *Biochem Biophys Res Commun* 305: 266-270, 2003.

29. **Burnett PE, Barrow RK, Cohen NA, Snyder SH and Sabatini DM**. Raft1 phosphorylation of the translational regulators p70 s6 kinase and 4e-bp1. *Proc Natl Acad Sci U S A* 95: 1432-1437, 1998.

30. **Cachaco AS, Chuva de Sousa Lopes SM, Kuikman I, Bajanca F, Abe K, Baudoin C, Sonnenberg A, Mummery CL and Thorsteinsdottir S**. Knock-in of integrin beta 1d affects primary but not secondary myogenesis in mice. *Development* 130: 1659-1671, 2003.

31. **Cai D, Frantz JD, Tawa NE, Jr., Melendez PA, Oh BC, Lidov HG, Hasselgren PO, Frontera WR, Lee J, Glass DJ and Shoelson SE**. Ikkbeta/nf-kappab activation causes severe muscle wasting in mice. *Cell* 119: 285-298, 2004.

32. **Chang WJ, Iannaccone ST, Lau KS, Masters BS, McCabe TJ, McMillan K, Padre RC, Spencer MJ, Tidball JG and Stull JT**. Neuronal nitric oxide synthase and dystrophin-deficient muscular dystrophy. *Proc Natl Acad Sci U S A* 93: 9142-9147, 1996.

33. **Chao DS, Silvagno F, Xia H, Cornwell TL, Lincoln TM and Bredt DS**. Nitric oxide synthase and cyclic gmp-dependent protein kinase concentrated at the neuromuscular endplate. *Neuroscience* 76: 665-672, 1997.

34. **Chaubourt E, Fossier P, Baux G, Leprince C, Israel M and De La Porte S**. Nitric oxide and l-arginine cause an accumulation of utrophin at the sarcolemma: A possible compensation for dystrophin loss in duchenne muscular dystrophy. *Neurobiol Dis* 6: 499-507, 1999.

35. **Chrzanowska-Wodnicka M and Burridge K**. Rho-stimulated contractility drives the formation of stress fibers and focal adhesions. *J Cell Biol* 133: 1403-1415, 1996.

36. **Clark CB, McKnight NL and Frangos JA**. Stretch activation of gtp-binding proteins in c2c12 myoblasts. *Exp Cell Res* 292: 265-273, 2004.

37. **Clark EA, King WG, Brugge JS, Symons M and Hynes RO**. Integrin-mediated signals regulated by members of the rho family of gtpases. *J Cell Biol* 142: 573-586, 1998.

38. **Collins RA and Grounds MD**. The role of tumor necrosis factor-alpha (tnf-alpha) in skeletal muscle regeneration. Studies in tnf-alpha(-/-) and tnf-alpha(-/-)/lt-alpha(-/-) mice. *J Histochem Cytochem* 49: 989-1001, 2001.

39. **Collinsworth AM, Torgan CE, Nagda SN, Rajalingam RJ, Kraus WE and Truskey GA**. Orientation and length of mammalian skeletal myocytes in response to a unidirectional stretch. *Cell Tissue Res* 302: 243-251, 2000.

40. **da Costa N, Edgar J, Ooi PT, Su Y, Meissner JD and Chang KC**. Calcineurin differentially regulates fast myosin heavy chain genes in oxidative muscle fibre type conversion. *Cell Tissue Res* 329: 515-527, 2007.

41. **Datta S, Brunet A and Greenberg M**. Cellular survival: A play in three akts. *Genes Dev* 13: 2925-2927, 1999.

42. **De Bleecker JL, Meire VI, Declercq W and Van Aken EH**. Immunolocalization of tumor necrosis factor-alpha and its receptors in inflammatory myopathies. *Neuromuscul Disord* 9: 239-246, 1999.

43. **DeMartino G and Ordway G**. Ubiquitin-proteasome pathway of intracellular protein degradation: Implications for muscle atrophy during unloading. *Exerc Sport Sci Rev* 26: 219-252, 1998.

44. **Dennis PB, Pullen N, Kozma SC and Thomas G**. The principal rapamycin-sensitive p70(s6k) phosphorylation sites, t-229 and t-389, are differentially regulated by rapamycin-insensitive kinase kinases. *Mol Cell Biol* 16: 6242-6251, 1996.

45. **Di Marco S, Mazroui R, Dallaire P, Chittur S, Tenenbaum SA, Radzioch D, Marette A and Gallouzi IE**. Nf-kappa b-mediated myod decay during muscle wasting requires nitric oxide synthase mrna stabilization, hur protein, and nitric oxide release. *Mol Cell Biol* 25: 6533-6545, 2005.

46. **Dias P, Dilling M and Houghton P**. The molecular basis of skeletal muscle differentiation. *Semin Diagn Pathol* 11: 3-14, 1994.

47. **Dogra C, Changotra H, Wergedal JE and Kumar A**. Regulation of phosphatidylinositol 3-kinase (pi3k)/akt and nuclear factor-kappa b signaling pathways in dystrophin-deficient skeletal muscle in response to mechanical stretch. *J Cell Physiol* 208: 575-585, 2006.

48. **Drenning J**. *Nitric oxide facilitates nuclear factor of activated t-cell (nfat) activity through akt-induced glycogen synthase kinase-3beta phosphorylation* (Dissertation). Gainesville: University of Florida, 2008.

49. **Du J, Mitch WE, Wang X and Price SR**. Glucocorticoids induce proteasome c3 subunit expression in l6 muscle cells by opposing the suppression of its transcription by nf-kappa b. *J Biol Chem* 275: 19661-19666, 2000.

50. **Du J, Wang X, Miereles C, Bailey J, Debigare R, Zheng B, Price S and Mitch W**. Activation of caspase-3 is an initial step triggering accelerated muscle proteolysis in catabolic conditions. *J Clin Invest* 113: 115-123, 2004.

51. **Ervasti JM**. Costameres: The achilles' heel of herculean muscle. *J Biol Chem* 278: 13591-13594, 2003.

52. **Etgen GJ, Jr., Fryburg DA and Gibbs EM**. Nitric oxide stimulates skeletal muscle glucose transport through a calcium/contraction- and phosphatidylinositol-3-kinase-independent pathway. *Diabetes* 46: 1915-1919, 1997.

53. **Fath KR, Edgell CJ and Burridge K**. The distribution of distinct integrins in focal contacts is determined by the substratum composition. *J Cell Sci* 92 (Pt 1): 67-75, 1989.

54. **Flinn HM and Ridley AJ**. Rho stimulates tyrosine phosphorylation of focal adhesion kinase, p130 and paxillin. *J Cell Sci* 109 (Pt 5): 1133-1141, 1996.

55. **Frisch S and Ruoslahti E**. Integrins and anoikis. *Curr Opin Cell Biol* 9: 701-706, 1997.

56. **Frost RA and Lang CH**. Skeletal muscle cytokines: Regulation by pathogen-associated molecules and catabolic hormones. *Curr Opin Clin Nutr Metab Care* 8: 255-263, 2005.

57. **Fujita T, Nolan GP, Liou HC, Scott ML and Baltimore D**. The candidate proto-oncogene bcl-3 encodes a transcriptional coactivator that activates through nf-kappa b p50 homodimers. *Genes Dev* 7: 1354-1363, 1993.

58. **Furuno K and Goldberg A**. The activation of protein degradation in muscle by ca2+ or muscle injury does not involve a lysosomal mechanism. *Biochem J* 237: 859-864, 1986.

59. **Gadjeva M, Tomczak MF, Zhang M, Wang YY, Dull K, Rogers AB, Erdman SE, Fox JG, Carroll M and Horwitz BH**. A role for nf-kappa b subunits p50 and p65 in the inhibition of lipopolysaccharide-induced shock. *J Immunol* 173: 5786-5793, 2004.

60. **Gath HJ, Heissler E, Hell B, Bier J, Riethmuller G and Pantel K**. Immunocytologic detection of isolated tumor cells in bone marrow of patients with squamous cell carcinomas of the head and neck region. *Int J Oral Maxillofac Surg* 24: 351-355, 1995.

61. **Gath I, Closs EI, Godtel-Armbrust U, Schmitt S, Nakane M, Wessler I and Forstermann U**. Inducible no synthase ii and neuronal no synthase i are constitutively expressed in different structures of guinea pig skeletal muscle: Implications for contractile function. *Faseb J* 10: 1614-1620, 1996.

62. **Gath I, Ebert J, Godtel-Armbrust U, Ross R, Reske-Kunz AB and Forstermann U**. No synthase ii in mouse skeletal muscle is associated with caveolin 3. *Biochem J* 340 (Pt 3): 723-728, 1999.

63. **Ghosh S and Karin M**. Missing pieces in the nf-kappab puzzle. *Cell* 109 Suppl: S81-96, 2002.

64. **Gius D, Botero A, Shah S and Curry HA**. Intracellular oxidation/reduction status in the regulation of transcription factors nf-kappab and ap-1. *Toxicol Lett* 106: 93-106, 1999.

65. **Goll D, Thompson V, Li H, Wei W and Cong J**. The calpain system. *Physiol Rev* 83: 731-801, 2003.

66. **Goll DE, Thompson VF, Taylor RG and Christiansen JA**. Role of the calpain system in muscle growth. *Biochimie* 74: 225-237, 1992.

67. **Gomes M, Lecker S, Jagoe R, Navon A and Goldberg A**. Atrogin-1, a muscle-specific f-box protein highly expressed during muscle atrophy. *Proc Natl Acad Sci* 98: 14440-14445, 2001.

68. **Grange RW, Isotani E, Lau KS, Kamm KE, Huang PL and Stull JT**. Nitric oxide contributes to vascular smooth muscle relaxation in contracting fast-twitch muscles. *Physiol Genomics* 5: 35-44, 2001.

69. **Grozdanovic Z, Nakos G, Dahrmann G, Mayer B and Gossrau R**. Species-independent expression of nitric oxide synthase in the sarcolemma region of visceral and somatic striated muscle fibers. *Cell Tissue Res* 281: 493-499, 1995.

70. **Guttridge DC**. Signaling pathways weigh in on decisions to make or break skeletal muscle. *Curr Opin Clin Nutr Metab Care* 7: 443-450, 2004.

71. **Guttridge DC, Mayo MW, Madrid LV, Wang CY and Baldwin AS, Jr.** Nf-kappab-induced loss of myod messenger rna: Possible role in muscle decay and cachexia. *Science* 289: 2363-2366, 2000.

72. **Haddad F, Roy RR, Zhong H, Edgerton VR and Baldwin KM**. Atrophy responses to muscle inactivity. I. Cellular markers of protein deficits. *J Appl Physiol* 95: 781-790, 2003.

73. **Hasselgreen P and Fischer J**. The ubiquitin-proteosome pathway: Review of a novel intracellular mechanism of muscle protein breakdown during sepsis and other catabolic conditions. *Ann Surg* 225: 307-316, 1997.

74. **Hasselgreen P, Wray C and Mammen J**. Molecular regulation of muscle cachexia: It may be more than the proteasome. *Biochem Biophys Res Commun* 290: 1-10, 2002.

75. **Heissmeyer V, Krappmann D, Wulczyn FG and Scheidereit C**. Nf-kappab p105 is a target of ikappab kinases and controls signal induction of bcl-3-p50 complexes. *Embo J* 18: 4766-4778, 1999.

76. **Hirschfield W, Moody MR, O'Brien WE, Gregg AR, Bryan RM, Jr. and Reid MB**. Nitric oxide release and contractile properties of skeletal muscles from mice deficient in type iii nos. *Am J Physiol Regul Integr Comp Physiol* 278: R95-R100, 2000.

77. **Ho RC, Hirshman MF, Li Y, Cai D, Farmer JR, Aschenbach WG, Witczak CA, Shoelson SE and Goodyear LJ**. Regulation of ikappab kinase and nf-kappab in contracting adult rat skeletal muscle. *Am J Physiol Cell Physiol* 289: C794-801, 2005.

78. **Hollander J, Fiebig R, Gore M, Bejma J, Ookawara T, Ohno H and Ji LL**. Superoxide dismutase gene expression in skeletal muscle: Fiber-specific adaptation to endurance training. *Am J Physiol* 277: R856-862, 1999.

79. **Hong DH and Forsberg NE**. Effects of dexamethasone on protein degradation and protease gene expression in rat l8 myotube cultures. *Mol Cell Endocrinol* 108: 199-209, 1995.

80. **Hornberger TA, Armstrong DD, Koh TJ, Burkholder TJ and Esser KA**. Intracellular signaling specificity in response to uniaxial vs. Multiaxial stretch: Implications for mechanotransduction. *Am J Physiol Cell Physiol* 288: C185-194, 2005.

81. **Hornberger TA, Stuppard R, Conley KE, Fedele MJ, Fiorotto ML, Chin ER and Esser KA**. Mechanical stimuli regulate rapamycin-sensitive signalling by a phosphoinositide 3-kinase-, protein kinase b- and growth factor-independent mechanism. *Biochem J* 380: 795-804, 2004.

82. **Huang J and Forsberg NE**. Role of calpain in skeletal-muscle protein degradation. *Proc Natl Acad Sci U S A* 95: 12100-12105, 1998.

83. **Hunter RB and Kandarian SC**. Disruption of either the nfkb1 or the bcl3 gene inhibits skeletal muscle atrophy. *J Clin Invest* 114: 1504-1511, 2004.

84. **Hunter RB, Stevenson E, Koncarevic A, Mitchell-Felton H, Essig DA and Kandarian SC**. Activation of an alternative nf-kappab pathway in skeletal muscle during disuse atrophy. *Faseb J* 16: 529-538, 2002.

85. **Isotani S, Hara K, Tokunaga C, Inoue H, Avruch J and Yonezawa K**. Immunopurified mammalian target of rapamycin phosphorylates and activates p70 s6 kinase alpha in vitro. *J Biol Chem* 274: 34493-34498, 1999.

86. **Iwata M, Hayakawa K, Murakami T, Naruse K, Kawakami K, Inoue-Miyazu M, Yuge L and Suzuki S**. Uniaxial cyclic stretch-stimulated glucose transport is mediated by a ca-dependent mechanism in cultured skeletal muscle cells. *Pathobiology* 74: 159-168, 2007.

87. **Jagoe R and Goldberg A**. What do we really know about the ubiquitin-proteasome pathway in muscle atrophy? *Curr Opin Clin Nutr Metab Care* 4: 183-190, 2001.

88. **Jefferies HB, Fumagalli S, Dennis PB, Reinhard C, Pearson RB and Thomas G**. Rapamycin suppresses 5'top mrna translation through inhibition of p70s6k. *Embo J* 16: 3693-3704, 1997.

89. **Ji LL, Gomez-Cabrera MC, Steinhafel N and Vina J**. Acute exercise activates nuclear factor (nf)-kappab signaling pathway in rat skeletal muscle. *Faseb J* 18: 1499-1506, 2004.

90. **Joshi SG, Francis CW, Silverman DJ and Sahni SK**. Nuclear factor kappa b protects against host cell apoptosis during rickettsia rickettsii infection by inhibiting activation of apical and effector caspases and maintaining mitochondrial integrity. *Infect Immun* 71: 4127-4136, 2003.

91. **Judge AR, Koncarevic A, Hunter RB, Liou HC, Jackman RW and Kandarian SC**. Role for ikappabalpha, but not c-rel, in skeletal muscle atrophy. *Am J Physiol Cell Physiol* 292: C372-382, 2007.

92. **Karayiannakis AJ, Syrigos KN, Polychronidis A, Pitiakoudis M, Bounovas A and Simopoulos K**. Serum levels of tumor necrosis factor-alpha and nutritional status in pancreatic cancer patients. *Anticancer Res* 21: 1355-1358, 2001.

93. **Katsumi A, Naoe T, Matsushita T, Kaibuchi K and Schwartz MA**. Integrin activation and matrix binding mediate cellular responses to mechanical stretch. *J Biol Chem* 280: 16546-16549, 2005.

94. **Katsumi A, Orr AW, Tzima E and Schwartz MA**. Integrins in mechanotransduction. *J Biol Chem* 279: 12001-12004, 2004.

95. **Kawasome H, Papst P, Webb S, Keller GM, Johnson GL, Gelfand EW and Terada N**. Targeted disruption of p70(s6k) defines its role in protein synthesis and rapamycin sensitivity. *Proc Natl Acad Sci U S A* 95: 5033-5038, 1998.

96. **Kimball SR, Farrell PA and Jefferson LS**. Invited review: Role of insulin in translational control of protein synthesis in skeletal muscle by amino acids or exercise. *J Appl Physiol* 93: 1168-1180, 2002.

97. **Kobzik L, Reid MB, Bredt DS and Stamler JS**. Nitric oxide in skeletal muscle. *Nature* 372: 546-548, 1994.

98. **Kobzik L, Stringer B, Balligand JL, Reid MB and Stamler JS**. Endothelial type nitric oxide synthase in skeletal muscle fibers: Mitochondrial relationships. *Biochem Biophys Res Commun* 211: 375-381, 1995.

99. **Koh TJ and Tidball JG**. Nitric oxide inhibits calpain-mediated proteolysis of talin in skeletal muscle cells. *Am J Physiol Cell Physiol* 279: C806-812, 2000.

100. **Kondo H**. Oxidative stress in skeletal muscle atrophy. In: *Handbook of oxidants and antioxidants in exercise*, edited by Chandan Sen L and Hanninen O. Amsterdam: Elsevier, 2000, p. 631–653.

101. **Kondo H, Nakagaki I, Sasaki S, Hori S and Itokawa Y**. Trace element movement and oxidative stress in skeletal muscle atrophied by immobilization. *Am J Physiol Endocrinol Metab* 262: E583-E590, 1992.

102. **Kumar A and Boriek AM**. Mechanical stress activates the nuclear factor-kappab pathway in skeletal muscle fibers: A possible role in duchenne muscular dystrophy. *Faseb J* 17: 386-396, 2003.

103. **Kumar A, Lnu S, Malya R, Barron D, Moore J, Corry DB and Boriek AM**. Mechanical stretch activates nuclear factor-kappab, activator protein-1, and mitogen-activated protein kinases in lung parenchyma: Implications in asthma. *Faseb J* 17: 1800-1811, 2003.

104. **Kumar A, Murphy R, Robinson P, Wei L and Boriek AM**. Cyclic mechanical strain inhibits skeletal myogenesis through activation of focal adhesion kinase, rac-1 gtpase, and nf-kappab transcription factor. *Faseb J* 18: 1524-1535, 2004.

105. **Kumar A, Takada Y, Boriek AM and Aggarwal BB**. Nuclear factor-kappab: Its role in health and disease. *J Mol Med* 82: 434-448, 2004.

106. **Ladner KJ, Caligiuri MA and Guttridge DC**. Tumor necrosis factor-regulated biphasic activation of nf-kappa b is required for cytokine-induced loss of skeletal muscle gene products. *J Biol Chem* 278: 2294-2303, 2003.

107. **Langenbach K and Rando T**. Inhibition of dystroglycan binding to laminin disrupts the pi3k/akt pathway and survival signaling in muscle cells. *Muscle Nerve* 26: 644-653, 2002.

108. **Lawler JM, Song W and Demaree SR**. Hindlimb unloading increases oxidative stress and disrupts antioxidant capacity in skeletal muscle. *Free Radic Biol Med* 35: 9-16, 2003.

109. **Lecker SH, Solomon V, Mitch WE and Goldberg AL**. Muscle protein breakdown and the critical role of the ubiquitin-proteasome pathway in normal and disease states. *J Nutr* 129: 227S-237S, 1999.

110. **Lee SW, Dai G, Hu Z, Wang X, Du J and Mitch WE**. Regulation of muscle protein degradation: Coordinated control of apoptotic and ubiquitin-proteasome systems by phosphatidylinositol 3 kinase. *J Am Soc Nephrol* 15: 1537-1545, 2004.

111. **Leger B, Cartoni R, Praz M, Lamon S, Deriaz O, Crettenand A, Gobelet C, Rohmer P, Konzelmann M, Luthi F and Russell AP**. Akt signalling through gsk-3beta, mtor and foxo1 is involved in human skeletal muscle hypertrophy and atrophy. *J Physiol* 576: 923-933, 2006.

112. **Li Y, Chen Y, Li A and Reid M**. Hydrogen peroxide stimulates ubiquitin-conjugating activity and expression of gene for specific e2 and e3 proteins in skeletal muscle myotubes. *Am J Physiol Cell Physiol* 285: C806-C812, 2003.

113. **Li YP, Chen Y, John J, Moylan J, Jin B, Mann DL and Reid MB**. Tnf-alpha acts via p38 mapk to stimulate expression of the ubiquitin ligase atrogin1/mafbx in skeletal muscle. *Faseb J* 19: 362-370, 2005.

114. **Li YP, Lecker SH, Chen Y, Waddell ID, Goldberg AL and Reid MB**. Tnf-alpha increases ubiquitin-conjugating activity in skeletal muscle by up-regulating ubch2/e220k. *Faseb J* 17: 1048-1057, 2003.

115. **Li YP and Schwartz RJ**. Tnf-alpha regulates early differentiation of c2c12 myoblasts in an autocrine fashion. *Faseb J* 15: 1413-1415, 2001.

116. **Lim CC, Zuppinger C, Guo X, Kuster GM, Helmes M, Eppenberger HM, Suter TM, Liao R and Sawyer DB**. Anthracyclines induce calpain-dependent titin proteolysis and necrosis in cardiomyocytes. *J Biol Chem* 279: 8290-8299, 2004.

117. **Lin L and Ghosh S**. A glycine-rich region in nf-kappab p105 functions as a processing signal for the generation of the p50 subunit. *Mol Cell Biol* 16: 2248-2254, 1996.

118. **Long JH, Lira VA, Soltow QA, Betters JL, Sellman JE and Criswell DS**. Arginine supplementation induces myoblast fusion via augmentation of nitric oxide production. *J Muscle Res Cell Motil* 27: 577-584, 2006.

119. **Lundberg IE and Dastmalchi M**. Possible pathogenic mechanisms in inflammatory myopathies. *Rheum Dis Clin North Am* 28: 799-822, 2002.

120. **McClung JM, Lee WJ, Thompson RW, Lowe LL and Carson JA**. Rhoa induction by functional overload and nandrolone decanoate administration in rat skeletal muscle. *Pflugers Arch* 447: 345-355, 2003.

121. **McElhinny AS, Kakinuma K, Sorimachi H, Labeit S and Gregorio CC**. Muscle-specific ring finger-1 interacts with titin to regulate sarcomeric m-line and thick filament structure and may have nuclear functions via its interaction with glucocorticoid modulatory element binding protein-1. *J Cell Biol* 157: 125-136, 2002.

122. **McKoy G, Ashley W, Mander J, Yang SY, Williams N, Russell B and Goldspink G**. Expression of insulin growth factor-1 splice variants and structural genes in rabbit skeletal muscle induced by stretch and stimulation. *J Physiol* 516 (Pt 2): 583-592, 1999.

123. **Michetti M, Salamino F, Melloni E and Pontremoli S**. Reversible inactivation of calpain isoforms by nitric oxide. *Biochem Biophys Res Commun* 207: 1009-1014, 1995.

124. **Miranti CK and Brugge JS**. Sensing the environment: A historical perspective on integrin signal transduction. *Nat Cell Biol* 4: E83-90, 2002.

125. **Misko TP, Schilling RJ, Salvemini D, Moore WM and Currie MG**. A fluorometric assay for the measurement of nitrite in biological samples. *Anal Biochem* 214: 11-16, 1993.

126. **Moylan JS, Smith JD, Chambers MA, McLoughlin TJ and Reid MB**. Tnf induction of atrogin-1/mafbx mrna depends on foxo4 expression but not akt-foxo1/3 signaling. *Am J Physiol Cell Physiol*, 2008.

127. **Naumann M and Scheidereit C**. Activation of nf-kappa b in vivo is regulated by multiple phosphorylations. *Embo J* 13: 4597-4607, 1994.

128. **Nieman DC, Davis JM, Henson DA, Gross SJ, Dumke CL, Utter AC, Vinci DM, Carson JA, Brown A, McAnulty SR, McAnulty LS and Triplett NT**. Muscle cytokine mrna changes after 2.5 h of cycling: Influence of carbohydrate. *Med Sci Sports Exerc* 37: 1283-1290, 2005.

129. **Nolan GP, Fujita T, Bhatia K, Huppi C, Liou HC, Scott ML and Baltimore D**. The bcl-3 proto-oncogene encodes a nuclear i kappa b-like molecule that preferentially interacts with nf-kappa b p50 and p52 in a phosphorylation-dependent manner. *Mol Cell Biol* 13: 3557-3566, 1993.

130. **Orian A, Schwartz AL, Israel A, Whiteside S, Kahana C and Ciechanover A**. Structural motifs involved in ubiquitin-mediated processing of the nf-kappab precursor p105: Roles of the glycine-rich region and a downstream ubiquitination domain. *Mol Cell Biol* 19: 3664-3673, 1999.

131. **Ostrowski K, Rohde T, Asp S, Schjerling P and Pedersen BK**. Pro- and anti-inflammatory cytokine balance in strenuous exercise in humans. *J Physiol* 515 (Pt 1): 287-291, 1999.

132. **Palombella VJ, Rando OJ, Goldberg AL and Maniatis T**. The ubiquitin-proteasome pathway is required for processing the nf-kappa b1 precursor protein and the activation of nf-kappa b. *Cell* 78: 773-785, 1994.

133. **Pan J and McEver RP**. Regulation of the human p-selectin promoter by bcl-3 and specific homodimeric members of the nf-kappa b/rel family. *J Biol Chem* 270: 23077-23083, 1995.

134. **Pardo PS, Lopez MA and Boriek AM**. Foxo transcription factors are mechanosensitive and their regulation is altered with aging in the respiratory pump. *Am J Physiol Cell Physiol* 294: C1056-1066, 2008.

135. **Park CS, Park R and Krishna G**. Constitutive expression and structural diversity of inducible isoform of nitric oxide synthase in human tissues. *Life Sci* 59: 219-225, 1996.

136. **Pavlath GK, Thaloor D, Rando TA, Cheong M, English AW and Zheng B**. Heterogeneity among muscle precursor cells in adult skeletal muscles with differing regenerative capacities. *Dev Dyn* 212: 495-508, 1998.

137. **Peng HB, Libby P and Liao JK**. Induction and stabilization of i kappa b alpha by nitric oxide mediates inhibition of nf-kappa b. *J Biol Chem* 270: 14214-14219, 1995.

138. **Pisconti A, Brunelli S, Di Padova M, De Palma C, Deponti D, Baesso S, Sartorelli V, Cossu G and Clementi E**. Follistatin induction by nitric oxide through cyclic gmp: A tightly regulated signaling pathway that controls myoblast fusion. *J Cell Biol* 172: 233-244, 2006.

139. **Purintrapiban J, Wang M and Forsberg N**. Degradation of sarcomeric and cytoskeletal proteins in cultured skeletal muscle cells. *Comp Biochem Physiol B Biochem Mol Biol* 136: 393-401, 2003.

140. **Qi WN, Chen LE, Zhang L, Eu JP, Seaber AV and Urbaniak JR**. Reperfusion injury in skeletal muscle is reduced in inducible nitric oxide synthase knockout mice. *J Appl Physiol* 97: 1323-1328, 2004.

141. **Quevedo C, Alcazar A and Salinas M**. Two different signal transduction pathways are implicated in the regulation of initiation factor 2b activity in insulin-like growth factor-1-stimulated neuronal cells. *J Biol Chem* 275: 19192-19197, 2000.

142. **Rando T**. The dystrophin-glycoprotein complex, cellular signaling, and the regulation of cell survival in the muscular dystrophies. *Muscle Nerve* 24: 1575-1594, 2001.

143. **Rauch C and Loughna PT**. Static stretch promotes mef2a nuclear translocation and expression of neonatal myosin heavy chain in c2c12 myocytes in a calcineurin- and p38-dependent manner. *Am J Physiol Cell Physiol* 288: C593-605, 2005.

144. **Reid MB and Li YP**. Cytokines and oxidative signalling in skeletal muscle. *Acta Physiol Scand* 171: 225-232, 2001.

145. **Reiser PJ, Kline WO and Vaghy PL**. Induction of neuronal type nitric oxide synthase in skeletal muscle by chronic electrical stimulation in vivo. *J Appl Physiol* 82: 1250-1255, 1997.

146. **Reynolds THt, Bodine SC and Lawrence JC, Jr.** Control of ser2448 phosphorylation in the mammalian target of rapamycin by insulin and skeletal muscle load. *J Biol Chem* 277: 17657-17662, 2002.

147. **Rubinstein I, Abassi Z, Coleman R, Milman F, Winaver J and Better OS**. Involvement of nitric oxide system in experimental muscle crush injury. *J Clin Invest* 101: 1325-1333, 1998.

148. **Rudnick J, Puttmann B, Tesch PA, Alkner B, Schoser BG, Salanova M, Kirsch K, Gunga HC, Schiffl G, Luck G and Blottner D**. Differential expression of nitric oxide synthases (nos 1-3) in human skeletal muscle following exercise countermeasure during 12 weeks of bed rest. *Faseb J* 18: 1228-1230, 2004.

149. **Sacheck JM, Ohtsuka A, McLary SC and Goldberg AL**. Igf-i stimulates muscle growth by suppressing protein breakdown and expression of atrophy-related ubiquitin ligases, atrogin-1 and murf1. *Am J Physiol Endocrinol Metab* 287: E591-601, 2004.

150. **Saghizadeh M, Ong JM, Garvey WT, Henry RR and Kern PA**. The expression of tnf alpha by human muscle. Relationship to insulin resistance. *J Clin Invest* 97: 1111-1116, 1996.

151. **Sakamoto K, Aschenbach WG, Hirshman MF and Goodyear LJ**. Akt signaling in skeletal muscle: Regulation by exercise and passive stretch. *Am J Physiol Endocrinol Metab* 285: E1081-1088, 2003.

152. **Sakamoto K, Hirshman MF, Aschenbach WG and Goodyear LJ**. Contraction regulation of akt in rat skeletal muscle. *J Biol Chem* 277: 11910-11917, 2002.

153. **Salmeron A, Janzen J, Soneji Y, Bump N, Kamens J, Allen H and Ley SC**. Direct phosphorylation of nf-kappab1 p105 by the ikappab kinase complex on serine 927 is essential for signal-induced p105 proteolysis. *J Biol Chem* 276: 22215-22222, 2001.

154. **Sandri M, Sandri C, Gilbert A, Skurk C, Calabria E, Picard A, Walsh K, Schiaffino S, Lecker SH and Goldberg AL**. Foxo transcription factors induce the atrophy-related ubiquitin ligase atrogin-1 and cause skeletal muscle atrophy. *Cell* 117: 399-412, 2004.

155. **Sasa T, Sairyo K, Yoshida N, Fukunaga M, Koga K, Ishikawa M and Yasui N**. Continuous muscle stretch prevents disuse muscle atrophy and deterioration of its oxidative capacity in rat tail-suspension models. *Am J Phys Med Rehabil* 83: 851-856, 2004.

156. **Sastry SK and Burridge K**. Focal adhesions: A nexus for intracellular signaling and cytoskeletal dynamics. *Exp Cell Res* 261: 25-36, 2000.

157. **Schultz E and McCormick KM**. Skeletal muscle satellite cells. *Rev Physiol Biochem Pharmacol* 123: 213-257, 1994.

158. **Schwander M, Leu M, Stumm M, Dorchies OM, Ruegg UT, Schittny J and Muller U**. Beta1 integrins regulate myoblast fusion and sarcomere assembly. *Dev Cell* 4: 673-685, 2003.

159. **Senf SM, Dodd SL, McClung JM and Judge AR**. Hsp70 overexpression inhibits nf-{kappa}b and foxo3a transcriptional activities and prevents skeletal muscle atrophy. *Faseb J*, 2008.

160. **Siems W, Capuozzo E, Lucano A, Salerno C and Crifo C**. High sensitivity of plasma membrane ion transport atpases from human neutrophils towards 4-hydroxy-2,3-trans-nonenal. *Life Sci* 73: 2583-2590, 2003.

161. **Sjakste N, Sjakste J, Boucher JL, Baumane L, Sjakste T, Dzintare M, Meirena D, Sharipova J and Kalvinsh I**. Putative role of nitric oxide synthase isoforms in the changes of nitric oxide concentration in rat brain cortex and cerebellum following sevoflurane and isoflurane anaesthesia. *Eur J Pharmacol* 513: 193-205, 2005.

162. **Smith LW, Smith JD and Criswell DS**. Involvement of nitric oxide synthase in skeletal muscle adaptation to chronic overload. *J Appl Physiol* 92: 2005-2011, 2002.

163. **Soltow QA, Betters JL, Sellman JE, Lira VA, Long JH and Criswell DS**. Ibuprofen inhibits skeletal muscle hypertrophy in rats. *Med Sci Sports Exerc* 38: 840-846, 2006.

164. **Sonoda Y, Watanabe S, Matsumoto Y, Aizu-Yokota E and Kasahara T**. Fak is the upstream signal protein of the phosphatidylinositol 3-kinase-akt survival pathway in hydrogen peroxide-induced apoptosis of a human glioblastoma cell line. *J Biol Chem* 274: 10566-10570, 1999.

165. **Starkie RL, Rolland J, Angus DJ, Anderson MJ and Febbraio MA**. Circulating monocytes are not the source of elevations in plasma il-6 and tnf-alpha levels after prolonged running. *Am J Physiol Cell Physiol* 280: C769-774, 2001.

166. **Stitt TN, Drujan D, Clarke BA, Panaro F, Timofeyva Y, Kline WO, Gonzalez M, Yancopoulos GD and Glass DJ**. The igf-1/pi3k/akt pathway prevents expression of muscle atrophy-induced ubiquitin ligases by inhibiting foxo transcription factors. *Mol Cell* 14: 395-403, 2004.

167. **Stoyanovsky D, Murphy T, Anno PR, Kim YM and Salama G**. Nitric oxide activates skeletal and cardiac ryanodine receptors. *Cell Calcium* 21: 19-29, 1997.

168. **Sultan KR, Henkel B, Terlou M and Haagsman HP**. Quantification of hormone-induced atrophy of large myotubes from c2c12 and l6 cells: Atrophy-inducible and atrophy-resistant c2c12 myotubes. *Am J Physiol Cell Physiol* 290: C650-659, 2006.

169. **Suzuki N, Motohashi N, Uezumi A, Fukada S, Yoshimura T, Itoyama Y, Aoki M, Miyagoe-Suzuki Y and Takeda S**. No production results in suspension-induced muscle atrophy through dislocation of neuronal nos. *J Clin Invest* 117: 2468-2476, 2007.

170. **Taillandier D, Aurousseau E, Meynial-Denis D, Bechet D, Ferrara M, Cottin P, Ducastaing A, Bigard X, Guezennec CY, Schmid HP and et al.** Coordinate activation of lysosomal, ca 2+-activated and atp-ubiquitin-dependent proteinases in the unweighted rat soleus muscle. *Biochem J* 316 (Pt 1): 65-72, 1996.

171. **Takamure M, Murata KY, Tamada Y, Azuma M and Ueno S**. Calpain-dependent alpha-fodrin cleavage at the sarcolemma in muscle diseases. *Muscle Nerve* 32: 303-309, 2005.

172. **Tang H, Cheung WM, Ip FC and Ip NY**. Identification and characterization of differentially expressed genes in denervated muscle. *Mol Cell Neurosci* 16: 127-140, 2000.

173. **Testa JR and Bellacosa A**. Akt plays a central role in tumorigenesis. *Proc Natl Acad Sci U S A* 98: 10983-10985, 2001.

174. **Tews DS and Goebel HH**. Cell death and oxidative damage in inflammatory myopathies. *Clin Immunol Immunopathol* 87: 240-247, 1998.

175. **Tews DS and Goebel HH**. DNA fragmentation and bcl-2 expression in infantile spinal muscular atrophy. *Neuromuscul Disord* 6: 265-273, 1996.

176. **Thomason D, Biggs R and Booth F**. Protein metabolism and beta-myosin heavy-chain mrna in unweighted soleus muscle. *Am J Physiol Regul Integr Comp Physiol* 257: R300-R305, 1989.

177. **Thompson M, Becker L, Bryant D, Williams G, Levin D, Margraf L and Giroir BP**. Expression of the inducible nitric oxide synthase gene in diaphragm and skeletal muscle. *J Appl Physiol* 81: 2415-2420, 1996.

178. **Tidball JG, Lavergne E, Lau KS, Spencer MJ, Stull JT and Wehling M**. Mechanical loading regulates nos expression and activity in developing and adult skeletal muscle. *Am J Physiol* 275: C260-266, 1998.

179. **Tidball JG, Spencer MJ, Wehling M and Lavergne E**. Nitric-oxide synthase is a mechanical signal transducer that modulates talin and vinculin expression. *J Biol Chem* 274: 33155-33160, 1999.

180. **Tidball JG and Wehling-Henricks M**. Expression of a nos transgene in dystrophin-deficient muscle reduces muscle membrane damage without increasing the expression of membrane-associated cytoskeletal proteins. *Mol Genet Metab* 82: 312-320, 2004.

181. **Toker A and Cantley LC**. Signalling through the lipid products of phosphoinositide-3-oh kinase. *Nature* 387: 673-676, 1997.

182. **Torgan CE and Daniels MP**. Regulation of myosin heavy chain expression during rat skeletal muscle development in vitro. *Mol Biol Cell* 12: 1499-1508, 2001.

183. **Tracey KJ and Cerami A**. Tumor necrosis factor, other cytokines and disease. *Annu Rev Cell Biol* 9: 317-343, 1993.

184. **Tsivitse SK, Mylona E, Peterson JM, Gunning WT and Pizza FX**. Mechanical loading and injury induce human myotubes to release neutrophil chemoattractants. *Am J Physiol Cell Physiol* 288: C721-729, 2005.

185. **Turinsky J and Damrau-Abney A**. Akt kinases and 2-deoxyglucose uptake in rat skeletal muscles in vivo: Study with insulin and exercise. *Am J Physiol* 276: R277-282, 1999.

186. **Van Der Heide LP, Hoekman MF and Smidt MP**. The ins and outs of foxo shuttling: Mechanisms of foxo translocation and transcriptional regulation. *Biochem J* 380: 297-309, 2004.

187. **van Weeren PC, de Bruyn KM, de Vries-Smits AM, van Lint J and Burgering BM**. Essential role for protein kinase b (pkb) in insulin-induced glycogen synthase kinase 3 inactivation. Characterization of dominant-negative mutant of pkb. *J Biol Chem* 273: 13150-13156, 1998.

188. **Vandenburgh H and Kaufman S**. In vitro model for stretch-induced hypertrophy of skeletal muscle. *Science* 203: 265-268, 1979.

189. **Vandenburgh HH, Hatfaludy S, Karlisch P and Shansky J**. Mechanically induced alterations in cultured skeletal muscle growth. *J Biomech* 24 Suppl 1: 91-99, 1991.

190. **Viatour P, Dejardin E, Warnier M, Lair F, Claudio E, Bureau F, Marine JC, Merville MP, Maurer U, Green D, Piette J, Siebenlist U, Bours V and Chariot A**. Gsk3-mediated bcl-3 phosphorylation modulates its degradation and its oncogenicity. *Mol Cell* 16: 35-45, 2004.

191. **Viner RI, Ferrington DA, Williams TD, Bigelow DJ and Schoneich C**. Protein modification during biological aging: Selective tyrosine nitration of the serca2a isoform of the sarcoplasmic reticulum ca2+-atpase in skeletal muscle. *Biochem J* 340 (Pt 3): 657-669, 1999.

192. **Voisin L, Breuille D, Combaret L, Pouyet C, Taillandier D, Aurousseau E, Obled C and Attaix D**. Muscle wasting in a rat model of long-lasting sepsis results from the activation of lysosomal, ca2+ -activated, and ubiquitin-proteasome proteolytic pathways. *J Clin Invest* 97: 1610-1617, 1996.

193. **Volberg T, Sabanay H and Geiger B**. Spatial and temporal relationships between vinculin and talin in the developing chicken gizzard smooth muscle. *Differentiation* 32: 34-43, 1986.

194. **Wakayama Y, Inoue M, Murahashi M, Shibuya S, Jimi T, Kojima H and Oniki H**. Ultrastructural localization of alpha 1-syntrophin and neuronal nitric oxide synthase in normal skeletal myofiber, and their relation to each other and to dystrophin. *Acta Neuropathol* 94: 455-464, 1997.

195. **Wang X, Janmaat M, Beugnet A, Paulin FE and Proud CG**. Evidence that the dephosphorylation of ser(535) in the epsilon-subunit of eukaryotic initiation factor (eif) 2b is insufficient for the activation of eif2b by insulin. *Biochem J* 367: 475-481, 2002.

196. **Warren GL, Hulderman T, Jensen N, McKinstry M, Mishra M, Luster MI and Simeonova PP**. Physiological role of tumor necrosis factor alpha in traumatic muscle injury. *Faseb J* 16: 1630-1632, 2002.

197. **Wehling M, Spencer MJ and Tidball JG**. A nitric oxide synthase transgene ameliorates muscular dystrophy in mdx mice. *J Cell Biol* 155: 123-131, 2001.

198. **Whipple G and Koohmaraie M**. Degradation of myofibrillar proteins by extractable lysosomal enzymes and m-calpain, and the effects of zinc chloride. *J Anim Sci* 69: 4449-4460, 1991.

199. **Williams AB, Decourten-Myers GM, Fischer JE, Luo G, Sun X and Hasselgren PO**. Sepsis stimulates release of myofilaments in skeletal muscle by a calcium-dependent mechanism. *Faseb J* 13: 1435-1443, 1999.

200. **Williams G, Brown T, Becker L, Prager M and Giroir BP**. Cytokine-induced expression of nitric oxide synthase in c2c12 skeletal muscle myocytes. *Am J Physiol* 267: R1020-1025, 1994.

201. **Wozniak AC and Anderson JE**. The dynamics of the nitric oxide release-transient from stretched muscle cells. *Int J Biochem Cell Biol*, 2008.

202. **Xie QW, Kashiwabara Y and Nathan C**. Role of transcription factor nf-kappa b/rel in induction of nitric oxide synthase. *J Biol Chem* 269: 4705-4708, 1994.

203. **Xu L, Eu JP, Meissner G and Stamler JS**. Activation of the cardiac calcium release channel (ryanodine receptor) by poly-s-nitrosylation. *Science* 279: 234-237, 1998.

204. **Yaffe D and Saxel O**. A myogenic cell line with altered serum requirements for differentiation. *Differentiation* 7: 159-166, 1977.

205. **Yang B, Jung D, Motto D, Meyer J, Koretzky G and Campbell K**. Sh3 domain-mediated interaction of dystroglycan and grb2. *J Biol Chem* 270: 11711-11714, 1995.

206. **Yang CC, Alvarez RB, Engel WK, Haun CK and Askanas V**. Immunolocalization of nitric oxide synthases at the postsynaptic domain of human and rat neuromuscular junctions--light and electron microscopic studies. *Exp Neurol* 148: 34-44, 1997.

207. **Yasukawa T, Tokunaga E, Ota H, Sugita H, Martyn JA and Kaneki M**. S-nitrosylation-dependent inactivation of akt/protein kinase b in insulin resistance. *J Biol Chem* 280: 7511-7518, 2005.

208. **Yoshida T, Pan Y, Hanada H, Iwata Y and Shigekawa M**. Bidirectional signaling between sarcoglycans and the integrin adhesion system in cultured l6 myocytes. *J Biol Chem* 273: 1583-1590, 1998.

209. **Young ME and Leighton B**. Evidence for altered sensitivity of the nitric oxide/cgmp signalling cascade in insulin-resistant skeletal muscle. *Biochem J* 329 (Pt 1): 73-79, 1998.

210. **Zador E, Mendler L, Takacs V, de Bleecker J and Wuytack F**. Regenerating soleus and extensor digitorum longus muscles of the rat show elevated levels of tnf-alpha and its receptors, tnfr-60 and tnfr-80. *Muscle Nerve* 24: 1058-1067, 2001.

211. **Zhan M, Jin B, Chen SE, Reecy JM and Li YP**. Tace release of tnf-alpha mediates mechanotransduction-induced activation of p38 mapk and myogenesis. *J Cell Sci* 120: 692-701, 2007.

212. **Zhang JS, Kraus WE and Truskey GA**. Stretch-induced nitric oxide modulates mechanical properties of skeletal muscle cells. *Am J Physiol Cell Physiol* 287: C292-299, 2004.

213. **Zhang SJ, Truskey GA and Kraus WE**. Effect of cyclic stretch on beta1d-integrin expression and activation of fak and rhoa. *Am J Physiol Cell Physiol* 292: C2057-2069, 2007.

214. **Zhao L, Lee JY and Hwang DH**. The phosphatidylinositol 3-kinase/akt pathway negatively regulates nod2-mediated nf-kappab pathway. *Biochem Pharmacol* 75: 1515-1525, 2008.

BIOGRAPHICAL SKETCH

Quinlyn Soltow is the daughter of Kimberly Bonner and Frederick Soltow, Jr. Quinlyn was born and raised in Canaan Valley, WV, where she attended Tucker County High School and graduated at the top of her class in 1999. Quinlyn then moved to Atlanta, Georgia, where she received her joint BS/MS degree with high honors in 2003 from Emory University. There she studied inorganic chemistry under the advisement of Dr. Luigi Marzilli. Her master's thesis was titled "Spectroscopic studies of tris(4-sulfonatophenyl) porphyrin and the binding to human serum albumin." Quinlyn chose to continue research with her pursuit of a doctoral degree at the University of Florida in exercise physiology. For the next 5 years, Quinlyn studied muscle physiology under Dr. David Criswell. In 2008, Quinlyn obtained her terminal degree and plans to continue her research aspirations by completing a postdoctoral fellow position with Dr. Dean Jones at the Emory University School of Medicine.